Multivariable fuzzy control with its applications in multi-evaporator refrigeration systems

Liao, Qianfang

2015

Liao, Q. (2015). Multivariable fuzzy control with its applications in multi-evaporator refrigeration systems. Doctoral thesis, Nanyang Technological University, Singapore.

https://hdl.handle.net/10356/62928

https://doi.org/10.32657/10356/62928

MULTIVARIABLE FUZZY CONTROL WITH ITS APPLICATIONS IN MULTI–EVAPORATOR REFRIGERATION SYSTEMS

LIAO QIANFANG

School of Electrical and Electronic Engineering

A thesis submitted to the Nanyang Technological University

in partial fulfillment of the requirement for the degree of

Doctor of Philosophy

2015

Acknowledgement

First and foremost, I would like to express my sincere gratitude to my supervisors, Prof. Cai Wenjian and Prof. Wang Youyi, for their patient supervision, tremendous support and invaluable guidance throughout the course of my research work. Their insightful comments and thoughtful discussions greatly inspire me. It is a big honor and pleasure to have them as my advisors.

I would like to particularly thank Prof. Li Shaoyuan and Prof. Li Ning of Shanghai Jiao Tong University for their patient supervision and constructive guidance during my graduate study and encouraging me to pursue a higher degree. And they still give me their precious support during my Ph.D study, which I am so grateful for.

I want to thank Dr. Yan Jia and Dr. Ding Xudong for their continuous guidance and help throughout the duration of my research. I also thank my colleagues, classmates and friends in Process Instrumentation Laboratory: Xu Di, Yang Chen, Liu Changxia, Yin Xiaohong, Wu Bingjie, Wu Qiong, Cui Can, Zhao Lei, Wang Xinli, Li Chao, Chen Can, Hu Shen, Chen Haoran, Ji Yongfeng, etc., and the laboratory supervisor, Mr. Yock, for their help and support during the course of my study.

I would like to acknowledge School of Electrical and Electronic Engineering, Nanyang Technological University and Energy Research Institute @ NTU (ERI@N) for providing the financial support, research facilities and opportunities for this study.

Last but not least, I want to express my deepest thanks to all members of my beloved family: my father, my mother, my sister and my brother. They give me steadfast love, support and understanding, and stand by me through thick and thin. I couldn’t realize my dreams without them. From the bottom of my heart, I love them always and forever.

Table of Contents

Summary

Multi–evaporator refrigeration (MER) system is a cost–effective device for a building with different cooling requirements because it is comprised of a single compressor and a single condenser but multiple evaporators each operating at a specified temperature to simultaneously cater to different cooling loads such that the efficiency can be improved and the economic cost can be reduced. Compared with a single–evaporator refrigeration system, an MER system is more difficult to control due to its complex structure with cross–coupling effects among different evaporators. This thesis presents a series of novel Type–1 and Type–2 Takagi–Sugeno (T–S) fuzzy model based studies for multivariable process control to manipulate MER systems. The methodologies and the contributions are summarized as follows:

1. Decentralized control is predominant in multivariable process control applications because of its simplicity and effectiveness. The first task for devising decentralized control is to determine a control configuration where the paired input–output loops have minimum cross–coupling effects. In this thesis, by defining the steady–state gain and normalized integrated error on a T–S fuzzy model, a relative normalized gain array (RNGA) based loop pairing criterion is presented to analyze the interactions and pair inputs and outputs to determine the control–loop configuration for decentralized control of an MER system. Simple calculation procedures based on both Type–1 and Type–2 T–S fuzzy models are provided. Compared with the existing fuzzy–model–based loop pairing approaches using only steady–state gain, the proposed method employs both steady and dynamic information of the process to pair the control–loops such that a more proper control configuration can be given for manipulating an MER system.
2. When devising a decentralized controller after control configuration determined, the local controller design for one loop requires the information of other loops since there are interactions among the control–loops. A manner called effective T–S fuzzy model (ETSM) is presented to describe the interacting effects on a certain loop caused by other closed–loops for controller design of an MER system.

The ETSM of a certain loop is derived by incorporating the quantified interactions provided by RNGA based pairing criterion into the coefficients of its individual T–S fuzzy model. Simple calculation methods to obtain Type–1 and Type–2 ETSMs are given. With the ETSMs of paired loops, a multi–input–multi–output (MIMO) process can be approximately considered as multiple independent single–input–single–output (SISO) processes and then the decentralized controller design can be greatly facilitated by linear SISO control algorithms. Compared with existing T–S fuzzy model based decentralized control adding extra terms to the individual fuzzy models to express the interacting effects, ETSM is a practical way that can reduce the complexity in both modeling and controller design.

3. To further improve the control performance in handling the strong interactions of an MER system, a guideline to devise sparse control based on both Type–1 and Type–2 T–S fuzzy models is presented, which includes, first, a method in terms of RNGA based pairing criterion is introduced to analyze the interactions between paired and unpaired loops and then select a sparse control structure by adding several unpaired elements to the paired structure; second, based on the ETSMs of selected loops, an independent controller design approach is given that an MIMO process can be approximately regarded as a group of non–interacting SISO processes, and then the linear SISO control algorithms can be applied to manipulate nonlinear closed–coupled MER systems. Sparse control can achieve improved performance over decentralized control when cost fewer calculations than full–dimensional control.
4. The applications of the proposed Type–1 and Type–2 T–S fuzzy model based methods in an experimental MER system with three evaporators to cater to the cooling requirements for air–conditioning, perishable food storage and freezing are presented. The experimental results validate the practicability and effectiveness of the proposed control structure selections and ETSM methods for decentralized and sparse control. And the comparative results of Type–1 and Type–2 T–S fuzzy systems in terms of robustness and computational cost are given.

Figure list

Table list

Chapter 1. Introduction

1.1 Overview of multi–evaporator refrigeration system control

Refrigeration systems move heat from one physical location to another. Because of this remarkable property, it has been widely used in modern society and plays an important role in air conditioning for comfort, food production and distribution, chemical and industry processes, and special applications [1]. The electricity consumption of refrigeration systems in a building accounts for relatively large proportion of the total energy usage. In countries and regions with mild climates, the usage of refrigeration systems costs up to 30% of the total electric energy consumption. In a tropical zone, such as Singapore, with an average annual ambient temperature of 29.40℃ and an average annual ambient relative humidity of 85%, the electricity consumption for refrigeration systems can be much higher. According to Building & Construction Authority (BCA)'s Green Mark program [2], more than 52% of the total electric energy consumption of Singapore is used for running air conditioning systems, which costs a large amount of money. Therefore, even a small improvement of efficiency in running refrigeration systems could save considerable energy and greatly reduce the expenditure in energy consumption.

In a general building, such as a household estate, a commercial complex or an office building, typically, there are three cooling demands for air–conditioning, perishable food storage and freezing, respectively. A convenient manner to meet different demands is to use different refrigeration systems that cater to different cooling loads independently. However, this approach may not be economically feasible due to the high initial cost, space requirements and redundant expenditures in operation and maintenance. Another alternative is to adopt a multi–evaporator refrigeration (MER) system constructed by a single compressor and a single condenser with three evaporators each operating at a specific evaporating temperature. Compared with using multiple independent single–evaporator refrigeration systems, an MER system can satisfy different cooling requirements simultaneously so that the efficiency in

running refrigeration systems can be improved and then the economic cost can be reduced. The schematic of an MER system with three evaporators is shown in Fig. 1.1.

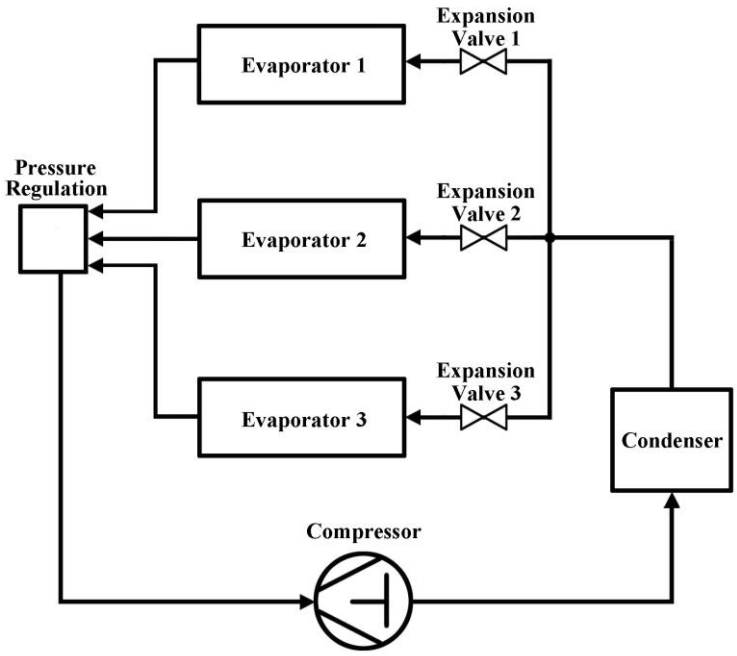

Figure 1.1 Schematic of an MER system

The working principle of this MER system is: circulating refrigerant as a saturated vapor enters the compressor and is compressed into a superheated vapor with higher pressure and temperature. Then the refrigerant is cooled and condensed into liquid phase in the condenser. Afterwards, the sub–cooled liquid refrigerant with a high pressure is divided into three flows that go through three expansion valves where their pressures are reduced abruptly. And then the three cold liquid refrigerant flows enter the evaporators, where they evaporate at different temperatures to absorb the heat of ambient environments and become saturated vapors with different pressures. To reduce the refrigerant vapor pressure from the evaporators with higher temperatures to that from the one with lowest temperature, a pressure regulation device is used to maintain the required pressure differences. After pressure regulation, the three flows with the same pressure are merged into one, and the refrigerant is routed back into the compressor to complete the refrigeration cycle.

Compared with the conventional single–evaporator refrigeration cycle, an MER system as shown in Fig. 1.1 is more difficult to regulate and control since it has a more

complex structure that consists of three cycles which inevitably interact with each other and can introduce strong cross–coupling effects. In the literature to date, only a limited number of studies can be found regarding controller designs for MER systems. For example, [3] presented an approach to controlling the evaporating temperatures and superheat values of a multi–unit air–conditioning system that uses feedback linearization to compensate for the nonlinearity in the system dynamics with a proportional–integral (PI) controller design. [4] developed a method to produce a first–order linear transfer function matrix to describe a triple–evaporator air–conditioner for a cascade controller design, and [5] used the same identification method to obtain a first–order transfer function matrix for the flow distribution control in a dual–evaporator air–conditioner. Several model predictive control methods for multi–evaporator air conditioners were given in [6-8]. A capacity control approach for a multi–evaporator air conditioning system was developed and validated by experimental tests in [9]. In [10] an optimal control strategy was presented to determine the maximum coefficient of performance (COP) for a dual–evaporator refrigeration system with different cold storage rooms where the setting temperatures were –5℃ and –23℃ respectively. In addition, methods using fuzzy logical reasoning to derive controllers for multi–evaporator systems were proposed in [11, 12]. It is noted that the overwhelming majority of existing control methods for MER systems are developed for multi–evaporator air conditioners where all the evaporators work at similar temperatures (air–conditioning), while very few are available for an MER system where the evaporators operate at different temperatures to satisfy different cooling loads (air–conditioning, food storage and freezing).

1.2 Motivations and objectives

An MER system with evaporators working at different temperatures is an effective device to save the energy cost for a building that has different cooling requirements. And a proper control method is necessary and important for running such an MER system. The lack of this type of control method, as introduced in the last section, has motivated the author to do the relevant studies and develop appropriate and practical

approaches to manipulating this type of MER system.

The conventional and classical control methods are developed based on essentially qualitative and quantitative techniques that require more or less accurate mathematical modeling [13]. However, for an MER system as shown in Fig. 1.1, because of its complex structure, strong nonlinearity and the influence of disturbances and interactions, an accurate mathematical model is generally difficult to derive. On the other hand, fuzzy control can be carried out without requiring accurate mathematical models since a fuzzy model can be built based on data samples, human experience or both [14-17]. Moreover, fuzzy control has proved to be an effective, robust and powerful tool to manipulate complex, ill–defined or even non–analytic processes [13, 18]. Thus fuzzy control has been recommended as an alternative to conventional control approaches [13, 18]. Currently, two fuzzy model structures are popular in research and application, one is Mamdani fuzzy model [19], and the other is the Takagi–Sugeno (T–S) fuzzy model [20]. Both of them consist of a group of "IF (antecedent)–THEN (consequent)" fuzzy rules. The difference between them is that Mamdani fuzzy model uses fuzzy sets as its consequents, while T–S uses real–valued dynamic linear polynomials instead. A T–S fuzzy model can describe a global nonlinear process by a group of local linear polynomials which are smoothly merged by fuzzy membership functions. And theoretical proof has been given that a T–S fuzzy model is a universal approximator for any smooth nonlinear systems with arbitrary degree of accuracy in any convex compact area [15-17]. Compared to the Mamdani fuzzy model, T–S fuzzy model can greatly reduce the number of fuzzy rules when modeling higher order systems and subsequently is less prone to the curse of dimensionality [18]. Furthermore, it provides a platform to develop methodologies that combine intelligent human reasoning and classical mathematical approaches for system analysis and controller design. Therefore, author has been motivated to study novel and efficacious methods based on T–S fuzzy models to manipulate MER systems.

Regulating an MER system as shown in Fig. 1.1 requires multi–input–multi–output

(MIMO) process control because it generally needs to adjust several variables such as the valve openings, fan speeds and compressor power to cater to different cooling loads. Compared to single–input–single–output (SISO) counterparts, the MIMO process controllers are much more difficult to realize because of the existence of interactions between process inputs and outputs. At present, a number of T–S fuzzy model based control methods for MIMO processes are available [21-32]. According to the control structure, the existing methods can be classified into two groups: centralized control and decentralized control. Centralized control can handle the interactions if it is well designed since a full–dimensional control structure is employed. However, the full–dimensional control works with acceptable computational cost only in manipulating low–dimensional processes. For large–scale processes, it will lead to greatly increased complexity for controller design because the calculations of high–dimensional matrices are involved, and may result in difficult or even impossible to implement control strategies. Decentralized control could be much simpler than centralized control since it uses a diagonal control structure instead of full–dimensional control structure. In contemporary industrial control practices, decentralized control is the predominant approach to regulating MIMO processes because of its simplicity in design, tuning and implementation, and maintenance with less cost [33-35]. However, using the limited control structure may give deteriorated closed–loop performance because of the interactions caused by the existence of non–zero off–diagonal elements in the matrix describing input–output relationships for an MIMO process [35]. Therefore, the primary step for decentralized control design is to pair the inputs and outputs to determine a control configuration with minimum cross–coupling effects such that the burden in handling the interactions can be reduced as much as possible. Currently very few published studies can be found with respect to interaction analysis and control structure selection based on fuzzy models. Among the few, [36] proposed a method to utilize steady–state gains calculated based on fuzzy basis function networks models to evaluate interactions for an MIMO process. However, for an MER system which is a dynamic process, using only steady–state gains to measure the interacting effects may give inaccurate results for control

structure selection since no dynamic information is taken into account; subsequently, the cost for controllers to cope with interactions will increase and the control performance may be deteriorated. Therefore, the author was motivated to investigate a T–S fuzzy model based method considering both steady–state gains and dynamic information to analyze the interactions and select a proper control configuration for an MER system that ensures the minimized interacting effects for a decentralized control system.

When devising a decentralized controller for an MER system after the control configuration has been determined, the performance of one control–loop cannot be assessed without the information of other loops since they interact with each other [37]. In the existing T–S fuzzy model based decentralized control laws, for a certain diagonal control–loop, extra terms that characterize the interacting effects are added to its individual open–loop model to express the interacting results. A simple example is given as follows:

$$\begin{aligned} R^l : IF \quad & u_i \ is \ C^l \\ THEN \quad & y_i = a^l \cdot u_i + \sum_{j=1, j\neq i}^{n} f_j(u_j) \end{aligned} \tag{1.1}$$

where R^l denotes the *l*th fuzzy rule, u_i is the *i*th input, C^l is the *l*th fuzzy cluster, y_i is the *i*th output. $y_i = a^l \cdot u_i$ is the model of individual open–loop $y_i - u_i$ in *l*th fuzzy rule, $f_j(u_j)$ is an extra term that denotes the interacting effects caused by u_j and $\sum_{j=1, j\neq i}^{n} f_j(u_j)$ is the sum of extra terms that describe the interactions from other loops. The local controller for control–loop $y_i - x_i$ of a decentralized control system is designed based on the model with extra terms as in Eq. (1.1) to handle or eliminate the influence of interactions. However, using extra terms in controller design for an MER system which is used to simultaneously cater for different cooling demands may not be feasible because:

- An MER system can form a large–scale process since it has plenty of variables to be chosen as the inputs and the outputs. For a large–scale process, the number of

extra terms in the model would be large. The identification of these extra terms may drastically increase the cost and complexity in process modeling.

- An MER system generally has intricate structure and considerable unmeasured physical changes. The interactions among the control–loops may be very difficult or even impossible to directly gauge or evaluate, which causes obstacles to obtain the extra terms.
- An MER system is nonlinear. For a nonlinear MIMO process, different working conditions may require different control configurations, and then result in changed interacting effects, which lead to challenges in finding suitable extra terms to describe the variant interactions.

In light of these issues, the author was motivated to investigate an alternative method instead of using extra terms to describe the interactions for decentralized controller design of MER systems.

For an MIMO process where the interactions among the loops are weak or modest, decentralized control using the simplest control structure can generally work with satisfactory results. However, strong coupling effects may exist in an MER system that decentralized control would give degraded performance due to its limited control structure. In this case, a more complicated control structure should be employed while generally not necessarily going to full–dimensional structure, which leads to the study of sparse control. Based on the diagonal decentralized control structure, by adding several off–diagonal controllers, sparse control, including "block diagonal control" and "triangular control", has the ability to achieve better performance than decentralized control [38]. To the best of author's knowledge, no study regarding sparse control structure selection and sparse control design based on fuzzy model has been proposed, which motivated the author to develop a fuzzy–model–based criterion for analyzing the interactions between diagonal and off–diagonal elements to select a proper sparse control structure, and then devise sparse fuzzy controllers for an MER system with closely–coupled effects.

The study in this thesis aims to develop a series of T–S fuzzy model based practical

methods for MER system control. According to the motivations described previously, the objectives of this thesis are summarized as follows:

- Based on T–S fuzzy models, study a method that employs both steady and dynamic information to evaluate the interactions and then pair the loops to determine the decentralized control configuration with minimum cross–coupling effects for an MER system.
- Investigate an alternative method which is simple, feasible and effective in MER system control applications to express the interacting effects based on T–S fuzzy models without using extra terms for decentralized control design.
- Develop a criterion to determine whether an MIMO process of an MER system has strong inner interactions that decentralized control may not fully handle. Afterwards, select a proper sparse control structure by adding several off–diagonal controllers to the diagonal control–loops, and then design sparse controllers based on T–S fuzzy models for the MER system.
- Apply the methods to control an experimental MER system to validate their practicability and effectiveness.

1.3 Major contributions of the thesis

In this thesis, a series of novel and practical T–S fuzzy model based methods for MER system control are presented. And these methods are studied based on both Type–1 and Type–2 T–S fuzzy models. The major contributions are described as follows:

1. Loop pairing based on T–S fuzzy models

For an MIMO process of an MER system, a T–S fuzzy model based loop pairing criterion is proposed that utilizing steady–state gains and normalized integrated errors of individual loops to measure the interactions and then determine the decentralized control configuration. Normalized integrated error accounts for the response speed that can be used to represent the dynamic property of a process. Compared with the existing fuzzy–model–based loop pairing methods using only steady–state gain, the

proposed method can give a more proper control structure for an MER system since both steady and dynamic information of the process are considered to pair the control–loops. Moreover, simple procedures to calculate steady–state gain and normalized integrated error based on both Type–1 and Type–2 T–S fuzzy models are given.

2. Effective T–S fuzzy model (ETSM) for decentralized control

In order to assist decentralized controller designs for MER systems in handling the interactions, a novel manner, called effective T–S fuzzy model (ETSM), is presented as an alternative to the model with extra terms as in Eq. (1.1). For a certain control–loop in a process of an MER system, an ETSM is derived by incorporating the interacting effects, quantified by the loop pairing criterion, into the coefficients of its individual T–S fuzzy model thus the ETSM has same structure but revised coefficients from that of its individual fuzzy model. Simple approaches to calculating the coefficients of both Type–1 and Type–2 ETSMs are provided. Based on the ETSMs of paired loops, an MIMO process can be approximately regarded as multiple non–interacting SISO processes for decentralized controller design. Compared with the existing decentralized fuzzy control methods adding extra terms to the individual model to characterize interacting results, ETSM method is a feasible way that can greatly reduce the cost in process modeling and the following controller design. Moreover, the local model of an ETSM has the same linear structure as that of its individual T–S fuzzy model, thus linear SISO control techniques can be applied to design decentralized control through parallel distributed compensation (PDC) [15] for the MER systems.

3. Sparse fuzzy control

In terms of the proposed loop pairing method, a criterion is given to determine whether a process of an MER system has strong coupling effects among loops that decentralized control may not fully handle, and then to select an appropriate sparse control structure based on T–S fuzzy models. Afterwards, by virtue of ETSMs of the selected loops, an independent design approach is given that the sparse controller

design for an MIMO process can be converted to a group of independent single–loop controller designs using linear control algorithms. Sparse control is able to achieve greatly improved performance by employing a little more complex control structure than decentralized control, and save the cost by utilizing simpler control structure when compared to full–dimensional control. Furthermore, this study provides a platform to utilize mature and developed linear SISO control schemes to manipulate nonlinear and strong coupled MER systems.

4. Applications

The proposed T–S fuzzy model based methods are applied to an experimental MER system with three evaporators for air–conditioning, perishable food storage and freezing to demonstrate their practicability and effectiveness. The experimental results prove that the proposed methods are feasible in using linear SISO control algorithm to regulate this MER system so that the outputs can track their reference values. And the comparisons of decentralized and sparse control are given to demonstrate that sparse control is able to achieve more satisfactory results when the interaction analysis indicates that the coupling effects among part of loops are strong that several off–diagonal controllers should be added to diagonal decentralized control structure. And the comparisons between Type–1 and Type–2 T–S fuzzy control systems are given to analyze the performances of these two types of fuzzy model in terms of robustness and computational cost.

1.4 Organization of the thesis

The rest of this thesis is organized as follows:

Chapter 2 introduces fuzzy modeling for an MIMO process that a T–S fuzzy model is built for each individual loop and then a T–S fuzzy model matrix can be formed for the overall process by collecting all these individual open–loop models. The detailed Type–1 and Type–2 T–S fuzzy modeling methods are introduced and a simulation example is given to demonstrate and compare their errors.

Chapter 3 describes a T–S fuzzy model based loop pairing method to determine the

control configuration with minimum cross–coupling effects for decentralized control. And the calculation procedures based on both Type–1 and Type–2 T–S fuzzy models are presented. A simulation example is used to show and compare the results obtained from these two types of T–S fuzzy model.

Chapter 4 presents an ETSM method to assist decentralized control in handling interactions. Simple calculations to obtain both Type–1 and Type–2 ETSMs are provided. The approach to devising controllers based on Type–1 and Type–2 ETSMs using linear SISO control algorithms is given. A nonlinear process is used as an example to demonstrate and compare the performances of Type–1 and Type–2 ETSM based decentralized controllers and their effective transfer function (ETF) based counterpart.

Chapter 5 provides a guideline for devising sparse control for a closely–coupled MIMO process including a criterion of sparse control structure selection and an independent design method based on ETSMs to facilitate sparse controller design in dealing with the interactions. The nonlinear process in Chapter 4 is used as the example to compare the performances among the decentralized and sparse controllers designed based on ETF, Type–1 and Type–2 ETSMs.

Chapter 6 presents the applications of the proposed methods of Chapter 2–5 on an experimental MER system. The performances of decentralized and sparse control based on Type–1 and Type–2 ETSMs are compared and analyzed.

Chapter 7 concludes the thesis and provides some possible future research directions.

Chapter 2. T–S fuzzy modeling for MIMO processes

2.1 Introduction

In an MER system, plenty of variables can be selected as inputs and outputs to form an MIMO process, such as valve openings, fan speeds and compressor power. These variables can be utilized to regulate refrigerant flow rates or the temperatures of the evaporators to satisfy different cooling loads. In this thesis, it is assumed that the processes to deal with are open–loop stable, nonsingular at steady–state conditions and square ($n \times n$), which can generally be expressed by Fig. 2.1, where y_i's ($i = 1, \cdots, n$) are outputs and u_j's ($j = 1, \cdots, n$) are inputs. Modeling and identification are key steps in devising control systems for an MIMO process since an accurate model can provide useful information for developing and testing different types of advanced approaches. This chapter describes T–S fuzzy modeling methods. In a process as shown in Fig. 2.1, there are $n!$ input–output configurations for a closed–loop control system. And when all loops open, there are n^2 individual single open–loop processes (denoted by loop $y_i - u_j$, $i, j = 1, \cdots, n$). The individual loop properties are important for the following studies in this thesis such as interaction analysis, loop pairing, ETSM method, etc. To completely reflect the steady and dynamic information of individual loops, a novel modeling manner is adopted in this thesis where a SISO T–S fuzzy model is built for each individual loop. When all loops open, the individual open–loop models are always identifiable with proper persistent excitations since there are no interactions from closed–loops to affect the identification results [39]. Denote the T–S fuzzy model for the individual open–loop $y_i - u_j$ as $f_{TS,ij}$, for the whole process, a fuzzy model matrix can be formed by collecting all these individual models as:

$$\boldsymbol{F}_{TS} = \left[f_{TS,ij} \right]_{n \times n} = \begin{bmatrix} f_{TS,11} & f_{TS,12} & \cdots & f_{TS,1n} \\ f_{TS,21} & f_{TS,22} & \cdots & f_{TS,2n} \\ \vdots & \vdots & \ddots & \vdots \\ f_{TS,n1} & f_{TS,n2} & \cdots & f_{TS,nn} \end{bmatrix} \tag{2.1}$$

Consequently, the information of individual loops can be obtained from $\boldsymbol{F}_{TS}$ to carry out interaction analysis, control structure selection and controller design for the MIMO process.

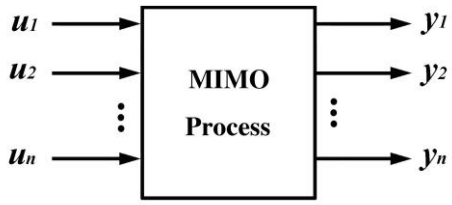

Figure 2.1 A $n \times n$ MIMO process

T–S fuzzy model can be constructed based on the input–output data pairs sampled from the original MIMO process. Generally, the construction includes two parts: one is the identification for antecedents, which is to divide the data into several fuzzy clusters. The other is the identification for consequents, which is to identify the parameters of the local linear polynomials. In this chapter, the methods to construct both Type–1 and Type–2 T–S fuzzy models are presented. Type–2 fuzzy theory was proposed in [40] as an extension of Type–1 (traditional) fuzzy theory [41]. Compared with Type–1 fuzzy set where the fuzzy memberships are crisp, Type–2 fuzzy set has the fuzzy memberships that are themselves fuzzy [42]. With this increased fuzziness, Type–2 fuzzy set can describe levels of uncertainty, vagueness and imprecision with which Type–1 fuzzy set struggles [43], and provides additional degrees of freedom for design that make it possible to directly describe the influence of uncertainties [44]. A completed theory of Type–2 Mamdani fuzzy logic systems was developed by [42, 44-46] at the end of last century. Soon after, Type–2 T–S fuzzy system was introduced and discussed in 1999 [47], which provided additional choice and gave the chance to combine Type–2 fuzzy theory and conventional mathematical approaches for the systematic method development. At the end of this chapter, simulation results are provided to show and compare the errors of Type–1 and Type–2 T–S fuzzy models.

2.2 Type–1 T–S fuzzy modeling

For loop $y_i - u_j$ in a $n \times n$ MIMO process, when its individual open–loop model

$f_{TS,ij}$ is a Type–1 T–S fuzzy system, the "IF–THEN" fuzzy rules of $f_{TS,ij}$ can be expressed as:

$$\begin{aligned} &R^l: \text{IF} \quad \boldsymbol{x}_{ij}(k) \quad is \quad C_{ij}^l \\ &\text{THEN} \quad y_i^l(k) = a_{ij,0}^l \cdot u_j(k-\tau_{ij}) + a_{ij,1}^l \cdot u_j(k-\tau_{ij}-1) + \cdots + a_{ij,p}^l \cdot u_j(k-\tau_{ij}-p) \\ &\qquad\qquad + b_{ij,1}^l \cdot y_i(k-1) + \cdots + b_{ij,q}^l \cdot y_i(k-q) \end{aligned} \tag{2.2}$$

where $l = 1, 2, \cdots, M_{ij}$, M_{ij} is the number of fuzzy rules in $f_{TS,ij}$; $\boldsymbol{x}_{ij}(k)$ is a vector that is constructed of the past inputs and outputs:

$$\boldsymbol{x}_{ij}(k) = [u_j(k-\tau_{ij}) \quad u_j(k-\tau_{ij}-1) \quad \cdots \quad u_j(k-\tau_{ij}-p) \quad y_i(k-1) \quad \cdots \quad y_i(k-q)]$$

p and q are integers that $p \geq 0$ and $q \geq 1$, $\tau_{ij} = \tau'_{ij} / T$, τ'_{ij} is the time delay in loop $y_i - u_j$ and T is the sampling interval; C_{ij}^l represents the lth fuzzy cluster; $y_i^l(k)$ is the output of lth rule; $a_{ij,r}^l (r = 0,1,\cdots, p)$ and $b_{ij,s}^l (s = 1,\cdots, q)$ are the coefficients of the linear polynomial in lth rule. The total output $y_i(k)$ is the weighted sum of local outputs as:

$$y_i(k) = \frac{\sum_{l=1}^{M_{ij}} \mu_{ij}^l(\boldsymbol{x}_{ij}(k)) \cdot y_i^l(k)}{\sum_{l=1}^{M_{ij}} \mu_{ij}^l(\boldsymbol{x}_{ij}(k))} = \sum_{l=1}^{M_{ij}} \mu_{ij}^l(\boldsymbol{x}_{ij}(k)) \cdot y_i^l(k) \tag{2.3}$$

where $\mu_{ij}^l(\boldsymbol{x}_{ij}(k))$ is the fuzzy membership function of $\boldsymbol{x}_{ij}(k)$ in fuzzy cluster C_{ij}^l that $0 \leq \mu_{ij}^l(\boldsymbol{x}_{ij}(k)) \leq 1$ and $\sum_{l=1}^{M_{ij}} \mu_{ij}^l(\boldsymbol{x}_{ij}(k)) = 1$.

The input–output data pairs of loop $y_i - u_j$ can be denoted as $\boldsymbol{z}_{ij}(k) = [\boldsymbol{x}_{ij}(k) \quad y_i(k)]$, $k = 1, \cdots, N_{ij}$, where N_{ij} is the number of data pairs sampled from individual loop $y_i - u_j$. These data pairs are divided into M_{ij} fuzzy clusters: $\left\{C_{ij}^1, C_{ij}^2, \cdots, C_{ij}^{M_{ij}}\right\}$, then $f_{TS,ij}$ is correspondingly characterized by M_{ij} fuzzy rules: $\left\{R^1, R^2, \cdots, R^{M_{ij}}\right\}$. A method is introduced here to construct Type–1 T–S fuzzy model

as in Eq. (2.2). In this method, for antecedents, Gustafson–Kessel (G–K) clustering algorithm [48], which employs the adaptive distance norm to detect clusters of different geometrical shapes, is used to classify the data pairs. And for consequents, least square method is adopted to identify the parameters of the local linear polynomials. The detailed steps are given as follows:

1. Randomly initialize a fuzzy membership matrix U_{ij}^{0} for the data samples

$$U_{ij}^{0}=\left[\mu_{ij}^{0,l}(\boldsymbol{z}_{ij}(k))\right]_{M_{ij}\times N_{ij}}=\begin{bmatrix}\mu_{ij}^{0,1}(\boldsymbol{z}_{ij}(1)) & \mu_{ij}^{0,1}(\boldsymbol{z}_{ij}(2)) & \cdots & \mu_{ij}^{0,1}(\boldsymbol{z}_{ij}(N_{ij}))\\ \mu_{ij}^{0,2}(\boldsymbol{z}_{ij}(1)) & \mu_{ij}^{0,2}(\boldsymbol{z}_{ij}(2)) & \cdots & \mu_{ij}^{0,2}(\boldsymbol{z}_{ij}(N_{ij}))\\ \vdots & \vdots & \ddots & \vdots\\ \mu_{ij}^{0,M_{ij}}(\boldsymbol{z}_{ij}(1)) & \mu_{ij}^{0,M_{ij}}(\boldsymbol{z}_{ij}(2)) & \cdots & \mu_{ij}^{0,M_{ij}}(\boldsymbol{z}_{ij}(N_{ij}))\end{bmatrix} \quad (2.4)$$

where $0\le\mu_{ij}^{0,l}(\boldsymbol{z}_{ij}(k))\le 1$ denotes the initialized fuzzy membership value of $\boldsymbol{z}_{ij}(k)=[\boldsymbol{x}_{ij}(k)\quad y_i(k)]$ in lth cluster, and $\sum_{l=1}^{M_{ij}}\mu_{ij}^{0,l}(\boldsymbol{z}_{ij}(k))=1$ for $k=1,\cdots,N_{ij}$.

2. Based on U_{ij}^{0}, the center of the lth cluster, denoted by $\boldsymbol{z}_{c,ij}^{l}$ $(l=1,\cdots,M_{ij})$ can be calculated by

$$\boldsymbol{z}_{c,ij}^{l}=\frac{\sum_{k=1}^{N_{ij}}\boldsymbol{z}_{ij}(k)\cdot\left(\mu_{ij}^{0,l}(\boldsymbol{z}_{ij}(k))\right)^{2}}{\sum_{k=1}^{N_{ij}}\left(\mu_{ij}^{0,l}(\boldsymbol{z}_{ij}(k))\right)^{2}} \quad (2.5)$$

where $\boldsymbol{z}_{c,ij}^{l}=[\boldsymbol{x}_{c,ij}^{l}\quad y_{c,i}^{l}]$, $\boldsymbol{x}_{c,ij}^{l}$ is the center of input vectors and $y_{c,i}^{l}$ is the center of outputs in lth cluster.

3. Based on the centers $\boldsymbol{z}_{c,ij}^{l}$ $(l=1,\cdots,M_{ij})$, the fuzzy covariance matrix for the lth cluster, denoted by F^{l}, can be computed by

$$F^{l}=\frac{\sum_{k=1}^{N_{ij}}\left(\mu_{ij}^{0,l}(\boldsymbol{z}_{ij}(k))\right)^{2}\cdot\left(\boldsymbol{z}_{ij}(k)-\boldsymbol{z}_{c,ij}^{l}\right)^{T}\cdot\left(\boldsymbol{z}_{ij}(k)-\boldsymbol{z}_{c,ij}^{l}\right)}{\sum_{k=1}^{N_{ij}}\left(\mu_{ij}^{0,l}(\boldsymbol{z}_{ij}(k))\right)^{2}} \quad (2.6)$$

4. Each fuzzy cluster has its own norm–inducing matrix , denoted by A^{l}, which can

be obtained by

$$A^l = \det\left(F^l\right)^{1/(p+q+2)} \cdot \left(F^l\right)^{-1} \tag{2.7}$$

where $\det(\cdot)$ denotes the value of the determinant.

5. Based on A^l, the adaptive distance between $\boldsymbol{z}_{ij}(k)$ and $\boldsymbol{z}_{c,ij}^l$, denoted by $\bar{D}(\boldsymbol{z}_{ij}(k), \boldsymbol{z}_{c,ij}^l)$, can be yielded

$$\bar{D}(\boldsymbol{z}_{ij}(k), \boldsymbol{z}_{c,ij}^l) = \left(\boldsymbol{z}_{ij}(k) - \boldsymbol{z}_{c,ij}^l\right) \cdot A^l \cdot \left(\boldsymbol{z}_{ij}(k) - \boldsymbol{z}_{c,ij}^l\right)^T \tag{2.8}$$

6. Based on the adaptive distances $\bar{D}(\boldsymbol{z}_{ij}(k), \boldsymbol{z}_{c,ij}^l)$ $(l = 1, \cdots, M_{ij})$, the updated fuzzy membership of $\boldsymbol{z}_{ij}(k)$ in lth cluster C_{ij}^l can be calculated by

$$\mu_{ij}^l(\boldsymbol{z}_{ij}(k)) = \begin{cases} \dfrac{1}{\sum_{s=1}^{M_{ij}} \dfrac{\bar{D}(\boldsymbol{z}_{ij}(k), \boldsymbol{z}_{c,ij}^l)}{\bar{D}(\boldsymbol{z}_{ij}(k), \boldsymbol{z}_{c,ij}^s)}}, & \text{if} \quad \text{all } \bar{D}(\boldsymbol{z}_{ij}(k), \boldsymbol{z}_{c,ij}^s) \neq 0, \\ & s = 1, \cdots, M_{ij} \\ 0, & \text{if} \quad \text{any } \bar{D}(\boldsymbol{z}_{ij}(k), \boldsymbol{z}_{c,ij}^s) = 0, \\ & s = 1, \cdots, M_{ij}, s \neq l \\ 1, & \text{if} \quad \bar{D}(\boldsymbol{z}_{ij}(k), \boldsymbol{z}_{c,ij}^l) = 0 \end{cases} \tag{2.9}$$

then the updated fuzzy membership matrix can be obtained as: $U_{ij} = \left[\mu_{ij}^l(\boldsymbol{z}_{ij}(k))\right]_{M_{ij} \times N_{ij}}$.

7. Given a termination tolerance $\varepsilon > 0$, if $\left\|U_{ij} - U_{ij}^0\right\| < \varepsilon$, it means the data classification is satisfactory; otherwise, let $U_{ij}^0 = U_{ij}$, repeat Step 2–6.

8. Assign $\boldsymbol{z}_{ij}(k)$ to the cluster in which it has the largest fuzzy membership such that the data samples are divided into M_{ij} clusters. For each cluster, using least square algorithm to identify the coefficients of polynomial in consequents ($a_{ij,r}^l (r = 0, 1, \cdots, p)$ and $b_{ij,s}^l (s = 1, \cdots, q)$). The T–S fuzzy modeling is completed.

When given an new input $\boldsymbol{x}_{ij}(k)$ to the $f_{TS,ij}$, its membership $\mu_{ij}^l(\boldsymbol{x}_{ij}(k))$ in lth fuzzy rule can be calculated by

$$\mu_{ij}^{l}(\boldsymbol{x}_{ij}(k))=\begin{cases}\dfrac{1}{\sum_{s=1}^{M_{ij}}\dfrac{D(\boldsymbol{x}_{ij}(k),\boldsymbol{x}_{c,ij}^{l})}{D(\boldsymbol{x}_{ij}(k),\boldsymbol{x}_{c,ij}^{s})}}, & if \quad all \;\; D(\boldsymbol{x}_{ij}(k),\boldsymbol{x}_{c,ij}^{s})\neq 0, \\ & s=1,\cdots,M_{ij} \\ 0, & if \quad any \;\; D(\boldsymbol{x}_{ij}(k),\boldsymbol{x}_{c,ij}^{s})=0, \\ & s=1,\cdots,M_{ij},\ s\neq l \\ 1, & if \quad D(\boldsymbol{x}_{ij}(k),\boldsymbol{x}_{c,ij}^{l})=0 \end{cases} \tag{2.10}$$

where $D(\boldsymbol{x}_{ij}(k),\boldsymbol{x}_{c,ij}^{l})=\left(\boldsymbol{x}_{ij}(k)-\boldsymbol{x}_{c,ij}^{l}\right)\cdot\left(\boldsymbol{x}_{ij}(k)-\boldsymbol{x}_{c,ij}^{l}\right)^{T}$. And then the output of the T–S fuzzy model can be obtained by Eq. (2.3).

Remark 2.1: The operating condition range that a T–S fuzzy model can cover is determined by the range that the data sampled from the process. To guarantee the performance of fuzzy–model–based controller, the data pairs should be sampled from the entire operating range of the process. And the selection of fuzzy rule number depends on the process properties, the operating range and the precision requirement, etc. The minimal number that can satisfy the demand for accuracy should be chosen such that the computational complexity in the following fuzzy model based studies can be minimized.

2.3 Type–2 T–S fuzzy modeling

When there are a large number of uncertainties that the Type–1 fuzzy model may not be able to fully handle, Type–2 fuzzy model can be used to describe the process. Type–2 fuzzy set was proposed based on a concept of “Words mean different things to different people” [40]. Its examples are given in Fig. 2.2. The fuzzy membership grade of an element in a Type–2 fuzzy set can be considered as a Type–1 fuzzy set that includes primary and secondary memberships. In the left side of Fig. 2.2, the perpendicular width of the “footprint” denotes the range of primary memberships, and the color depth of the “footprint” characterizes the values of secondary memberships: lighter color means smaller value and darker means larger. Part (a) of Fig. 2.2 is an example of general Type–2 fuzzy set. When all the secondary membership values are 1, which means the primary memberships are elements of an interval Type–1 fuzzy set

(can be called interval set, which is actually a classical set) as shown in Part (b) of Fig. 2.2, it becomes interval Type–2 fuzzy set [45]. It is noted that because of the increased fuzziness, the identification or the controller design using Type–2 fuzzy model require much more computational cost than that using Type–1 fuzzy model. In order to reduce the cost, the majority of existing Type–2 fuzzy methods for controller designs are developed based on interval Type–2 fuzzy model because the computations associated with it are very manageable.

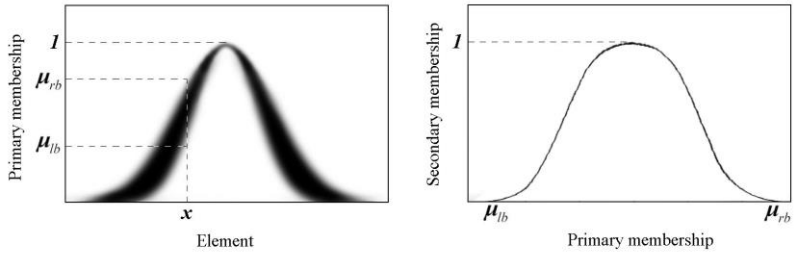

(*a*) A general Type-2 fuzzy set

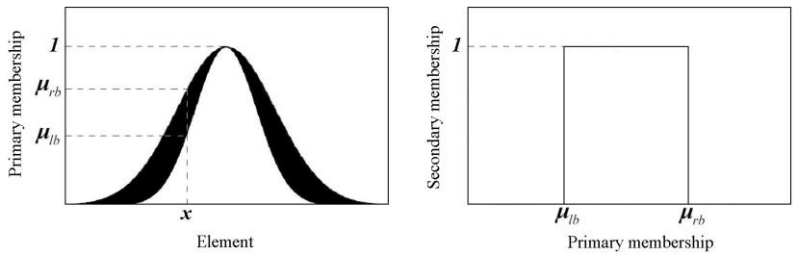

(*b*) An interval Type-2 fuzzy set

Figure 2.2 Type–2 fuzzy sets

For the Type–2 T–S fuzzy model, several results can be found [24, 49, 50] to demonstrate that it offers a significant improvement on its Type–1 counterpart in terms of robustness under the influence of uncertainty. There are three different structures of Type–2 T–S fuzzy model proposed in [47] as shown in Table 2.1, all of which can describe processes with inexact information better than Type–1 T–S fuzzy model [47].

Table 2.1 Type–2 T–S fuzzy models

Type–2 T–S fuzzy models	Model–I	Model–II	Model–III
Fuzzy sets in Antecedents	Type–2 fuzzy sets	Type–2 fuzzy sets	Type–1 fuzzy sets
Coefficients in Consequents	Type–1 fuzzy sets	Crisp numbers	Type–1 fuzzy sets

As described in Table 2.1, Model–I can describe the process with uncertainties more completely than Model–II and Model–III since it has additional degree of fuzziness in both antecedents and consequents. In this section a modeling method to construct Type–2 T–S fuzzy Model–I using interval Type–2 sets as the antecedents and interval sets as the parameters in consequents is introduced. Since Model–II and Model–III have a part (antecedent or consequent) same as that of Type–1 fuzzy model, combine this Type–2 T–S fuzzy Model–I construction method with the Type–1 T–S fuzzy modeling approach introduced in Section 2.2, it is easy to obtain Type–2 T–S fuzzy Model–II or Model–III for the process.

For loop $y_i - u_j$ in a $n \times n$ MIMO process, when its individual open–loop model $f_{TS,ij}$ is a Type–2 T–S fuzzy system, the "IF–THEN" fuzzy rules of $f_{TS,ij}$ can be expressed as

$$\begin{aligned} &R^l: \text{IF} \quad \boldsymbol{x}_{ij}(k) \quad is \quad \tilde{C}_{ij}^l \\ &\text{THEN} \quad \tilde{y}_i^l(k) = \tilde{a}_{ij,0}^l \cdot u_j(k-\tau_{ij}) + \tilde{a}_{ij,1}^l \cdot u_j(k-\tau_{ij}-1) + \cdots + \tilde{a}_{ij,p}^l \cdot u_j(k-\tau_{ij}-p) \\ &\qquad\qquad + \tilde{b}_{ij,1}^l \cdot y_i(k-1) + \cdots + \tilde{b}_{ij,q}^l \cdot y_i(k-q) \end{aligned} \tag{2.11}$$

where $\tilde{C}_{ij}^l$ ($l = 1, \cdots, M_{ij}$) denotes the lth interval Type–2 fuzzy set, the fuzzy membership of $\boldsymbol{x}_{ij}(k)$ in $\tilde{C}_{ij}^l$ is an interval that can be denoted as $\tilde{\mu}_{ij}^l(\boldsymbol{x}_{ij}(k)) = \left[\mu_{ij,lb}^l(\boldsymbol{x}_{ij}(k)), \quad \mu_{ij,rb}^l(\boldsymbol{x}_{ij}(k))\right]$, where $\mu_{ij,lb}^l(\boldsymbol{x}_{ij}(k))$ and $\mu_{ij,rb}^l(\boldsymbol{x}_{ij}(k))$ are the left and the right bounds. $\tilde{a}_{ij,r}^l$ ($r = 0, 1, \cdots, p$) and $\tilde{b}_{ij,s}^l$ ($s = 1, \cdots, q$) are also intervals with left and right bounds as $\tilde{a}_{ij,r}^l = \left[a_{ij,lb,r}^l, \quad a_{ij,rb,r}^l\right]$ ($r = 0, 1, \cdots, p$) and $\tilde{b}_{ij,s}^l = \left[b_{ij,lb,s}^l, \quad b_{ij,rb,s}^l\right]$ ($s = 1, \cdots, q$). And the output of lth fuzzy rule is $\tilde{y}_i^l(k) = \left[y_{i,lb}^l(k), \quad y_{i,rb}^l(k)\right]$ that can be calculated by [24]

$$\begin{cases} y_{i,lb}^l(k) = a_{ij,lb,0}^l \cdot u_j(k-\tau_{ij}) + a_{ij,lb,1}^l \cdot u_j(k-\tau_{ij}-1) + \cdots + a_{ij,lb,p}^l \cdot u_j(k-\tau_{ij}-p) \\ \qquad\qquad + b_{ij,lb,1}^l \cdot y_i(k-1) + \cdots + b_{ij,lb,q}^l \cdot y_i(k-q) \\ y_{i,rb}^l(k) = a_{ij,rb,0}^l \cdot u_j(k-\tau_{ij}) + a_{ij,rb,1}^l \cdot u_j(k-\tau_{ij}-1) + \cdots + a_{ij,rb,p}^l \cdot u_j(k-\tau_{ij}-p) \\ \qquad\qquad + b_{ij,rb,1}^l \cdot y_i(k-1) + \cdots + b_{ij,rb,q}^l \cdot y_i(k-q) \end{cases} \tag{2.12}$$

Based on these M_{ij} fuzzy rules, a type–reduced set can be obtained [24, 47] as

$$\tilde{y}_i(k) = f_{TS,ij}(\boldsymbol{x}_{ij}(k)) = \left[y_{i,lb}(k), \quad y_{i,rb}(k) \right] \tag{2.13}$$

An approach to calculating $y_{i,lb}(k)$ and $y_{i,rb}(k)$ is given in [47] which is an iterative process. In this thesis, a simpler way as follows is adopted for saving computations as

$$\begin{cases} y_{i,lb}(k) = \dfrac{\sum_{l=1}^{M_{ij}} \mu_{ij,lb}^{l}(\boldsymbol{x}_{ij}(k)) \cdot y_{i,lb}^{l}(k)}{\sum_{l=1}^{M_{ij}} \mu_{ij,lb}^{l}(\boldsymbol{x}_{ij}(k))} \\ y_{i,rb}(k) = \dfrac{\sum_{l=1}^{M_{ij}} \mu_{ij,rb}^{l}(\boldsymbol{x}_{ij}(k)) \cdot y_{i,rb}^{l}(k)}{\sum_{l=1}^{M_{ij}} \mu_{ij,rb}^{l}(\boldsymbol{x}_{ij}(k))} \end{cases} \tag{2.14}$$

Based on Eq. (2.14) the crisp output can be derived by defuzzifying the type–reduced set $\tilde{y}_i(k)$ as

$$y_i(k) = \frac{y_{i,lb}(k) + y_{i,rb}(k)}{2} \tag{2.15}$$

It should be noted that different from the fuzzy memberships in Type–1 fuzzy model, $\sum_{l=1}^{M_{ij}} \mu_{ij,lb}^{l}(\boldsymbol{x}_{ij}(k))$ and $\sum_{l=1}^{M_{ij}} \mu_{ij,rb}^{l}(\boldsymbol{x}_{ij}(k))$ in Type–2 fuzzy model may not equal 1.

Type–2 T–S fuzzy modeling method is an extension of the Type–1 fuzzy modeling method. The steps are presented as follows [24].

For antecedents: Based on the data samples $\boldsymbol{z}_{ij}(k) = [\boldsymbol{x}_{ij}(k) \quad y_i(k)]$ $(k = 1, \cdots, N_{ij})$, M_{ij} fuzzy cluster centers can be determined by G–K algorithm as introduced in Section 2.2. And then a crisp fuzzy membership $\mu_{ij}^{l}(\boldsymbol{z}_{ij}(k))$ can be calculated by Eq. (2.9) for each sample in *l*th cluster, which is utilized as the center of Type–2 fuzzy membership $\tilde{\mu}_{ij}^{l}(\boldsymbol{z}_{ij}(k))$ for $\boldsymbol{z}_{ij}(k)$ as

$$\mu_{ij}^{l}(\boldsymbol{z}_{ij}(k)) = \frac{\mu_{ij,lb}^{l}(\boldsymbol{z}_{ij}(k)) + \mu_{ij,rb}^{l}(\boldsymbol{z}_{ij}(k))}{2} \tag{2.16}$$

where

$$\begin{cases} \mu_{ij,lb}^{l}(\boldsymbol{z}_{ij}(k)) = \mu_{ij}^{l}(\boldsymbol{z}_{ij}(k)) - \Delta\mu_{ij}^{l} \\ \mu_{ij,rb}^{l}(\boldsymbol{z}_{ij}(k)) = \mu_{ij}^{l}(\boldsymbol{z}_{ij}(k)) + \Delta\mu_{ij}^{l} \end{cases} \tag{2.17}$$

where $\Delta\mu_{ij}^{l}$ denotes the radius of the interval $\tilde{\mu}_{ij}^{l}(\boldsymbol{z}_{ij}(k))$. The value of $\Delta\mu_{ij}^{l}$ represents the degree of influence from uncertainties. It can be determined by expert experience, or calculated from the data samples as follows.

Firstly, assign $\boldsymbol{z}_{ij}(k)\,(k=1,\cdots,N_{ij})$ to the cluster in which it has the largest fuzzy membership to divide data samples into M_{ij} clusters. In each cluster, choose R $(R>1)$ groups of data samples. The selection criterion is that the distances among the data in a group should be smaller than a given limit denoted by δ^1, which is $\left\|\boldsymbol{z}_{ij}(k)-\boldsymbol{z}_{ij}(s)\right\| < \delta^1$, where $\boldsymbol{z}_{ij}(k)$ and $\boldsymbol{z}_{ij}(s)$ are different samples in a group.

Secondly, in each group, define the maximum membership value as $\max_r(\mu_{ij}^{l})$ and the minimum as $\min_r(\mu_{ij}^{l})$, $r=1,\cdots,R$. And then $\Delta\mu_{ij}^{l}$ can be approximately evaluated by the following equation.

$$\Delta\mu_{ij}^{l} = \frac{1}{R}\sum_{r=1}^{R}\frac{\max_r(\mu_{ij}^{l}) - \min_r(\mu_{ij}^{l})}{2} \tag{2.18}$$

Afterwards the interval $\tilde{\mu}_{ij}^{l}(\boldsymbol{z}_{ij}(k))$ of $\boldsymbol{z}_{ij}(k)$ can be obtained by $\mu_{ij}^{l}(\boldsymbol{z}_{ij}(k))$ and $\Delta\mu_{ij}^{l}$ according to Eq. (2.17).

For consequents: In order to identify the bounds of $\tilde{a}_{ij,r}^{l}$ $(r=0,1,\cdots,p)$ and $\tilde{b}_{ij,s}^{l}$ $(s=1,\cdots,q)$, the fluctuating range of output y_i caused by the uncertainties, denoted by Δy_i $(\Delta y_i>0)$, needs to be assessed. One way to determine Δy_i is based on the expert experience, another way is based on the data samples as follows.

Firstly, in each cluster, choose R $(R>1)$ groups of data samples. The selection criterion is that the distances among the input vectors of the samples in a group are not

larger than a given limit denoted by δ^2, which means $\left\|\boldsymbol{x}_{ij}(k)-\boldsymbol{x}_{ij}(s)\right\|<\delta^2$, where $\boldsymbol{x}_{ij}(k)$ and $\boldsymbol{x}_{ij}(s)$ are different sampled input vectors in a group.

Secondly, in each group, define the maximum value of the output as $\max_r(y_i)$ and minimum as $\min_r(y_i)$, $r=1,\cdots,R$, and then the fluctuating range of the output, denoted by Δy_i, can be evaluated as

$$\begin{cases}\Delta y_i^l=\max\left\{\dfrac{\max_r(y_i)-\min_r(y_i)}{2}\right\}, & r=1,\cdots,R\\ \Delta y_i=\max\left\{\Delta y_i^l\right\}, & l=1,\cdots,M_{ij}\end{cases} \tag{2.19}$$

After obtain the value of Δy_i, two data pairs can be obtain from each sample $\boldsymbol{z}_{ij}(k)=[\boldsymbol{x}_{ij}(k)\quad y_i(k)]$ as

$$\begin{cases}\boldsymbol{z}_{ij,lb}(k)=[\boldsymbol{x}_{ij}(k)\quad y_{i,lb}(k)] & \text{where } y_{i,lb}(k)=y_i(k)-\Delta y_i\\ \boldsymbol{z}_{ij,rb}(k)=[\boldsymbol{x}_{ij}(k)\quad y_{i,rb}(k)] & \text{where } y_{i,rb}(k)=y_i(k)+\Delta y_i\end{cases} \tag{2.20}$$

Consequently, in each cluster, the coefficients in the two linear polynomials of Eq. (2.12) can be identified by least square algorithm based on $\boldsymbol{z}_{ij,lb}(k)$ and $\boldsymbol{z}_{ij,rb}(k)$ respectively, such that the following equations with intervals as its coefficients can be acquired for each fuzzy rule.

$$\begin{aligned}\tilde{y}_i^l(k)&=\left[y_{i,lb}^l(k),\quad y_{i,rb}^l(k)\right]\\ &=\left[a_{ij,lb,0}^l,\quad a_{ij,rb,0}^l\right]\cdot u_j(k-\tau_{ij})+\left[a_{ij,lb,1}^l,\quad a_{ij,rb,1}^l\right]\cdot u_j(k-\tau_{ij}-1)\\ &\quad+\cdots+\left[a_{ij,lb,p}^l,\quad a_{ij,rb,p}^l\right]\cdot u_j(k-\tau_{ij}-p)\\ &\quad+\left[b_{ij,lb,1}^l,\quad b_{ij,rb,1}^l\right]\cdot y_i(k-1)+\cdots+\left[b_{ij,lb,q}^l,\quad b_{ij,rb,q}^l\right]\cdot y_i(k-q)\end{aligned} \tag{2.21}$$

When given a new input $\boldsymbol{x}_{ij}(k)$ to the Type–2 T–S fuzzy model $f_{TS,ij}$, the center of its fuzzy membership in each fuzzy cluster can be calculated by Eq. (2.10), and the left and the right bounds can be determined with $\Delta\mu_{ij}^l$ ($l=1,\cdots,M_{ij}$) by Eq. (2.17). Afterwards, using Eq. (2.12), (2.14) and (2.15) to obtain the crisp output $y_i(k)$.

Remark 2.2: The value of a fuzzy membership should be in the interval [0, 1], which

means the left and the right bounds of $\tilde{\mu}_{ij}^{l}(\mathbf{z}_{ij}(k))$ should satisfy $0 \le \mu_{ij,lb}^{l}(\mathbf{z}_{ij}(k)) \le \mu_{ij,rb}^{l}(\mathbf{z}_{ij}(k)) \le 1$. Therefore, when the values of $\Delta\mu_{ij}^{l}$ $(l = 1, \cdots, M_{ij})$ are obtained, if $\mu_{ij}^{l}(\mathbf{z}_{ij}(k)) - \Delta\mu_{ij}^{l} < 0$, then let $\mu_{ij,lb}^{l}(\mathbf{z}_{ij}(k)) = 0$; If $\mu_{ij}^{l}(\mathbf{z}_{ij}(k)) + \Delta\mu_{ij}^{l} > 1$, then let $\mu_{ij,rb}^{l}(\mathbf{z}_{ij}(k)) = 1$.

Remark 2.3: With the increased fuzziness in the parameters, the Type–2 fuzzy model has stronger ability to describe uncertainties, while the computational cost of its modeling procedure and the following controller design is increased accordingly even though using interval Type–2 fuzzy model. Therefore, when the degree of uncertainty is in the range that traditional fuzzy models can fully handle, using Type–1 fuzzy model instead of Type–2 fuzzy model is able to reduce the complexity in both process modeling and controller design.

2.4 Simulation

Since the modeling method in this thesis is to construct T–S fuzzy models for individual loops which are SISO processes, in this section, the introduced Type–1 and Type–2 T–S fuzzy modeling methods are applied on a SISO nonlinear process to demonstrate and compare their accuracies. Consider the following nonlinear function,

$$\frac{\mathrm{d}y}{\mathrm{d}t} = \frac{36 \cdot y^2}{5 - u} + 21 \cdot u - (11 + u) \cdot y^2 \tag{2.22}$$

where the time delay is $\tau' = 0.1\text{sec}$, the sampling interval is $T = 0.1\text{sec}$, thus $\tau = \tau' / T = 1$. And the range of input is [0, 2]. Suppose there are disturbances with random values limited in [–0.8, 0.8] on the output, choose the values of *p* and *q* in Eq. (2.2) and Eq. (2.11) as $p = 0$ and $q = 1$, and then the sampled data pairs are in the form of $\mathbf{z}(k) = [\mathbf{x}(k) \quad y(k)]$, where $\mathbf{x}(k) = \begin{bmatrix} u(k-\tau) & y(k-1) \end{bmatrix}$. Collect 200 data pairs from Eq. (2.22), and set the number of fuzzy rules as 5. Based on these sampled data pairs, a Type–1 and a Type–2 T–S fuzzy model for this nonlinear process can be constructed using the modeling methods introduced in this chapter. The identified

centers of fuzzy clusters, denoted by $\boldsymbol{z}_c^l = [\boldsymbol{x}_c^l(k) \quad y_c^l(k)]$, where $\boldsymbol{x}_c^l = \left[u_c^l(k-\tau) \quad y_c^l(k-1)\right]$, ($l = 1, \cdots, 5$), are given in Table 2.2. The radius of the interval $\tilde{\mu}^l(\boldsymbol{x}(k))$ for Type–2 fuzzy model is $\Delta\mu^l = 0.12$ ($l = 1, \cdots, 5$). The identified parameters of the consequents in Type–1 and Type–2 T–S fuzzy models are presented in Table 2.3. The errors of two types of T–S models are illustrated in Fig. 2.3, and root–mean–square errors (RMSE) are employed to characterize the accuracies of the models, which are presented in Table 2.4. As can be seen in Fig. 2.3 and Table 2.4, Type–2 T–S fuzzy model can achieve higher degree of accuracy than Type–1 T–S fuzzy model when the process is under the influence of disturbance.

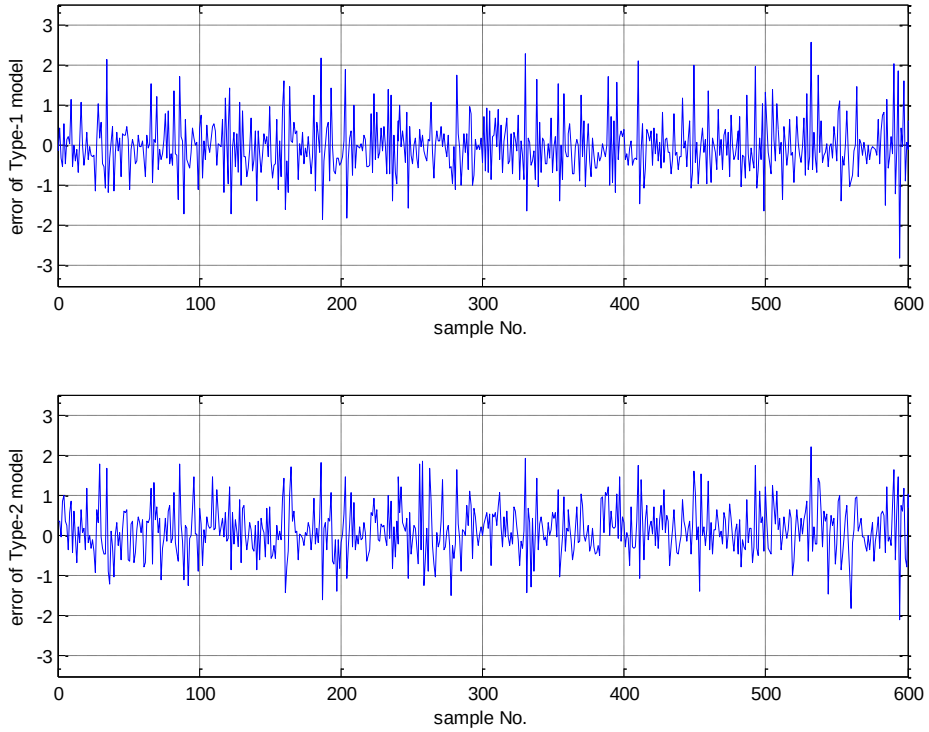

Figure 2.3 The errors of Type–1 and Type–2 fuzzy models

Table 2.2 The centers of fuzzy clusters for Eq. (2.22)

Centers of clusters C^l	No. of fuzzy clusters				
	$R^1(l=1)$	$R^2(l=2)$	$R^3(l=3)$	$R^4(l=4)$	$R^5(l=5)$
$u_c^l(k-\tau)$	0.4602	0.6735	1.5263	1.5188	0.7658
$y_c^l(k-1)$	2.3804	3.5853	3.2967	2.5627	2.5841
$y_c^l(k)$	3.0025	3.5697	2.4175	3.1873	2.2231

Table 2.3 The consequent parameters of Type–1 and Type–2 models for Eq. (2.22)

No. of	Type–1 model		Type–2 model			
Fuzzy rules	a_0^l	b_1^l	$a_{lb,0}^l$	$a_{rb,0}^l$	$b_{lb,1}^l$	$b_{rb,1}^l$
$R^1(l=1)$	1.6557	1.0463	1.5148	1.7966	0.8565	1.2361
$R^2(l=2)$	0.8756	0.7856	0.8418	0.9095	0.6621	0.9091
$R^3(l=3)$	0.4181	0.4963	0.2356	0.6006	0.4356	0.5569
$R^4(l=4)$	0.8647	0.7425	0.6150	1.1145	0.7031	0.7820
$R^5(l=5)$	0.8308	0.5737	0.6137	1.0479	0.4442	0.7031

Table 2.4 The RMSEs of Type–1 and Type–2 models for Eq. (2.22)

Type of T–S fuzzy model	RSME
Type–1	0.7153
Type–2	0.6596

2.5 Summary

In order to completely express the properties of individual loops in an MIMO process, in this chapter, a SISO T–S fuzzy model was established for each individual loop to form a fuzzy model matrix for an MIMO process. Both Type–1 and Type–2 T–S fuzzy modeling methods were introduced. Compared with a Type–1 fuzzy model, the Type–2 fuzzy model with increased fuzziness has stronger capability to describe the uncertainties and achieve higher accuracy, which has been proved by the simulation results. While the computational costs for the model construction and the following studies based on Type–2 fuzzy model are also increased. Which type of T–S fuzzy model should be chosen depends on the degree of uncertainties and the requirement of accuracy in the real applications. Based on the Type–1 and the Type–2 T–S fuzzy model matrices, useful information can be derived to carry out the studies in this thesis. In the next chapter, the interactions analysis and loop pairing to determine the optimal decentralized control configuration based on both Type–1 and Type–2 T–S fuzzy model matrices for an MIMO process are presented.

Chapter 3. Interaction analysis and loop pairing methods based on T–S fuzzy models for MIMO processes

3.1 Introduction

Although considerable sophisticated techniques have been proposed for multivariable control, decentralized control is more prevalent in industrial applications because it possesses outstanding advantages such as simplicity in design and implementation, fewer parameters for tuning, and low cost in maintenance [33, 34]. How to cope with the interactions among the loops in an MIMO process is the main problem for decentralized control to solve. The primary step for decentralized controller design is to pair the inputs and the outputs to obtain a control configuration where the paired loops have minimum crossing–coupled effects such that they can mostly resemble a group of SISO processes which are independent to each other, subsequently, the controller design and tuning can be largely facilitated by SISO control methods [35, 51].

Currently, a number of approaches for interaction analysis and loop pairing are available to determine the decentralized control structure. One of the most popular methods is the relative gain array (RGA) based criterion that was proposed by [52] in 1966. Generally, RGA–based pairing rules are used in conjunction with the Niederlinski index (NI) [53] to guarantee system stability. The RGA–NI based criterion only employs the open–loop steady–state gain matrix of an MIMO process to evaluate the interacting effects and determine control configuration. It is very simple in calculation and the scaling is independent because of its ratio nature [54]. However, since no dynamic properties of the process are considered, using only steady–state gain may result in incorrect pairing results, consequently, the control performance may be degraded. In order to overcome this limit, several loop pairing methods that using both steady–state gain and dynamic properties have been developed later. Such as the Dynamic RGA (DRGA) methods [55-59] which employ the transfer function matrix instead of the steady–state gain matrix for RGA calculation. And the effective relative

gain array (ERGA) based method [51] which adopts steady–state gain and bandwidth of the process transfer function element for interaction measurement. And the **relative normalized gain array (RNGA)** based criterion [35] uses **steady–state gain** matrix and **normalized integrated error** matrix of the process for loop pairing. Among these methods, RNGA based loop pairing criterion has prominent advantages: it gives a comprehensive description for dynamic interactions among individual loops without requiring the specification of the controllers, and it can provide unique loop pairing results. Moreover, it is very simple for researchers and engineers to understand and make pairing decisions in theoretic studies and real applications [35].

These criteria are all proposed and can be easily implemented based on transfer functions while cannot be directly applied to a fuzzy model that consists of "IF–THEN" rules and is intrinsically nonlinear. Multivariable fuzzy control requires the fuzzy–model–based method for interaction analysis and loop pairing. To the best of author's knowledge, very few published academic papers can be found in this area. Among the few, [36] has proposed a method to analyze the interactions among loops based on fuzzy basis function networks model using RGA. As described before, RGA based loop pairing rules may provide inaccurate results since no dynamic information of the process is included. Another problem in [36] is that it used a fuzzy modeling manner that n MISO fuzzy models were constructed for an $n \times n$ MIMO process, from which the characteristics of the individual loops may not be obtained. Furthermore, singleton rather than polynomial was adopted to be the consequents in the fuzzy rules, which may not have the capability to completely reflect the properties of the process.

In this chapter, based on the T–S fuzzy model matrix $\boldsymbol{F}_{TS}$ where a SISO model is constructed for each loop of an MIMO process as described in Chapter 2, the definitions of steady–state gain matrix and normalized integrated error matrix are given to present the RNGA based loop pairing rules. And the calculation procedures based on both Type–1 and Type–2 T–S fuzzy models are provided. The proposed method is simple in computation and gives an alternative to decide the control

configuration for an MIMO process where the exact mathematical models are difficult to derive. Compared with the existing fuzzy–model–based pairing approaches, the proposed method using RNGA criterion is able to give more appropriate control configurations since both steady and dynamic properties of the loops are considered. A simulation example is employed to compare the results obtained from T–S fuzzy models to that from accurate mathematical functions to demonstrate the simplicity, accuracy and effectiveness of the proposed method. And the comparison between Type–1 and Type–2 T–S fuzzy models is also provided to prove that Type–2 T–S fuzzy model can achieve more accurate results under the influence of uncertainties.

3.2 Loop pairing criteria

According to the definition proposed in [52], the relative gain for a loop in an MIMO process described by T–S fuzzy model can be defined as

$$\lambda_{TS,ij} = \frac{(\partial y_i / \partial u_j)_{\Delta u_{r\neq j}=0}}{(\partial y_i / \partial u_j)_{\Delta y_{r\neq i}=0}} \tag{3.1}$$

where $\lambda_{TS,ij}$ denotes the relative gain of loop $y_i - u_j$, $(\partial y_i / \partial u_j)_{\Delta u_{r\neq j}=0}$ is the steady–state gain of individual loop $y_i - u_j$, and $(\partial y_i / \partial u_j)_{\Delta y_{r\neq i}=0}$ is the process gain of the same loop when all other loops close. In order to calculate $\lambda_{TS,ij}$ from $f_{TS,ij}$, an operating point must be given due to the nonlinear nature of fuzzy model. Different operating points may result in different relative gains. Denote an operating point $\boldsymbol{x}_{0,ij}$ for loop $y_i - u_j$ of an $n \times n$ MIMO process as

$$\boldsymbol{x}_{0,ij} = [u_{0,j}(k_0 - \tau_{ij}) \quad \cdots \quad u_{0,j}(k_0 - \tau_{ij} - p) \quad y_{0,i}(k_0 - 1) \quad \cdots \quad y_{0,i}(k_0 - q)] \tag{3.2}$$

where $i, j = 1, \cdots, n$. Denote the steady–state gain of $f_{TS,ij}$ based on $\boldsymbol{x}_{0,ij}$ as $k_{TS,ij}$. In this thesis, the step response of the process is utilized to define the value of steady–state gain, which means $k_{TS,ij}$ is the gain in output of the process when the input is a unit step signal. Collect $k_{TS,ij}$ of each loop, the steady–state gain matrix of

$\boldsymbol{F}_{TS}$, denoted by $\boldsymbol{K}_{TS}$, can be formed as

$$\boldsymbol{K}_{TS} = \left[k_{TS,ij} \right]_{n\times n} = \begin{bmatrix} k_{TS,11} & k_{TS,12} & \cdots & k_{TS,1n} \\ k_{TS,21} & k_{TS,22} & \cdots & k_{TS,2n} \\ \vdots & \vdots & \ddots & \vdots \\ k_{TS,n1} & k_{TS,n2} & \cdots & k_{TS,nn} \end{bmatrix} \tag{3.3}$$

As the definition in Eq. (3.1), the relative gain for $f_{TS,ij}$ is the ratio of two gains, first, the steady–state gain of the isolated loop $y_i - u_j$, $k_{TS,ij}$, second, the steady–state gain in the same loop when all other loops are closed, denoted by $\hat{k}_{TS,ij}$.

$$\lambda_{TS,ij} = \frac{k_{TS,ij}}{\hat{k}_{TS,ij}} \tag{3.4}$$

Consequently, the RGA for $\boldsymbol{F}_{TS}$, denoted by $\boldsymbol{\Lambda}_{TS}$, is expressed as

$$\boldsymbol{\Lambda}_{TS} = \left[\lambda_{TS,ij} \right]_{n\times n} = \begin{bmatrix} \lambda_{TS,11} & \lambda_{TS,12} & \cdots & \lambda_{TS,1n} \\ \lambda_{TS,21} & \lambda_{TS,22} & \cdots & \lambda_{TS,2n} \\ \vdots & \vdots & \ddots & \vdots \\ \lambda_{TS,n1} & \lambda_{TS,n2} & \cdots & \lambda_{TS,nn} \end{bmatrix} \tag{3.5}$$

which can be calculated only using the steady–state gains of individual loops as [52]

$$\boldsymbol{\Lambda}_{TS} = \boldsymbol{K}_{TS} \otimes \boldsymbol{K}_{TS}^{-T} \tag{3.6}$$

where $\otimes$ indicates element–by–element product, and $\boldsymbol{K}_{TS}^{-T}$ is the transpose of the inverse of $\boldsymbol{K}_{TS}$.

Similar to the pairing rules for an MIMO process described by transfer function matrix, the RGA pairing rules for an MIMO process described by T–S fuzzy model matrix are that inputs and outputs in a decentralized fuzzy control system should be paired as follows.

(i) The paired RGA elements should be positive

(ii) The paired RGA elements should be closest to 1

(iii) Large RGA elements should be avoided.

By placing the paired loops at the diagonal position in $\boldsymbol{K}_{TS}$ through column swap, the Niederlinski index (NI) [53] for T–S fuzzy model, denoted by $\boldsymbol{N}_{TS}$, can be defined as

$$\boldsymbol{N}_{TS} = \frac{\det\left[\boldsymbol{K}_{TS}\right]}{\prod_{i=1}^{n} k_{TS,ii}} \tag{3.7}$$

where $\det\left[\boldsymbol{K}_{TS}\right]$ is the determinant of $\boldsymbol{K}_{TS}$ after column swap, and $k_{TS,ii}$'s ($i = 1, \cdots, n$) are the diagonal (paired) elements. NI provides a necessary condition for a stable paired system, that is: if the NI is negative, the processes will be unstable for all possible (any) values of controller parameters (i.e., it will be "structurally monotonic unstable") [35]. Therefore, an additional rule for RGA based loop pairing is

(iv) $\boldsymbol{N}_{TS} > 0$, for the paired structure.

The main advantage of RGA–NI based loop pairing criterion is that it is simple in calculation as it only depends on the steady–state gain matrix, which is generally easy to compute. However, a potential weakness of this criterion is the same fact that it only uses the steady–state gains which based on the assumption of perfect loop control to determine loop pairing, and no dynamic information of the process is considered. In order to make more accurate and effective evaluation of control–loop interactions, the normalized integrated error, which can be used to represent dynamic property of a process, is included into the assessment of interacting effects. The concept of normalized integrated error is introduced as follows.

Normalized Integrated Error: Normalized integrated error is the normalized sum of the errors between the steady–state value and the outputs of a process. Same as that of the definition of $k_{TS,ij}$, the normalized integrated error of $y_i - u_j$ based on the T–S fuzzy model, denoted by $e_{TS,ij}$, is defined from the step response of $y_i - u_j$ as

$$e_{TS,ij} = \sum_{r=0}^{\infty} \frac{y_i(\infty) - y_i(r \cdot T)}{k_{TS,ij}} \cdot T \tag{3.8}$$

where T is the sampling interval, $y_i(\infty) = y_i(k)\big|_{k\to\infty}$ is the steady–state output value

when the input is a unit step signal. And $y_i(r \cdot T)$ is the output at the *r*th sample time of $f_{TS,ij}$. Normalized integrated error is directly related to the process dynamics since it reflects the response speed of the y_i to u_j. Smaller absolute value of $e_{TS,ij}$ indicates that this loop has fast response to the particular input, while larger one indicates the loop has slower response [35]. Note that $e_{TS,ij}$ of a real process is generally not equal to 0, thus in this thesis, it is assumed that $e_{TS,ij} \neq 0$. Two typical examples are given in Fig. 3.1, where the shaded area determines the value of $e_{TS,ij}$.

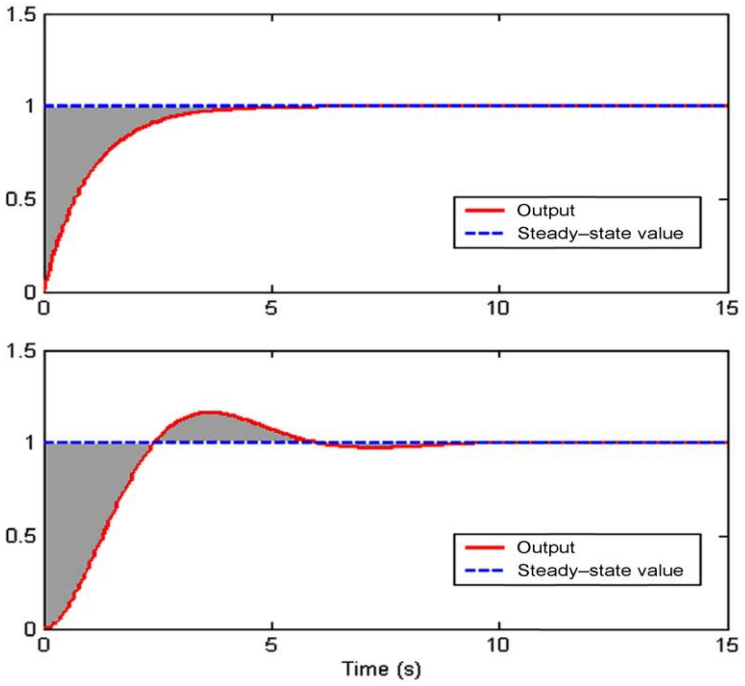

Figure 3.1 Typical waveforms for processes

For the overall process, the normalized integrated error matrix of $\boldsymbol{F}_{TS}$, denoted by $\boldsymbol{E}_{TS}$, is expressed as

$$\boldsymbol{E}_{TS} = \left[e_{TS,ij} \right]_{n \times n} = \begin{bmatrix} e_{TS,11} & e_{TS,12} & \cdots & e_{TS,1n} \\ e_{TS,21} & e_{TS,22} & \cdots & e_{TS,2n} \\ \vdots & \vdots & \ddots & \vdots \\ e_{TS,n1} & e_{TS,n2} & \cdots & e_{TS,nn} \end{bmatrix} \tag{3.9}$$

So far, two important factors from $f_{TS,ij}$ have been defined for interaction analysis:

(i) Steady–state gain $k_{TS,ij}$: it reflects the effect from u_j on the gain of y_i when the process reaches the steady–state condition;

(ii) Normalized integrated error $e_{TS,ij}$: it indicates the response speed of y_i to u_j.

In order to combine both steady–state gain and normalized integrated error for interaction measurement and loop pairing, the normalized gain of $f_{TS,ij}$, $k_{NTS,ij}$, as the ratio of steady–state gain to normalized integrated error, is utilized:

$$k_{NTS,ij} = \frac{k_{TS,ij}}{e_{TS,ij}} \tag{3.10}$$

Eq. (3.10) provides a total effects of u_j to y_i. For the overall process, the normalized gain matrix of $\boldsymbol{F}_{TS}$, denoted by $\boldsymbol{K}_{NTS}$, can be expressed as

$$\boldsymbol{K}_{NTS} = \left[k_{NTS,ij} \right]_{n\times n} = \begin{bmatrix} k_{NTS,11} & k_{NTS,12} & \cdots & k_{NTS,1n} \\ k_{NTS,21} & k_{NTS,22} & \cdots & k_{NTS,2n} \\ \vdots & \vdots & \ddots & \vdots \\ k_{NTS,n1} & k_{NTS,n2} & \cdots & k_{NTS,nn} \end{bmatrix} = \boldsymbol{K}_{TS} \odot \boldsymbol{E}_{TS} \tag{3.11}$$

where $\odot$ indicates the element–by–element division.

Denote the normalized gain of $f_{TS,ij}$ when all other loops close as $\hat{k}_{NTS,ij}$, $\hat{k}_{NTS,ij} = \hat{k}_{TS,ij} / \hat{e}_{TS,ij}$, and $\hat{e}_{TS,ij}$ is the normalized integrated error of loop $y_i - u_j$ when all other loops close. And then the relative normalized gain, $\phi_{TS,ij}$, can be defined as

$$\phi_{TS,ij} = \frac{k_{NTS,ij}}{\hat{k}_{NTS,ij}} \tag{3.12}$$

And then the RNGA, denoted by $\boldsymbol{\Phi}_{TS}$, is

$$\boldsymbol{\Phi}_{TS} = \left[\phi_{TS,ij} \right]_{n\times n} = \begin{bmatrix} \phi_{TS,11} & \phi_{TS,12} & \cdots & \phi_{TS,1n} \\ \phi_{TS,21} & \phi_{TS,22} & \cdots & \phi_{TS,2n} \\ \vdots & \vdots & \ddots & \vdots \\ \phi_{TS,n1} & \phi_{TS,n2} & \cdots & \phi_{TS,nn} \end{bmatrix} \tag{3.13}$$

which can be calculated by only using the information of individual loops as [35, 60, 61]

$$\boldsymbol{\Phi}_{TS} = \boldsymbol{K}_{NTS} \otimes \boldsymbol{K}_{NTS}^{-T} \tag{3.14}$$

The RNGA can be taken as a complement to RGA–NI based pairing criterion such that the dynamic property of the process can be included into the control structure decision. The updated pairing rules for an MIMO process are the following.

(i) All paired RGA and RNGA elements should be positive

(ii) The paired RNGA elements should be closest to 1

(iii) Large RNGA elements should be avoided

(iv) NI should be positive.

RNGA based loop pairing criterion provides important insights into the issue of control structure selection because it takes RNGA, RGA, and NI into consideration. The significances of this pairing method are:

- The pairing criterion is implemented on T–S fuzzy model constructed from data samples, which means the decision for control configuration can be made based on data samples without exactly knowing other information, such as the internal structure or parameters of the system. Therefore, it provides a simple and feasible way to evaluate the interactions among the loops and then determine an appropriate loop pairing structure.
- Compared with the existing loop pairing method based on fuzzy models in [36], the proposed method is based on the T–S fuzzy model matrix which can provide individual loop properties of an MIMO process, and using RNGA criterion that employs both steady–state and dynamic information to measure the interactions such that it is able to provide more accurate results for control–loop configuration.

3.3 Calculations based on Type–1 and Type–2 T–S fuzzy models

In this section, the calculations of RNGA loop pairing criterion based on both Type–1 and Type–2 T–S fuzzy models are presented.

1. Calculation based on Type–1 T–S fuzzy model

In the vicinity of the given operating point $\boldsymbol{x}_{0,ij}$ as in Eq. (3.2), nonlinear Type–1 T–S fuzzy model of Eq. (2.2) can be approximately represented by a linear function by letting $\mu_{ij}^{l}(\boldsymbol{x}_{ij}(k)) = \mu_{ij}^{l}(\boldsymbol{x}_{0,ij})$ $(l = 1, \cdots, M_{ij})$ as

$$\begin{aligned} y_i(k) &= f_{TS,ij}(\boldsymbol{x}_{ij}(k)) \\ &= a_{ij,0} \cdot u_j(k - \tau_{ij}) + \cdots + a_{ij,p} \cdot u_j(k - \tau_{ij} - p) + b_{ij,1} \cdot y_i(k-1) + \cdots + b_{ij,q} \cdot y_i(k-q) \end{aligned} \tag{3.15}$$

where $a_{ij,r} = \sum_{l=1}^{M_{ij}} \mu_{ij}^{l}(\boldsymbol{x}_{0,ij}) a_{ij,r}^{l}$ $(r = 0, 1, \cdots, p)$ and $b_{ij,s} = \sum_{l=1}^{M_{ij}} \mu_{ij}^{l}(\boldsymbol{x}_{0,ij}) b_{ij,s}^{l}$ $(s = 1, \cdots, q)$.

Through $\boldsymbol{Z}$–transform [62], Eq. (3.15) can be converted to a discrete transfer function as

$$G_{TS,ij}(z) = \frac{Y_i(z)}{U_j(z)} = \frac{a_{ij,0} + a_{ij,1} z^{-1} + \cdots + a_{ij,p} z^{-p}}{1 - (b_{ij,1} z^{-1} + b_{ij,2} z^{-2} + \cdots + b_{ij,q} z^{-q})} \cdot z^{-\tau_{ij}} \tag{3.16}$$

where $G_{TS,ij}(z)$ denotes the linearized function of loop $y_i - u_j$ in $\boldsymbol{Z}$–domain, $Y_i(z) = \boldsymbol{Z}[y_i]$ and $U_j(z) = \boldsymbol{Z}[u_j]$. Based on $G_{TS,ij}(z)$, the steady–state gain $k_{TS,ij}$ of loop $y_i - u_j$ at the operating point $\boldsymbol{x}_{0,ij}$ can be easily computed according to final value theorem as

$$\begin{aligned} k_{TS,ij} &= G_{TS,ij}(z)\big|_{z=1} = \left. \frac{a_{ij,0} + a_{ij,1} z^{-1} + \cdots + a_{ij,p} z^{-p}}{1 - (b_{ij,1} z^{-1} + b_{ij,2} z^{-2} + \cdots + b_{ij,q} z^{-q})} \cdot z^{-\tau_{ij}} \right|_{z=1} \\ &= \frac{a_{ij,0} + a_{ij,1} + \cdots + a_{ij,p}}{1 - (b_{ij,1} + b_{ij,2} + \cdots + b_{ij,q})} \end{aligned} \tag{3.17}$$

Note that using final value theorem of $\boldsymbol{Z}$–transform to calculate steady–state gain can greatly reduce the computational complexity when compared to the method proposed in [36].

According to the definition of normalized integrated error in Eq. (3.8), the input is a unit step signal that can be expressed by

$$
\begin{aligned}
&U_j(z) = \boldsymbol{Z}[u_j] \\
&= 1 + z^{-1} + z^{-2} + \cdots + z^{-r} + \cdots = \sum_{r=0}^{\infty} z^{-r} = \frac{z}{z-1}
\end{aligned}
\tag{3.18}
$$

Substitute Eq. (3.18) into Eq. (3.16), the output $Y_i(z) = \boldsymbol{Z}[y_i]$ becomes

$$
Y_i(z) = G_{TS,ij}(z) U_j(z) = \frac{a_{ij,0} + a_{ij,1} z^{-1} + \cdots + a_{ij,p} z^{-p}}{1 - (b_{ij,1} z^{-1} + b_{ij,2} z^{-2} + \cdots + b_{ij,q} z^{-q})} \cdot z^{-\tau_{ij}} \cdot \frac{z}{z-1} \tag{3.19}
$$

And according to the definition in $\boldsymbol{Z}$–transform, $Y_i(z)$ can be expressed as

$$
\begin{aligned}
Y_i(z) &= y_i(0 \cdot T) + y_i(T) z^{-1} + y_i(2 \cdot T) z^{-2} + \cdots + y_i(r \cdot T) z^{-r} + \cdots \\
&= \sum_{r=0}^{\infty} y_i(r \cdot T) z^{-r}
\end{aligned}
\tag{3.20}
$$

According to Eq. (3.20), Eq. (3.8) can be rewritten as

$$
\begin{aligned}
e_{TS,ij} &= \sum_{r=0}^{\infty} \frac{(y_i(\infty) - y_i(r \cdot T))}{k_{TS,ij}} \cdot T = \frac{\sum_{r=0}^{\infty} y_i(\infty) - \sum_{r=0}^{\infty} y_i(r \cdot T)}{k_{TS,ij}} \cdot T \\
&= \frac{y_i(\infty) \cdot \sum_{r=0}^{\infty} 1 - (y_i(0 \cdot T) + y_i(1 \cdot T) + \cdots + y_i(r \cdot T) + \cdots)}{k_{TS,ij}} \cdot T \\
&= \frac{y_i(\infty) \cdot (1 + z^{-1} + \cdots + z^{-r} + \cdots) - (y_i(0 \cdot T) + y_i(1 \cdot T) z^{-1} + \cdots + y_i(r \cdot T) z^{-r} + \cdots)}{k_{TS,ij}} \cdot T \Bigg|_{z=1} \\
&= \frac{y_i(\infty) \cdot \sum_{r=0}^{\infty} z^{-r} - Y_i(z)}{k_{TS,ij}} \cdot T \Bigg|_{z=1} = \left(\frac{y_i(\infty)}{k_{TS,ij}} \cdot \frac{z}{z-1} - \frac{Y_i(z)}{k_{TS,ij}} \right) \cdot T \Bigg|_{z=1}
\end{aligned}
\tag{3.21}
$$

For a stable process, when the input is a unit step signal, it is easy to learn that $y_i(\infty) = k_{TS,ij}$, thus Eq. (3.21) can be revised by

$$
e_{TS,ij} = \left(\frac{z}{z-1} - \frac{Y_i(z)}{k_{TS,ij}} \right) \cdot T \Bigg|_{z=1} \tag{3.22}
$$

Substituting Eq. (3.17) and (3.19) into Eq. (3.22) gives that

$$
\begin{aligned}
e_{TS,ij} &= \left(\frac{z}{z-1} - \frac{1-(b_{ij,1}+\cdots+b_{ij,q})}{a_{ij,0}+a_{ij,1}+\cdots+a_{ij,p}} \cdot \frac{a_{ij,0}+a_{ij,1}z^{-1}+\cdots+a_{ij,p}z^{-p}}{1-(b_{ij,1}z^{-1}+\cdots+b_{ij,q}z^{-q})} \cdot z^{-\tau_{ij}} \cdot \frac{z}{z-1} \right) \cdot T \Bigg|_{z=1} \\
&= \left(1 - \frac{1-(b_{ij,1}+\cdots+b_{ij,q})}{a_{ij,0}+a_{ij,1}+\cdots+a_{ij,p}} \cdot \frac{a_{ij,0}+a_{ij,1}z^{-1}+\cdots+a_{ij,p}z^{-p}}{1-(b_{ij,1}z^{-1}+\cdots+b_{ij,q}z^{-q})} \right) \cdot \frac{z}{z-1} \cdot T \Bigg|_{z=1} + \tau_{ij} \cdot T \\
&= \frac{\sum_{r=0}^{p} a_{ij,r}(1-z^{-r}) - \sum_{w=0}^{p}\sum_{s=1}^{q} a_{ij,w}b_{ij,s}\left(z^{-s}-z^{-w}\right)}{\left(a_{ij,0}+a_{ij,1}+\cdots+a_{ij,p}\right)\left(1-\left(b_{ij,1}z^{-1}+\cdots+b_{ij,q}z^{-q}\right)\right)} \cdot \frac{z}{z-1} \cdot T \Bigg|_{z=1} + \tau_{ij} \cdot T \\
&= \frac{\sum_{r=0}^{p} a_{ij,r}(1-z^{-r}) - \sum_{w=0}^{p}\sum_{s=1}^{q} a_{ij,w}b_{ij,s}z^{-\min(w,s)} \cdot \left(1-z^{-|w-s|}\right) \cdot \mathrm{sgn}\left(w-s\right)}{\left(a_{ij,0}+a_{ij,1}+\cdots+a_{ij,p}\right)\left(1-\left(b_{ij,1}z^{-1}+\cdots+b_{ij,q}z^{-q}\right)\right)} \cdot \frac{1}{1-z^{-1}} \cdot T \Bigg|_{z=1} + \tau_{ij} \cdot T \\
&= \frac{\sum_{r=0}^{p} a_{ij,r}\frac{1-z^{-r}}{1-z^{-1}} - \sum_{w=0}^{p}\sum_{s=1}^{q} a_{ij,w}b_{ij,s}z^{-\min(w,s)} \cdot \frac{1-z^{-|w-s|}}{1-z^{-1}} \cdot \mathrm{sgn}\left(w-s\right)}{\left(a_{ij,0}+a_{ij,1}+\cdots+a_{ij,p}\right)\left(1-\left(b_{ij,1}z^{-1}+\cdots+b_{ij,q}z^{-q}\right)\right)} \cdot T \Bigg|_{z=1} + \tau_{ij} \cdot T
\end{aligned}
$$

(3.23)

It is obvious that $(1-z^{-r})/(1-z^{-1}) = 1+z^{-1}+z^{-2}+\cdots+z^{-r+1}$, and $(1+z^{-1}+z^{-2}+\cdots+z^{-r+1})\big|_{z=1} = r$, therefore, it follows that

$$
\left.\frac{1-z^{-r}}{1-z^{-1}}\right|_{z=1} = r \text{, and } \left.\frac{1-z^{-|w-s|}}{1-z^{-1}}\right|_{z=1} = |w-s|
$$

Then Eq. (3.23) can be arranged to obtain

$$
e_{TS,ij} = \frac{\sum_{r=0}^{p} r a_{ij,r} - \sum_{w=0}^{p}\sum_{s=1}^{q} a_{ij,w} \cdot b_{ij,s} \cdot |w-s| \cdot \mathrm{sgn}\left(w-s\right)}{\left(a_{ij,0}+a_{ij,1}+\cdots+a_{ij,p}\right)\left(1-\left(b_{ij,1}+\cdots+b_{ij,q}\right)\right)} \cdot T + \tau_{ij} \cdot T \tag{3.24}
$$

Considering Eq. (3.17) and Eq. (3.24), the steady–state gain and normalized integrated error of each loop can be easily calculated from $f_{TS,ij}$ $(i, j = 1, \cdots, n)$. And then $\boldsymbol{K}_{TS}$ and $\boldsymbol{E}_{TS}$ can be formed to calculate $\boldsymbol{\Lambda}_{TS}$, $\boldsymbol{\Phi}_{TS}$ and $\boldsymbol{N}_{TS}$. Finally, the control configuration can be determined according to the rules of RNGA based loop pairing criterion.

2. Calculation based on Type–2 T–S fuzzy model

Compared with the calculation procedure based on Type–1 T–S fuzzy model, the calculation based on Type–2 T–S fuzzy model requires one more step of defuzzification since the parameters of Type–2 T–S fuzzy model are of increased fuzziness. Based on the fuzzy rules in Eq. (2.11), in the vicinity of the given operating point $\boldsymbol{x}_{0,ij}$ as in Eq. (3.2), the following type–reduced set of output can be obtained as

$$\begin{aligned}\tilde{y}_i(k) &= \left[y_{i,lb}(k), \quad y_{i,rb}(k) \right] \\ &= \tilde{a}_{ij,0} \cdot u_j(k-\tau_{ij}) + \tilde{a}_{ij,1} \cdot u_j(k-\tau_{ij}-1) + \cdots + \tilde{a}_{ij,p} \cdot u_j(k-\tau_{ij}-p) \\ &\quad + \tilde{b}_{ij,1} \cdot y_i(k-1) + \cdots + \tilde{b}_{ij,q} \cdot y_i(k-q).\end{aligned} \tag{3.25}$$

In Eq. (3.25), $\tilde{a}_{ij,r} = \left[a_{ij,lb,r}, \quad a_{ij,rb,r} \right]$ ($r = 0,1,\cdots,p$) and $\tilde{b}_{ij,s} = \left[b_{ij,lb,s}, \quad b_{ij,rb,s} \right]$ ($s = 1,\cdots,q$), where

$$a_{ij,lb,r} = \frac{\sum_{l=1}^{M_{ij}} \mu_{ij,lb}^{l}(\boldsymbol{x}_{0,ij}) \cdot a_{ij,lb,r}^{l}}{\sum_{l=1}^{M_{ij}} \mu_{ij,lb}^{l}(\boldsymbol{x}_{0,ij})}, \quad a_{ij,rb,r} = \frac{\sum_{l=1}^{M_{ij}} \mu_{ij,rb}^{l}(\boldsymbol{x}_{0,ij}) \cdot a_{ij,rb,r}^{l}}{\sum_{l=1}^{M_{ij}} \mu_{ij,rb}^{l}(\boldsymbol{x}_{0,ij})}, \text{ and}$$

$$b_{ij,lb,s} = \frac{\sum_{l=1}^{M_{ij}} \mu_{ij,lb}^{l}(\boldsymbol{x}_{0,ij}) \cdot b_{ij,lb,s}^{l}}{\sum_{l=1}^{M_{ij}} \mu_{ij,lb}^{l}(\boldsymbol{x}_{0,ij})}, \quad b_{ij,rb,s} = \frac{\sum_{l=1}^{M_{ij}} \mu_{ij,rb}^{l}(\boldsymbol{x}_{0,ij}) \cdot b_{ij,rb,s}^{l}}{\sum_{l=1}^{M_{ij}} \mu_{ij,rb}^{l}(\boldsymbol{x}_{0,ij})}, \text{ and}$$

$$\begin{aligned}y_{i,lb}(k) &= a_{ij,lb,0} \cdot u_j(k-\tau_{ij}) + a_{ij,lb,1} \cdot u_j(k-\tau_{ij}-1) + \cdots + a_{ij,lb,p} \cdot u_j(k-\tau_{ij}-p) \\ &\quad + b_{ij,lb,1} \cdot y_i(k-1) + \cdots + b_{ij,lb,q} \cdot y_i(k-q)\end{aligned}, \text{ and}$$

$$\begin{aligned}y_{i,rb}(k) &= a_{ij,rb,0} \cdot u_j(k-\tau_{ij}) + a_{ij,rb,1} \cdot u_j(k-\tau_{ij}-1) + \cdots + a_{ij,rb,p} \cdot u_j(k-\tau_{ij}-p) \\ &\quad + b_{ij,rb,1} \cdot y_i(k-1) + \cdots + b_{ij,rb,q} \cdot y_i(k-q)\end{aligned}.$$

And the following linear equation can be obtained by defuzzifying $\tilde{y}_i(k)$ in Eq. (3.25) according to the method presented in Eq. (2.15) as

$$\begin{aligned}y_i(k) &= \frac{y_{i,lb}(k) + y_{i,rb}(k)}{2} \\ &= a_{ij,0} \cdot u_j(k-\tau_{ij}) + \cdots + a_{ij,p} \cdot u_j(k-\tau_{ij}-p) + b_{ij,1} \cdot y_i(k-1) + \cdots + b_{ij,q} \cdot y_i(k-q)\end{aligned} \tag{3.26}$$

where $a_{ij,r} = (a_{ij,lb,r} + a_{ij,rb,r})/2$, $r = 0,1,\cdots, p$ and $b_{ij,s} = (b_{ij,lb,s} + b_{ij,rb,s})/2$, $s = 1,\cdots, q$. Eq. (3.26) can be used to approximately represent a Type–2 T–S fuzzy model $f_{TS,ij}$ in the area around $\boldsymbol{x}_{0,ij}$, and it can be converted to a discrete transfer function as the form in Eq. (3.16) by $\boldsymbol{Z}$–transform. Consequently, the steady–state gain $k_{TS,ij}$ and normalized integrated error $e_{TS,ij}$ of each loop can be easily calculated by using Eq. (3.17) and Eq. (3.24), and then $\boldsymbol{\Lambda}_{TS}$, $\boldsymbol{\Phi}_{TS}$ and $\boldsymbol{N}_{TS}$ can be calculated based on $\boldsymbol{K}_{TS}$ and $\boldsymbol{E}_{TS}$. Finally, the control structure can be determined in accordance with the rules of RNGA based loop paring criterion.

Eq. (3.17) and Eq. (3.24) seem to be complicated but actually very simple in real applications since the number of p and q are generally not large. For example, when $p = 0$ and $q = 1$, the Type–1 and the Type–2 T–S fuzzy rules are in the form of

$$\begin{aligned} &R^l : \text{IF} \quad \boldsymbol{x}_{ij}(k) \quad is \quad C_{ij}^l \\ &\text{THEN} \quad y_i^l(k) = a_{ij,0}^l \cdot u_j(k-\tau_{ij}) + b_{ij,1}^l \cdot y_i(k-1) \end{aligned}$$

and

$$\begin{aligned} &R^l : \text{IF} \quad \boldsymbol{x}_{ij}(k) \quad is \quad \tilde{C}_{ij}^l \\ &\text{THEN} \quad \tilde{y}_i^l(k) = \tilde{a}_{ij,0}^l \cdot u_j(k-\tau_{ij}) + \tilde{b}_{ij,1}^l \cdot y_i(k-1) \end{aligned}$$

In this case, $k_{TS,ij}$ and $e_{TS,ij}$ can be simply calculated by:

$$k_{TS,ij} = \frac{a_{ij,0}}{1-b_{ij,1}}, \quad e_{TS,ij} = \frac{b_{ij,1}}{1-b_{ij,1}} \cdot T + \tau_{ij} \cdot T$$

3.4 Simulation

In this section, both Type–1 and Type–2 T–S fuzzy model matrices are constructed for an MIMO process with bounded disturbance, and then the pairing structures are determined based on these two types of fuzzy models by using RNGA based loop pairing criterion. The comparisons are presented to demonstrate that both Type–1 and Type–2 fuzzy models can provide accurate pairing structure, and the results obtained

from Type–2 models are with smaller errors than that from Type–1 models when the process is under the influence of uncertainties.

Consider an $n \times n$ process where $n = 3$ as described in [35], its mathematical transfer function matrix is as follows.

$$\boldsymbol{G}(s) = \begin{bmatrix} \dfrac{e^{-9s}}{6s^2+17s+1} & \dfrac{-9e^{-5s}}{s^2+4s+1} & \dfrac{13e^{-3s}}{3s^2+35s+1} \\ \dfrac{-5e^{-13s}}{2s^2+19s+1} & \dfrac{8e^{-2s}}{s^2+33s+1} & \dfrac{7e^{-5s}}{s^2+3s+1} \\ \dfrac{-16e^{-3s}}{s^2+5s+1} & \dfrac{3e^{-7s}}{s^2+14s+1} & \dfrac{e^{-11s}}{3s^2+25s+1} \end{bmatrix} \tag{3.27}$$

Its accurate steady–state gain matrix, denoted by $\boldsymbol{K} = \left[k_{ij} \right]_{3\times3}$, and accurate normalized integrated error matrix, denoted by $\boldsymbol{E} = \left[e_{ij} \right]_{3\times3}$ are [35]

$$\boldsymbol{K} = \begin{bmatrix} 1 & -9 & 13 \\ -5 & 8 & 7 \\ -16 & 3 & 1 \end{bmatrix}, \text{ and } \boldsymbol{E} = \begin{bmatrix} 26 & 9 & 38 \\ 32 & 35 & 8 \\ 8 & 21 & 36 \end{bmatrix}$$

And then RGA $\boldsymbol{\Lambda} = \left[\lambda_{ij} \right]_{3\times3}$ and RNGA $\boldsymbol{\Phi} = \left[\phi_{ij} \right]_{3\times3}$ can be obtained as

$$\boldsymbol{\Lambda} = \begin{bmatrix} -0.0054 & 0.3981 & 0.6073 \\ -0.0992 & 0.6912 & 0.4080 \\ 1.1046 & -0.0893 & -0.0153 \end{bmatrix}, \text{ and } \boldsymbol{\Phi} = \begin{bmatrix} -0.0024 & 0.9237 & 0.0787 \\ -0.0063 & 0.0829 & 0.9235 \\ 1.0088 & -0.0066 & -0.0022 \end{bmatrix}$$

The loop pairing structure determined by RNGA based criterion is $y_1 - u_2 \,/\, y_2 - u_3 \,/\, y_3 - u_1$, where NI is $\boldsymbol{N} = 2.3998$.

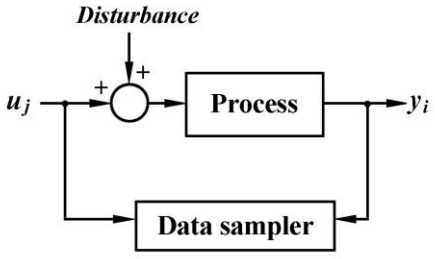

Figure 3.2 AN MIMO process with disturbances

Suppose there are disturbances added to the process when collecting data samples of individual loops as shown in Fig. 3.2, and the disturbances are random but bounded in

$[-0.3,\ 0.3]$. Choose $p=0$, $q=1$ and sampling interval $T=1\text{sec}$. For loop y_i-u_j, sample the data pairs as $\mathbf{z}_{ij}(k)=[\boldsymbol{x}_{ij}(k)\quad y_i(k)]$, where $\boldsymbol{x}_{ij}(k)=[u_j(k-\tau_{ij})\quad y_i(k-1)]$, $N_{ij}=300$. The constructed Type–1 and Type–2 T–S fuzzy models are presented in Appendix A. The operating points are $\boldsymbol{x}_{0,ij}=[u_{0,j}(k_0-\tau_{ij})\quad y_{0,i}(k_0-1)]=[0\quad 0]$ for $i,j=1,2,3$, from the Type–1 fuzzy models, the following results can be derived as

$$\boldsymbol{K}_{TS}=\begin{bmatrix} 1.0720 & -8.4602 & 8.2669 \\ -5.2928 & 8.1431 & 7.7005 \\ -15.0900 & 4.3773 & 1.0015 \end{bmatrix},\quad \boldsymbol{E}_{TS}=\begin{bmatrix} 28.2977 & 7.8913 & 19.4790 \\ 22.6081 & 48.5019 & 8.9191 \\ 7.2556 & 21.4491 & 30.3054 \end{bmatrix}$$

$$\boldsymbol{\Lambda}_{TS}=\begin{bmatrix} -0.0158 & 0.5407 & 0.4751 \\ -0.1362 & 0.5905 & 0.5457 \\ 1.1520 & -0.1312 & -0.0208 \end{bmatrix},\quad \boldsymbol{\Phi}_{TS}=\begin{bmatrix} -0.0032 & 0.9404 & 0.0628 \\ -0.0140 & 0.0728 & 0.9412 \\ 1.0172 & -0.0132 & -0.0040 \end{bmatrix}$$

According to these results, the pairing structure can be determined by RNGA based criterion as: $y_1-u_2\,/\,y_2-u_3\,/\,y_3-u_1$, where NI is $\boldsymbol{N}_{TS}=1.7650$.

From the Type–2 fuzzy models, the following results can be obtained as

$$\boldsymbol{K}_{TS}=\begin{bmatrix} 1.0228 & -8.7498 & 8.6927 \\ -5.5137 & 7.5198 & 8.0004 \\ -15.4664 & 4.0303 & 1.0440 \end{bmatrix},\quad \boldsymbol{E}_{TS}=\begin{bmatrix} 25.1327 & 7.9222 & 22.5794 \\ 24.1025 & 42.3875 & 8.7584 \\ 7.3578 & 21.2531 & 32.4872 \end{bmatrix}$$

$$\boldsymbol{\Lambda}_{TS}=\begin{bmatrix} -0.0137 & 0.5656 & 0.4481 \\ -0.1334 & 0.5583 & 0.5751 \\ 1.1471 & -0.1239 & -0.0232 \end{bmatrix},\quad \boldsymbol{\Phi}_{TS}=\begin{bmatrix} -0.0031 & 0.9462 & 0.0568 \\ -0.0111 & 0.0644 & 0.9467 \\ 1.0142 & -0.0106 & -0.0035 \end{bmatrix}$$

According to these results, the pairing structure can be determined by RNGA based criterion as: $y_1-u_2\,/\,y_2-u_3\,/\,y_3-u_1$, where NI is $\boldsymbol{N}_{TS}=1.6858$.

As demonstrated in the above results, both Type–1 and Type–2 T–S fuzzy models built based on the data with inexact information can give accurate pairing structures. In order to further compare the degrees of accuracy between these two types of fuzzy model, the mean absolute error (MAE) index is employed to show their errors. Since the RGA, RNGA and NI are all calculated from $\boldsymbol{K}_{TS}$ and $\boldsymbol{E}_{TS}$, we compare MAE of

$\boldsymbol{K}_{TS}$: $k_{MAE} = \sum_{i=1}^{n}\sum_{j=1}^{n}\left|k_{TS,ij} - k_{ij}\right| / n^2$, and MAE of $\boldsymbol{E}_{TS}$: $e_{MAE} = \sum_{i=1}^{n}\sum_{j=1}^{n}\left|e_{TS,ij} - e_{ij}\right| / n^2$

between Type–1 and Type–2 T–S fuzzy models. The results are given in Table 3.1.

Table 3.1 The comparisons of MAEs

Type of fuzzy model	k_{MAE}	e_{MAE}
Type–1	0.9745	5.8476
Type–2	0.9092	4.2019

As shown in Table 3.1, both k_{MAE} and e_{MAE} of Type–2 fuzzy model are less than that of Type–1 fuzzy model, which demonstrates that Type–2 fuzzy model can yield more accurate results than Type–1 fuzzy model under the influence of uncertainties.

3.5 Summary

This chapter introduced RNGA based loop pairing criterion for MIMO processes described by T–S fuzzy models, and the simple calculation procedures based on both Type–1 and Type–2 T–S fuzzy models were presented. The proposed method can analyze the interactions between process inputs and outputs and then pair the loops to determine the decentralized control configuration without requiring accurate mathematical functions of an MIMO process. Compared with the existing fuzzy–model–based approaches which only use steady–state gain for loop pairing, this method can provide a more proper control structure since both steady and dynamic information of the process were considered. The simulation demonstrated that under the influence of uncertainties, both Type–1 and Type–2 fuzzy models can give accurate control configuration, while the errors of the calculated results of Type–2 fuzzy models were smaller than that of Type–1 fuzzy models. Since this pairing criterion can quantify the interactions among the loops, an effective fuzzy model can be formed by incorporating the interactions into the individual fuzzy model for a certain paired loop. Effective fuzzy model is a simple and practical way without using extra terms to express the interacting results for decentralized controller design, which will be elaborated in the next chapter.

Chapter 4. Effective T–S fuzzy model for decentralized control of MIMO processes

4.1 Introduction

In decentralized controller design for an MIMO process, the performance of one loop cannot be assessed without the information of other loops since controllers interact with each other [37]. In the existing T–S fuzzy model based decentralized control methods, extra terms are added to the individual open–loop model to characterize the interacting effects as in Eq. (1.1). Since the extra terms will increase the complexity in both modeling and controller design for an MIMO process of an MER system, in this chapter, an alternative, called effective model, is presented to describe the interacting effects instead of using extra terms.

Effective models are used to describe a group of non–interacting equivalent SISO processes which are built based on the control–loops to represent an MIMO process for decentralized controller design. By virtue of different loop pairing criteria, recently, a number of effective model methods based on transfer functions, called effective transfer functions (ETF) have been developed. [37] proposed a method using dynamic relative gain to derive ETFs for equivalent open–loop processes without prior knowledge of controller dynamic properties, which is simple and effective for low–dimensional MIMO system but conservative for high–dimensional system due to the inevitable modeling errors in formulation. [63] presented an ETF method in terms of effective relative gain array (ERGA) for MIMO processes, several examples demonstrated its simplicity and effectiveness in both low and high dimensional system. The disadvantage of this method is that the computation of ERGA requires the value of critical frequency of each individual loop. Different criteria for selecting critical frequency points may result in different ERGAs, and then causes uncertainties in pairing structures and the ETFs. In order to overcome this weakness, the approaches using RNGA to obtain ETFs for controller designs were later developed [38, 64] which can obtain unique results of control structure and effective models for controller

designs, and achieve good performance with less computational complexity.

To the best of the author's knowledge, no published studies regarding loop pairing criterion based effective model have been found in fuzzy area. Because of the intrinsic nonlinearity and special structure of fuzzy models, the existing ETF methods are not directly applicable to fuzzy control systems. In order to facilitate decentralized fuzzy control, in this chapter, based on the T–S fuzzy model matrices introduced in Chapter 2 and the RNGA pairing criterion presented in Chapter 3, an **effective T–S fuzzy model (ETSM)** method is proposed. For a paired loop in an MIMO process, an ETSM can be obtained by simply scaling the coefficients of its individual open–loop T–S fuzzy model according to the quantified interactions provided by RNGA criterion, and the scaled coefficients are further revised to adapt different interacting cases. ETSM can reflect the interacting effects caused by all other closed–loops on both steady and dynamic properties through a simple and direct manner while the integrity of control system can be maintained. The consequents of an ETSM also have the same linear structure as that of its individual T–S fuzzy model. Hence, based on the ETSMs of paired loops, the local controllers of a decentralized control system can be independently designed using linear SISO control algorithms through parallel distributed compensation (PDC) [15]. Compared with the existing decentralized fuzzy control approaches, no extra terms to characterize interactions are required in the ETSM method, which can save considerable costs in modeling and controller design. When the pairing structure changes as the operating conditions vary in a nonlinear process, the ETSMs can be quickly updated since the calculation is simple, which makes it applicable in real–time controls. Compared with the ETF methods, ETSM can work without knowing exact mathematical functions of the process and provides a basis to develop robust controllers since fuzzy system is powerful to handle the uncertainties. In the simulation section, the performances of decentralized controllers based on ETFs and ETSMs for an MIMO process with and without parametric uncertainties are presented and compared to demonstrate the superiorities of the proposed ETSM method over its ETF counterpart. And the comparisons between

Type–1 and Type–2 ETSMs are also given to show that Type–2 fuzzy system can achieve more robust results under the influence of uncertainty.

4.2 ETSM

Denote the ETSM for loop $y_i - u_j$ in an $n \times n$ MIMO process as $\hat{f}_{TS,ij}$. At a certain operating condition, suppose the optimal control configuration has been determined. Since the control–loop when other loops close has similar frequency properties with that when other loops open if the process is well paired [63, 65], it is reasonable to let the structure and part of parameters of $\hat{f}_{TS,ij}$ be same as that of $f_{TS,ij}$. For Type–1 ETSM, the fuzzy rules of $\hat{f}_{TS,ij}$ can be expressed as

$$\begin{aligned} &R^l: \text{IF} \quad \boldsymbol{x}_{ij}(k) \quad is \quad C_{ij}^l \\ &\text{THEN} \quad y_i^l(k) = \hat{a}_{ij,0}^l \cdot u_j(k-\hat{\tau}_{ij}) + \hat{a}_{ij,1}^l \cdot u_j(k-\hat{\tau}_{ij}-1) + \cdots + \hat{a}_{ij,p}^l \cdot u_j(k-\hat{\tau}_{ij}-p) \\ &\qquad\qquad + b_{ij,1}^l \cdot y_i(k-1) + \cdots + b_{ij,q}^l \cdot y_i(k-q) \end{aligned} \tag{4.1}$$

where $\hat{a}_{ij,r}^l$ ($r = 0,1,\cdots,p$, $l = 1,\cdots,M_{ij}$) and $\hat{\tau}_{ij}$ are the different parameters from its original Type–1 T–S fuzzy model as in Eq. (2.2). And for Type–2 ETSM, the fuzzy rules of $\hat{f}_{TS,ij}$ can be expressed as

$$\begin{aligned} &R^l: \text{IF} \quad \boldsymbol{x}_{ij}(k) \quad is \quad \tilde{C}_{ij}^l \\ &\text{THEN} \quad \tilde{y}_i^l(k) = \hat{\tilde{a}}_{ij,0}^l \cdot u_j(k-\hat{\tau}_{ij}) + \hat{\tilde{a}}_{ij,1}^l \cdot u_j(k-\hat{\tau}_{ij}-1) + \cdots + \hat{\tilde{a}}_{ij,p}^l \cdot u_j(k-\hat{\tau}_{ij}-p) \\ &\qquad\qquad + \tilde{b}_{ij,1}^l \cdot y_i(k-1) + \cdots + \tilde{b}_{ij,q}^l \cdot y_i(k-q) \end{aligned} \tag{4.2}$$

where $\hat{\tilde{a}}_{ij,r}^l = \left[\hat{a}_{ij,lb,r}^l, \quad \hat{a}_{ij,rb,r}^l \right]$ ($r = 0,1,\cdots,p$, $l = 1,\cdots,M_{ij}$) and $\hat{\tau}_{ij}$ are the different parameters from its original Type–2 T–S fuzzy model as in Eq. (2.11).

The quantified interactions from RNGA based pairing criterion can be utilized to calculate the parameters of ETSMs. The interacting effects on steady–state gain can be derived by relative gain $\lambda_{TS,ij}$, while the interacting effects on dynamic property can be obtained from both relative gain $\lambda_{TS,ij}$ and relative normalized gain $\phi_{TS,ij}$ as

$$\frac{\phi_{TS,ij}}{\lambda_{TS,ij}} = \frac{\hat{e}_{TS,ij}}{e_{TS,ij}} \equiv \gamma_{TS,ij} \tag{4.3}$$

where $\gamma_{TS,ij}$, defined as relative normalized integrated error, represents the normalized integrated error change of loop $y_i - u_j$ when other loops close. The relative normalized integrated error array, denoted by $\boldsymbol{\Gamma}_{TS}$, can be calculated as

$$\boldsymbol{\Gamma}_{TS} = \left[\gamma_{TS,ij} \right]_{n \times n} = \boldsymbol{\Phi}_{TS} \odot \boldsymbol{\Lambda}_{TS} \tag{4.4}$$

Based on $\lambda_{TS,ij}$ and $\gamma_{TS,ij}$, the approaches to obtain Type–1 and Type–2 ETSMs are given as follows.

1. Calculations to determine coefficients of Type–1 ETSM

According to Eq. (3.17), the steady–state gain $\hat{k}_{TS,ij}$ at the given operating point $\boldsymbol{x}_{0,ij}$ of Type–1 ETSM $\hat{f}_{TS,ij}$ in Eq. (4.1) can be calculated as

$$\hat{k}_{TS,ij} = \frac{\hat{a}_{ij,0} + \hat{a}_{ij,1} \cdots + \hat{a}_{ij,p}}{1 - (b_{ij,1} + b_{ij,2} + \cdots + b_{ij,q})} \tag{4.5}$$

where $\hat{a}_{ij,r} = \sum_{l=1}^{M_{ij}} \mu_{ij}^{l}(\boldsymbol{x}_{0,ij}) \hat{a}_{ij,r}^{l}$, $r = 0,1,\cdots,p$. Submitting Eq. (3.4) and Eq. (3.17) into Eq. (4.5), the following equation to can be obtained.

$$\hat{a}_{ij,r} = \frac{a_{ij,r}}{\lambda_{TS,ij}} \tag{4.6}$$

And then $\hat{a}_{ij,r}^{l}$ in Eq. (4.1) can be calculated by

$$\hat{a}_{ij,r}^{l} = \frac{a_{ij,r}^{l}}{\lambda_{TS,ij}} \tag{4.7}$$

According to Eq. (3.24), the normalized integrated error $\hat{e}_{TS,ij}$ of $\hat{f}_{TS,ij}$ can be calculated by

$$\hat{e}_{TS,ij} = \frac{\sum_{r=0}^{p} r\hat{a}_{ij,r} - \sum_{w=0}^{p}\sum_{s=1}^{q} \hat{a}_{ij,w} \cdot b_{ij,s} \cdot |w-s| \cdot \operatorname{sgn}(w-s)}{\left(\hat{a}_{ij,0} + \hat{a}_{ij,1} + \cdots + \hat{a}_{ij,p}\right)\left(1 - \left(b_{ij,1} + \cdots + b_{ij,q}\right)\right)} \cdot T + \hat{\tau}_{ij} \cdot T \tag{4.8}$$

By considering Eq. (4.6), Eq. (4.8) can be rewritten as

$$\hat{e}_{TS,ij} = \frac{\sum_{r=0}^{p} r \cdot \frac{a_{ij,r}}{\lambda_{TS,ij}} - \sum_{w=0}^{p}\sum_{s=1}^{q} \frac{a_{ij,w}}{\lambda_{TS,ij}} \cdot b_{ij,s} \cdot |w-s| \cdot \mathrm{sgn}(w-s)}{\left(\frac{a_{ij,1}}{\lambda_{TS,ij}} + \frac{a_{ij,2}}{\lambda_{TS,ij}} + \cdots + \frac{a_{ij,p}}{\lambda_{TS,ij}}\right)\left(1-\left(b_{ij,1}+\cdots+b_{ij,q}\right)\right)} \cdot T + \hat{\tau}_{ij} \cdot T$$
$$= \frac{\sum_{r=0}^{p} r a_{ij,r} - \sum_{w=0}^{p}\sum_{s=1}^{q} a_{ij,w} \cdot b_{ij,s} \cdot |w-s| \cdot \mathrm{sgn}(w-s)}{\left(a_{ij,0}+a_{ij,1}+\cdots+a_{ij,p}\right)\left(1-\left(b_{ij,1}+\cdots+b_{ij,q}\right)\right)} \cdot T + \hat{\tau}_{ij} \cdot T \quad (4.9)$$

Substituting Eq. (3.24) and Eq. (4.3) into Eq. (4.9), after arrangement, gives the following equation to calculate $\hat{\tau}_{ij}$.

$$\hat{\tau}_{ij} = \frac{\sum_{r=0}^{p} r a_{ij,r} - \sum_{w=0}^{p}\sum_{s=1}^{q} a_{ij,w} \cdot b_{ij,s} \cdot |w-s| \cdot \mathrm{sgn}(w-s)}{\left(a_{ij,0}+a_{ij,1}+\cdots+a_{ij,p}\right)\left(1-\left(b_{ij,1}+\cdots+b_{ij,q}\right)\right)} \cdot (\gamma_{TS,ij}-1) + \tau_{ij} \cdot \gamma_{TS,ij} \quad (4.10)$$

Several experimental results demonstrate that for well paired MIMO processes, the values of $\gamma_{TS,ij}$'s of paired loops are close to 1. Therefore, the calculation of $\hat{\tau}_{ij}$ for paired loop in Eq. (4.10) can be simplified as

$$\hat{\tau}_{ij} \approx \tau_{ij} \cdot \gamma_{TS,ij} \quad (4.11)$$

Eq. (4.11) is a practical formula to calculate ETSMs. Even though it is less accurate than Eq. (4.10), a number of simulating examples prove that the control performances are comparable by these two formulas. Moreover, Eq. (4.11) is much more straightforward, explainable and understandable than Eq. (4.10).

Based on Eq. (4.7) and (4.11), Type–1 ETSMs can be obtained. While the Type–2 ETSM can be obtained by similar procedure with one more step of defuzzification.

2. Calculations to determine coefficients of Type–2 ETSM:

Based on the Type–2 T–S fuzzy model $f_{TS,ij}$ for loop $y_i - u_j$, the steady–state gain $k_{TS,ij}$ at the given operating point $\boldsymbol{x}_{0,ij}$ can be calculated by Eq. (3.17) where

$$a_{ij,r} = \frac{a_{ij,lb,r} + a_{ij,rb,r}}{2} = \frac{1}{2} \cdot \left(\frac{\sum_{l=1}^{M_{ij}} \mu_{ij,lb}^{l}(\boldsymbol{x}_{0,ij}) \cdot a_{ij,lb,r}^{l}}{\sum_{l=1}^{M_{ij}} \mu_{ij,lb}^{l}(\boldsymbol{x}_{0,ij})} + \frac{\sum_{l=1}^{M_{ij}} \mu_{ij,rb}^{l}(\boldsymbol{x}_{0,ij}) \cdot a_{ij,rb,r}^{l}}{\sum_{l=1}^{M_{ij}} \mu_{ij,rb}^{l}(\boldsymbol{x}_{0,ij})} \right) \quad (4.12)$$

$$b_{ij,s}=\frac{b_{ij,lb,s}+b_{ij,rb,s}}{2}=\frac{1}{2}\cdot\left(\frac{\sum_{l=1}^{M_{ij}}\mu_{ij,lb}^{l}(\boldsymbol{x}_{0,ij})\cdot b_{ij,lb,s}^{l}}{\sum_{l=1}^{M_{ij}}\mu_{ij,lb}^{l}(\boldsymbol{x}_{0,ij})}+\frac{\sum_{l=1}^{M_{ij}}\mu_{ij,rb}^{l}(\boldsymbol{x}_{0,ij})\cdot b_{ij,rb,s}^{l}}{\sum_{l=1}^{M_{ij}}\mu_{ij,rb}^{l}(\boldsymbol{x}_{0,ij})}\right) \tag{4.13}$$

$r=0,1,\cdots,p$, $s=1,\cdots,q$. The steady–state gain $\hat{k}_{TS,ij}$ for the Type–2 ETSM $\hat{f}_{TS,ij}$ can be derived by an equation with the same form as Eq. (4.5) where

$$\hat{a}_{ij,r}=\frac{\hat{a}_{ij,lb,r}+\hat{a}_{ij,rb,r}}{2}=\frac{1}{2}\cdot\left(\frac{\sum_{l=1}^{M_{ij}}\mu_{ij,lb}^{l}(\boldsymbol{x}_{0,ij})\cdot\hat{a}_{ij,lb,r}^{l}}{\sum_{l=1}^{M_{ij}}\mu_{ij,lb}^{l}(\boldsymbol{x}_{0,ij})}+\frac{\sum_{l=1}^{M_{ij}}\mu_{ij,rb}^{l}(\boldsymbol{x}_{0,ij})\cdot\hat{a}_{ij,rb,r}^{l}}{\sum_{l=1}^{M_{ij}}\mu_{ij,rb}^{l}(\boldsymbol{x}_{0,ij})}\right),\quad r=0,1,\cdots,p. \tag{4.14}$$

Considering Eq. (3.4), Eq. (3.17), Eq. (4.5) and Eqs (4.12)–(4.14) gives that

$$\hat{a}_{ij,lb,r}=\frac{a_{ij,lb,r}}{\lambda_{TS,ij}},\text{ and }\ \hat{a}_{ij,rb,r}=\frac{a_{ij,rb,r}}{\lambda_{TS,ij}} \tag{4.15}$$

The left and the right bound of $\hat{\tilde{a}}_{ij,r}^{l}=\left[\hat{a}_{ij,lb,r}^{l},\ \ \hat{a}_{ij,rb,r}^{l}\right]$ in Eq. (4.2) can be calculated as

$$\hat{a}_{ij,lb,r}^{l}=\frac{a_{ij,lb,r}^{l}}{\lambda_{TS,ij}},\text{ and }\ \hat{a}_{ij,rb,r}^{l}=\frac{a_{ij,rb,r}^{l}}{\lambda_{TS,ij}} \tag{4.16}$$

Similar to the method for determining Type–1 ETSM, the time delay $\hat{\tau}_{ij}$ of Type–2 ETSM can be calculated by an equation with the same form as Eq. (4.10), where the parameters $a_{ij,r}$ ($r=0,1,\cdots,p$) and $b_{ij,s}$ ($s=1,\cdots,q$) are determined by Eq. (4.12) and Eq. (4.13). And the calculation can also be simplified as Eq. (4.11) since the values of $\gamma_{TS,ij}$'s of paired loops are close to 1.

By the above simple calculating methods, it is easy to obtain a Type–1 and a Type–2 ETSM for a paired loop that can exhibit the interacting effects on both steady–state gain and dynamic property when all other loops close. However, it is required that the control system possesses integrity property, which means, the overall control system should remain stable whether other control–loops are put in and/or removed [38, 63]. And the integrity requires that when controlling a certain loop after all other loops

removed, the performance of the controller designed based on the ETSM should be no more aggressive than that of the controller designed based on the individual model [38]. Therefore, the coefficients in $\hat{f}_{TS,ij}$ must take different values for different interacting cases. There are four different interacting cases that are classified by four combinations of the values of $\lambda_{TS,ij}$ and $\gamma_{TS,ij}$. How to revise the coefficients in $\hat{f}_{TS,ij}$ to guarantee the integrity property of a control system is discussed below.

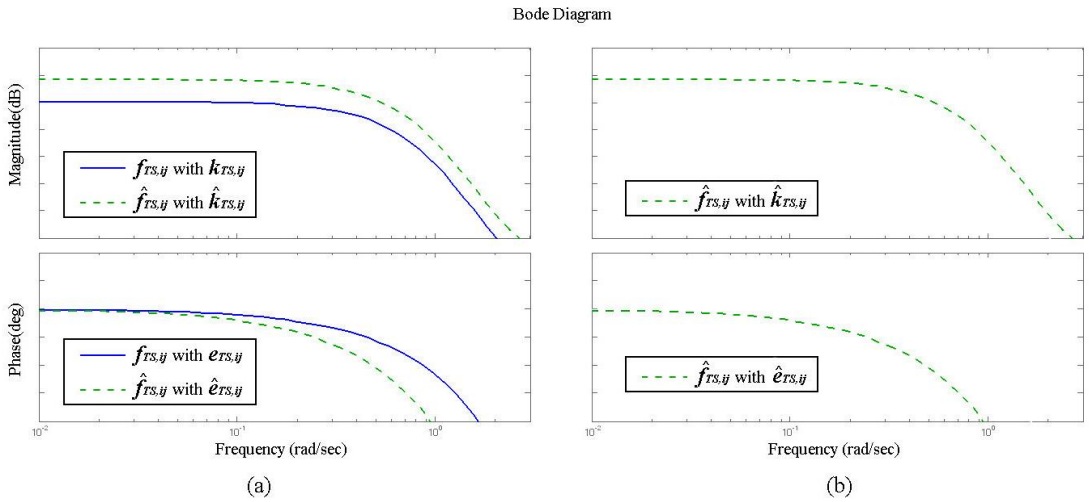

Figure 4.1 Interacting case with $\lambda_{TS,ij} \leq 1$ and $\gamma_{TS,ij} > 1$

Case 1: $\lambda_{TS,ij} \leq 1$ and $\gamma_{TS,ij} > 1$

In this case, $\lambda_{TS,ij} = k_{TS,ij} / \hat{k}_{TS,ij} \leq 1$ and $\gamma_{TS,ij} = \hat{e}_{TS,ij} / e_{TS,ij} > 1$, which means $\hat{k}_{TS,ij} \geq k_{TS,ij}$ and $\hat{e}_{TS,ij} > e_{TS,ij}$. An example of the Bode diagrams of $f_{TS,ij}$ and $\hat{f}_{TS,ij}$ can be seen in part (a) of Fig. 4.1.

- $\hat{k}_{TS,ij} \geq k_{TS,ij}$, means that the steady–state gain of loop $y_i - u_j$ when other loops close is not smaller than that of the individual loop. Since the interactions from the other loops enlarge the effect of u_j on y_i, the controller gains need reducing to guarantee the system stability. In this case, for Type–1 ETSM, $\hat{a}^l_{ij,r}$ ($r = 0,1,\cdots,p$, $l = 1,\cdots,M_{ij}$) is determined by Eq. (4.7), and for Type–2 ETSM, $\hat{a}^l_{ij,lb,r}$ and $\hat{a}^l_{ij,rb,r}$ ($r = 0,1,\cdots,p$, $l = 1,\cdots,M_{ij}$) are determined by Eq. (4.16), such that the

controller will be designed based on $\hat{f}_{TS,ij}$ where the steady–state gain is $\hat{k}_{TS,ij} = k_{TS,ij} / \lambda_{TS,ij}$.

- $\hat{e}_{TS,ij} > e_{TS,ij}$, means that the response speed of loop $y_i - u_j$ when other loops close is slower than that of the individual loop. The enlarged normalized integrated error will reduce the phase margin and may cause instability. In this case, we let the time delay $\hat{\tau}_{ij}$ in both Type–1 and Type–2 ETSMs be determined by Eq. (4.11), such that the controller will be designed based on $\hat{f}_{TS,ij}$ where the normalized integrated error is $\hat{e}_{ij} = e_{ij} \cdot \gamma_{TS,ij}$.

The Bode diagram of $\hat{f}_{TS,ij}$ with revised parameters in this case can be seen in part (b) of Fig. 4.1.

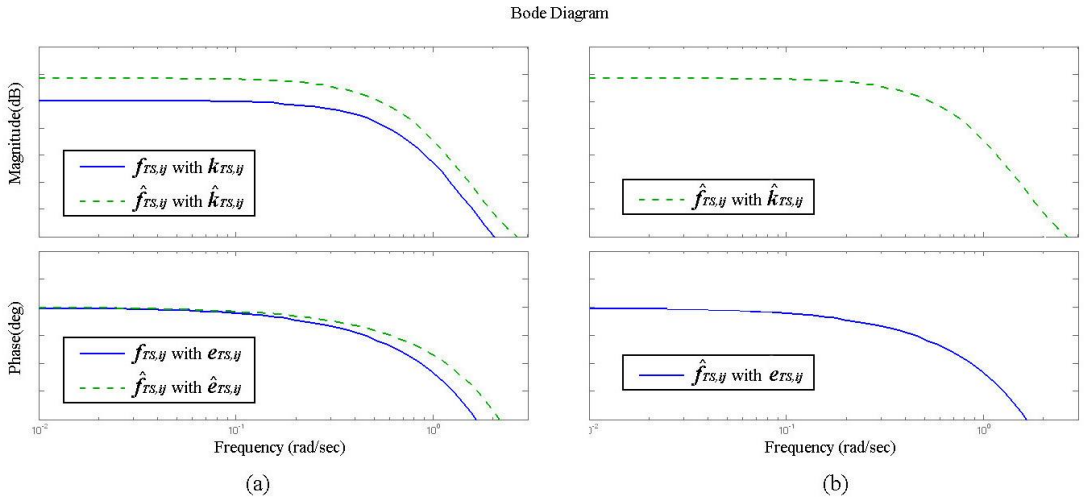

Figure 4.2 Interacting case with $\lambda_{TS,ij} \leq 1$ and $\gamma_{TS,ij} \leq 1$

Case 2: $\lambda_{TS,ij} \leq 1$ and $\gamma_{TS,ij} \leq 1$

In this case, $\lambda_{TS,ij} = k_{TS,ij} / \hat{k}_{TS,ij} \leq 1$ and $\gamma_{TS,ij} = \hat{e}_{TS,ij} / e_{TS,ij} \leq 1$, which means $\hat{k}_{TS,ij} \geq k_{TS,ij}$ and $\hat{e}_{TS,ij} \leq e_{TS,ij}$. An example of the Bode diagrams of $f_{TS,ij}$ and $\hat{f}_{TS,ij}$ can be seen in part (a) of Fig. 4.2.

- $\hat{k}_{TS,ij} \geq k_{TS,ij}$, same as that in **Case 1**.

- $\hat{e}_{TS,ij} \le e_{TS,ij}$, means that the response speed of loop $y_i - u_j$ when other loops close is not slower than that of the individual loop. The reduced normalized integrated error will enlarge the phase margin. However, in consideration of the control system integrity, the time delay of ETSMs should be same as that of their individual T–S fuzzy models, i.e., $\hat{\tau}_{ij} = \tau_{ij}$, such that the controller design will be based on the unchanged normalized integrated error: $\hat{e}_{ij} = e_{ij}$.

The Bode diagram of $\hat{f}_{TS,ij}$ with revised parameters in this case can be seen in part (b) of Fig. 4.2.

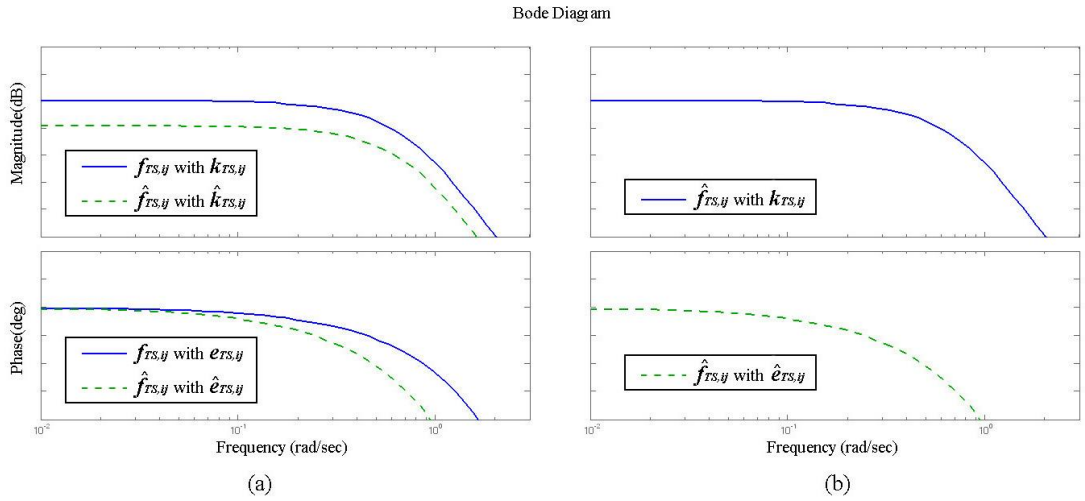

Figure 4.3 Interacting case with $\lambda_{TS,ij} > 1$ and $\gamma_{TS,ij} > 1$

Case 3: $\lambda_{TS,ij} > 1$ and $\gamma_{TS,ij} > 1$

In this case, $\lambda_{TS,ij} = k_{TS,ij} / \hat{k}_{TS,ij} > 1$ and $\gamma_{TS,ij} = \hat{e}_{TS,ij} / e_{TS,ij} > 1$, which means $\hat{k}_{TS,ij} < k_{TS,ij}$ and $\hat{e}_{TS,ij} > e_{TS,ij}$. An example of the Bode diagrams of $f_{TS,ij}$ and $\hat{f}_{TS,ij}$ can be seen in part (a) of Fig. 4.3.

- $\hat{k}_{TS,ij} < k_{TS,ij}$, means that the steady–state gain of loop $y_i - u_j$ when other loops close is smaller than that of the individual loop. Even though the interactions from other loops acts in opposition to the effect of u_j on y_i, the controller gain cannot be magnified for better performance due to the control system integrity

consideration. Hence, $\hat{a}^l_{ij,r}$ of Type–1 ETSM, and $\hat{a}^l_{ij,lb,r}$, $\hat{a}^l_{ij,rb,r}$ of Type–2 ETSM ($r = 0,1,\cdots,p$, $l = 1,\cdots,M_{ij}$) should be same as that of their individual models, i.e., $\hat{a}^l_{ij,r} = a^l_{ij,r}$, $\hat{a}^l_{ij,lb,r} = a^l_{ij,lb,r}$ and $\hat{a}^l_{ij,rb,r} = a^l_{ij,rb,r}$, such that the controller design will be based on the unchanged steady–state gain: $\hat{k}_{TS,ij} = k_{TS,ij}$.

- $\hat{e}_{TS,ij} > e_{TS,ij}$, same as that in **Case 1**.

The Bode diagram of $\hat{f}_{TS,ij}$ with revised parameters in this case can be seen in part (b) of Fig. 4.3.

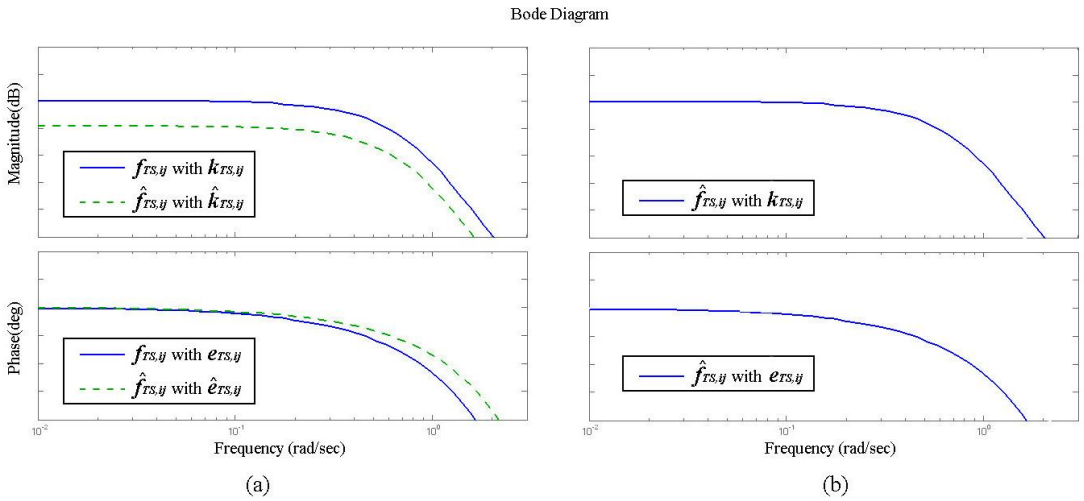

Figure 4.4 Interacting case with $\lambda_{TS,ij} > 1$ and $\gamma_{TS,ij} \leq 1$

Case 4: $\lambda_{TS,ij} > 1$ and $\gamma_{TS,ij} \leq 1$

In this case, $\lambda_{TS,ij} = k_{TS,ij} / \hat{k}_{TS,ij} > 1$ and $\gamma_{TS,ij} = \hat{e}_{TS,ij} / e_{TS,ij} \leq 1$, which means $\hat{k}_{TS,ij} < k_{TS,ij}$ and $\hat{e}_{TS,ij} \leq e_{TS,ij}$. An example of the Bode diagrams of $f_{TS,ij}$ and $\hat{f}_{TS,ij}$ can be seen in part (a) of Fig. 4.4.

- $\hat{k}_{TS,ij} < k_{TS,ij}$, same as that in **Case 3**.
- $\hat{e}_{TS,ij} \leq e_{TS,ij}$, same as that in **Case 2**.

The Bode diagram of $\hat{f}_{TS,ij}$ with revised parameters in this case can be seen in part (b) of Fig. 4.4.

After revising the coefficients, *n* ETSMs of *n* paired control–loops can be obtained to describe *n* non–interacting equivalent single loops to represent an $n \times n$ MIMO process. Afterwards, each local controller of a decentralized control system for this process can be independently designed based on an ETSM through linear SISO control algorithms. An example for a two–input–two–output process is shown in Fig. 4.5.

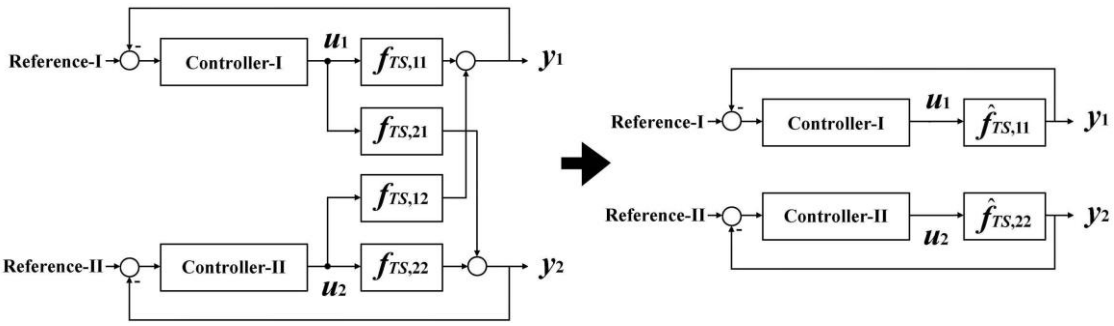

Figure 4.5 Decentralized control system based on ETSMs for a 2×2 process

The steps of using the presented loop pairing criterion based ETSM method to develop a decentralized controller for an MIMO process are given in the following.

i). At an operating condition, calculate the steady–state gain and the normalized integrated error from the T–S fuzzy model of each individual loop to select a control configuration for the overall process according to the RNGA based pairing criterion.

ii). According to the information provided by the RNGA based criterion, scale the individual T–S fuzzy model coefficients of paired control–loops to obtain ETSMs. Then each local decentralized controller can be independently derived based on an ETSM using linear SISO control approaches.

iii). When the operating condition changes, repeat step i) and step ii) to update control configuration and ETSMs for control variable calculations.

The significances of the proposed ETSM method are as follows.

- ETSM can describe the interacting effects on both steady and dynamic properties without using extra terms or changing the linear structure of local T–S fuzzy model, which provides a simple but effective manner to approximate the interacting results that can greatly reduce the complexity and cost of process modeling and the following controller designs especially for large–scale MIMO

processes.

- The calculations are quite simple such that in an MER system which is a nonlinear process the ETSM of updated control configuration for changed working condition can be obtained immediately. And it only utilizes the information of individual open–loop models which are always identifiable with proper persistent excitations. Moreover, fuzzy model can be identified based on data samples or human experience without requiring the knowledge of inner process information. Therefore, it is feasible and effective in complex MIMO process controls, and can be applied in real–time applications for manipulating MER systems.
- Compared with the existing loop pairing criteria based effective model methods that are all proposed based on linear transfer functions identified at certain working points, the ETSM method provides an alternative when the accurate mathematical functions are unavailable. And fuzzy model is a global description for the process that can save the computational cost and time for new transfer function identification when the working points change in real–time applications. Moreover, this method lays a foundation to develop robust controllers since fuzzy system is powerful to handle uncertainties.
- The ETSM can reflect proper steady and dynamic properties in different cases to guarantee the control system integrity. Based on ETSMs of paired loops, decentralized controller design for an MER system can be regarded as multiple independent single–loop controller designs and greatly facilitated by linear SISO control algorithms. Furthermore, this method presents Type–1 and Type–2 ETSMs under a unified framework where the comparative studies of Type–1 and Type–2 T–S fuzzy systems in terms of robustness and computational cost can be carried out to qualitatively and quantitatively analyze their properties and differences.

4.3 Controller design based on ETSMs

This section introduces how to design controllers based on Type–1 and Type–2 ETSMs. A closed–loop T–S fuzzy model based control system for an $n \times n$ MIMO process is shown in Fig. 4.6, where rv_i, $i = 1, \cdots, n$, denote the reference values;

control variables u_j ($j = 1, \cdots, n$) are determined through controller $\boldsymbol{G}_c$ according to d_i's ($i = 1, \cdots, n$), which are the differences between reference values and system outputs, $d_i = rv_i - y_i$. Suppose the control configuration has been determined and the paired loops have been placed in the diagonal positions through column swapping, by virtue of the ETSMs of the paired loops, the linear SISO control techniques can be employed to devise decentralized controllers for the MIMO process.

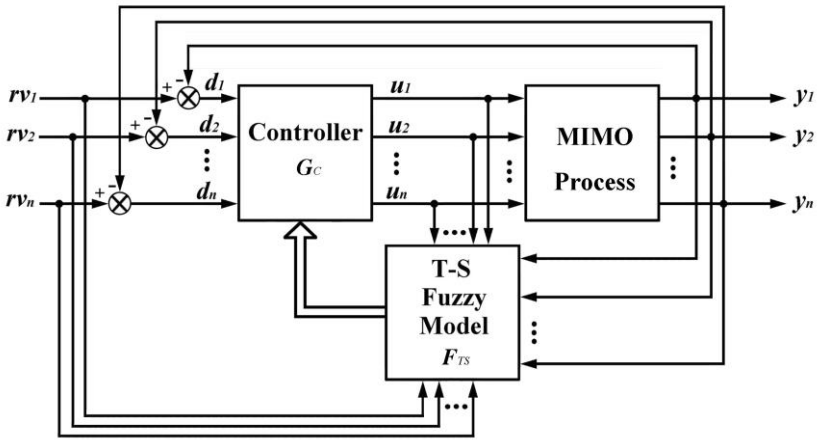

Figure 4.6 A fuzzy model based closed–loop control system for an MIMO process

Theoretically, any linear control algorithms can be applied to design controllers based on an ETSM through PDC [15]. In order to develop a practical controller for a real MIMO process, the control algorithms should be robust to the disturbance and simple in calculation and implementation. Currently, a number of control algorithms have been proposed to cope with the interactions and disturbance, such as model predictive control (MPC) and the robust control. They are more suitable to be used in higher level of a control strategy due to the computational complexity. While at the lower level, the control algorithms based on proportional–integral (PI) or proportional–integral–derivative (PID) controllers are widely used for regulating controls [38]. Different methods have been proposed to calculate the gains of a PID controller, such as Ziegler–Nichols with detuning factor method proposed in [66], the biggest log modulus tuning algorithm presented in [67], the relative gain based tuning approach given in [65], and the sequential loop tuning manner introduced by [68], etc..

Recently a PID controller tuning method based on gain and phase margins is proposed [69], which can guarantee both robustness and performance. Several examples have demonstrated that it can achieve better control performances for both set point change and load disturbance than many other PID control tuning methods in [63]. In this section, this gain and phase margins based algorithm is selected to present the controller designs based on Type–1 and Type–2 ETSMs.

For simplicity, the following Type–1 and Type–2 T–S fuzzy rules with $p=0$ and $q=2$, which can be used to approximate the majority of individual loops in the MIMO processes, are utilized to present controller designs.

The Type–1 T–S fuzzy rule expressed as

$$\begin{aligned} R^l:\ &\text{IF} \quad \boldsymbol{x}_{ij}(k) \quad is \quad C_{ij}^l \\ &\text{THEN} \quad y_i^l(k)=a_{ij,0}^l\cdot u_j(k-\tau_{ij})+b_{ij,1}^l\cdot y_i(k-1)+b_{ij,2}^l\cdot y_i(k-2) \end{aligned} \tag{4.17}$$

and the Type–2 T–S fuzzy rule expressed as

$$\begin{aligned} R^l:\ &\text{IF} \quad \boldsymbol{x}_{ij}(k) \quad is \quad \tilde{C}_{ij}^l \\ &\text{THEN} \quad \tilde{y}_i^l(k)=\tilde{a}_{ij,0}^l\cdot u_j(k-\tau_{ij})+\tilde{b}_{ij,1}^l\cdot y_i(k-1)+\tilde{b}_{ij,2}^l\cdot y_i(k-2) \end{aligned} \tag{4.18}$$

Based on Eq. (4.17) and Eq. (4.18), the procedures to devise controllers are given as follows.

1. Controller design based on Type–1 ETSM

For a certain paired loop y_i-u_i, its Type–1 ETSM $\hat{f}_{TS,ii}$ can be expressed as

$$\begin{aligned} R^l:\ &\text{IF} \quad \boldsymbol{x}_{ii}(k) \quad is \quad C_{ii}^l \\ &\text{THEN} \quad y_i^l(k)=\hat{a}_{ii,0}^l\cdot u_i(k-\hat{\tau}_{ii})+b_{ii,1}^l\cdot y_i(k-1)+b_{ii,2}^l\cdot y_i(k-2) \end{aligned} \tag{4.19}$$

The linear polynomial of *l*th fuzzy rule as in Eq. (4.19) can be converted to a discrete transfer function form by through ***Z***–transform

$$G_{TS,ii}^l(z)=\frac{Y_i(z)}{U_i(z)}=\frac{\hat{a}_{ii,0}^l}{1-b_{ii,1}^l z^{-1}-b_{ii,2}^l z^{-2}}\cdot z^{-\hat{\tau}_{ii}} \tag{4.20}$$

And a standard discrete PID controller for $G_{TS,ii}^l(z)$ in Eq. (4.20) using backward differencing approximation of derivative can be expressed by

$$G_{c,i}^{l}(z)=\frac{U_i(z)}{D_i(z)}=K_{P,i}^{l}+\frac{K_{I,i}^{l}T}{1-z^{-1}}+\frac{K_{D,i}^{l}}{T}(1-z^{-1}) \tag{4.21}$$

where $K_{P,i}^{l}$, $K_{I,i}^{l}$ and $K_{D,i}^{l}$ are proportional, integral and derivative gains respectively, and $D_i(z)=\boldsymbol{Z}[d_i]$. According to the gain and phase margins based PID tuning method [69], the parameters of the controller should be chosen to satisfy the following equation.

$$\hat{G}_{TS,ii}^{l}(z)G_{c,i}^{l}(z)=\frac{K_i^{l}T}{1-z^{-1}}z^{-\hat{\tau}_{ii}} \tag{4.22}$$

where $K_i^{l}=\pi/(2A_{m,i}\hat{\tau}_{ii}T)$, $A_{m,i}$ is the specified gain margin, which is interrelated to phase margin $\Psi_{m,i}$. Some typical gain–phase margin pairs are given in Table 4.1. Substitute Eq. (4.20) and Eq. (4.21) into Eq. (4.22) to have

$$\begin{aligned}
\hat{G}_{TS,ii}^{l}(z)G_{c,i}^{l}(z)&=\frac{\hat{a}_{ii,0}^{l}\cdot z^{-\hat{\tau}_{ii}}}{1-(b_{ii,1}^{l}z^{-1}+b_{ii,2}^{l}z^{-2})}\cdot\left(K_{P,i}^{l}+\frac{K_{I,i}^{l}T}{1-z^{-1}}+\frac{K_{D,i}^{l}}{T}(1-z^{-1})\right)\\
&=\frac{\hat{a}_{ii,0}^{l}\cdot z^{-\hat{\tau}_{ii}}}{1-b_{ii,1}^{l}z^{-1}-b_{ii,2}^{l}z^{-2}}\cdot\frac{(K_{P,i}^{l}+K_{I,i}^{l}T+\frac{K_{D,i}^{l}}{T})-(K_{P,i}^{l}+\frac{2K_{D,i}^{l}}{T})z^{-1}+\frac{K_{D,i}^{l}}{T}z^{-2}}{1-z^{-1}}\\
&=\frac{\hat{a}_{ii,0}^{l}\cdot(K_{P,i}^{l}+K_{I,i}^{l}T+K_{D,i}^{l}/T)\cdot z^{-\hat{\tau}_{ii}}}{1-b_{ii,1}^{l}z^{-1}-b_{ii,2}^{l}z^{-2}}\cdot\frac{1-\frac{K_{P,i}^{l}+2K_{D,i}^{l}/T}{K_{P,i}^{l}+K_{I,i}^{l}T+K_{D,i}^{l}/T}z^{-1}+\frac{K_{D,i}^{l}/T}{K_{P,i}^{l}+K_{I,i}^{l}T+K_{D,i}^{l}/T}z^{-2}}{1-z^{-1}}\\
&=\frac{K_i^{l}T}{1-z^{-1}}z^{-\hat{\tau}_{ii}}
\end{aligned} \tag{4.23}$$

Table 4.1 Typical gain and phase margin pairs

$\Psi_{m,i}$	$\pi/4$	$\pi/3$	$3\pi/8$	$2\pi/5$
$A_{m,i}$	2	3	4	5

In order to satisfy Eq. (4.23), the following equations are utilized.

$$K_i^l T = \hat{a}_{ii,0}^l \cdot (K_{P,i}^l + K_{I,i}^l T + K_{D,i}^l / T)$$

$$b_{ii,1}^l = \frac{K_{P,i}^l + 2K_{D,i}^l / T}{K_{P,i}^l + K_{I,i}^l T + K_{D,i}^l / T}$$

$$b_{ii,2}^l = \frac{-K_{D,i}^l / T}{K_{P,i}^l + K_{I,i}^l T + K_{D,i}^l / T}$$

Consequently the proportional, integral and derivative gains can be derived by

$$\begin{cases} K_{P,i}^l = \dfrac{K_i^l T}{\hat{a}_{ii,0}^l} \cdot (b_{ii,1}^l + 2b_{ii,2}^l) = \dfrac{\pi}{2\hat{a}_{ii,0}^l A_{m,i} \hat{\tau}_{ii}} \cdot (b_{ii,1}^l + 2b_{ii,2}^l) \\ K_{I,i}^l = \dfrac{K_i^l}{\hat{a}_{ii,0}^l} \cdot (1 - b_{ii,1}^l - b_{ii,2}^l) = \dfrac{\pi}{2\hat{a}_{ii,0}^l A_{m,i} \hat{\tau}_{ii} T} \cdot (1 - b_{ii,1}^l - b_{ii,2}^l) \\ K_{D,i}^l = \dfrac{K_i^l T^2}{\hat{a}_{ii,0}^l} \cdot (-b_{ii,2}^l) = \dfrac{\pi T}{2\hat{a}_{ii,0}^l A_{m,i} \hat{\tau}_{ii}} \cdot (-b_{ii,2}^l) \end{cases} \tag{4.24}$$

Submitting Eq. (4.24) into Eq. (4.21) to obtain $G_{c,i}^l(z)$ for *l*th fuzzy rule as

$$\begin{aligned} G_{c,i}^l(z) &= K_{P,i}^l + \frac{K_{I,i}^l T}{1 - z^{-1}} + \frac{K_{D,i}^l}{T}(1 - z^{-1}) \\ &= \frac{\pi \cdot (b_{ii,1}^l + 2b_{ii,2}^l)}{2\hat{a}_{ii,0}^l A_{m,i} \hat{\tau}_{ii}} + \frac{\pi \cdot (1 - b_{ii,1}^l - b_{ii,2}^l)}{2\hat{a}_{ii,0}^l A_{m,i} \hat{\tau}_{ii}} \cdot \frac{1}{1 - z^{-1}} + \frac{\pi \cdot (-b_{ii,2}^l)}{2\hat{a}_{ii,0}^l A_{m,i} \hat{\tau}_{ii}} \cdot (1 - z^{-1}) \\ &= \frac{\pi - \pi b_{ii,1}^l z^{-1} - \pi b_{ii,2}^l z^{-2}}{2\hat{a}_{ii,0}^l A_{m,i} \hat{\tau}_{ii} (1 - z^{-1})} \end{aligned} \tag{4.25}$$

And Eq. (4.25) gives the following equation to derive a control variable in time domain for *l*th fuzzy rule as

$$u_i^l(k) = u_i(k-1) + \frac{\pi}{2\hat{a}_{ii,0}^l A_{m,i} \hat{\tau}_{ii}} d_i(k) - \frac{\pi b_{ii,1}^l}{2\hat{a}_{ii,0}^l A_{m,i} \hat{\tau}_{ii}} d_i(k-1) - \frac{\pi b_{ii,2}^l}{2\hat{a}_{ii,0}^l A_{m,i} \hat{\tau}_{ii}} d_i(k-2) \tag{4.26}$$

According to PDC, the $u_i(k)$ is a weighted sum of local control variables $u_i^l(k)$ ($l = 1, \cdots, M_{ii}$) and shares the same membership functions of $\hat{f}_{TS,ii}$ as

$$u_i(k) = \sum_{l=1}^{M_{ii}} \mu_{ii}^l \left(\boldsymbol{x}_{ii}(k) \right) u_i^l(k) \tag{4.27}$$

2. Controller design based on Type–2 ETSM

For a certain paired loop $y_i - u_i$, its Type–2 ETSM $\hat{f}_{TS,ii}$ can be expressed as

$$\begin{aligned} R^l &: \text{IF} \quad \boldsymbol{x}_{ij}(k) \quad is \quad \tilde{C}_{ij}^l \\ &\text{THEN} \quad \tilde{y}_i^l(k) = \hat{\tilde{a}}_{ij,0}^l \cdot u_j(k-\hat{\tau}_{ij}) + \tilde{b}_{ij,1}^l \cdot y_i(k-1) + \cdots + \tilde{b}_{ij,2}^l \cdot y_i(k-2) \end{aligned} \tag{4.28}$$

where $\tilde{y}_i^l(k) = \left[y_{i,lb}^l(k), \quad y_{i,rb}^l(k) \right]$, $y_{i,lb}^l(k)$ and $y_{i,rb}^l(k)$ are expressed by

$$\begin{cases} y_{i,lb}^l(k) = \hat{a}_{ij,lb,0}^l \cdot u_j(k-\hat{\tau}_{ij}) + b_{ij,lb,1}^l y_i(k-1) + b_{ij,lb,2}^l \cdot y_i(k-2) \\ y_{i,rb}^l(k) = \hat{a}_{ij,rb,0}^l \cdot u_j(k-\hat{\tau}_{ij}) + b_{ij,rb,1}^l y_i(k-1) + b_{ij,rb,2}^l \cdot y_i(k-2) \end{cases} \tag{4.29}$$

Eq. (4.29) can be converted to two discrete linear functions through ***Z***–transform as

$$\begin{cases} G_{TS,ii,lb}^l(z) = \dfrac{\hat{a}_{ii,lb,0}^l}{1 - b_{ii,lb,1}^l z^{-1} - b_{ii,lb,2}^l z^{-2}} \cdot z^{-\hat{\tau}_{ii}} \\ G_{TS,ii,rb}^l(z) = \dfrac{\hat{a}_{ii,rb,0}^l}{1 - b_{ii,rb,1}^l z^{-1} - b_{ii,rb,2}^l z^{-2}} \cdot z^{-\hat{\tau}_{ii}} \end{cases} \tag{4.30}$$

According to the gain and phase margins based tuning method, a control variable interval for *l*th rule: $\tilde{u}_i^l(k) = \left[u_{i,lb}^l(k), \quad u_{i.rb}^l(k) \right]$ can be calculated based on Eq. (4.30):

$$\begin{cases} u_{i,lb}^l(k) = u_i(k-1) + \dfrac{\pi \cdot d_i(k) - \pi b_{ii,lb,1}^l \cdot d_i(k-1) - \pi b_{ii,lb,2}^l \cdot d_i(k-2)}{2\hat{a}_{ii,lb,0}^l A_{m,i} \hat{\tau}_{ii}} \\ u_{i,rb}^l(k) = u_i(k-1) + \dfrac{\pi \cdot d_i(k) - \pi b_{ii,rb,1}^l \cdot d_i(k-1) - \pi b_{ii,rb,2}^l \cdot d_i(k-2)}{2\hat{a}_{ii,rb,0}^l A_{m,i} \hat{\tau}_{ii}} \end{cases} \tag{4.31}$$

and the control variable interval for loop $y_i - u_i$ can be obtained through PDC as

$$\begin{aligned} \tilde{u}_i(k) &= \left[u_{i,lb}(k), \quad u_{i,rb}(k) \right] \\ &= \left[\frac{\sum_{l=1}^{M_{ii}} \mu_{ii,lb}^l \left(\boldsymbol{x}_{ii}(k) \right) u_{i,lb}^l(k)}{\sum_{l=1}^{M_{ii}} \mu_{ii,lb}^l \left(\boldsymbol{x}_{ii}(k) \right)}, \quad \frac{\sum_{l=1}^{M_{ii}} \mu_{ii,rb}^l \left(\boldsymbol{x}_{ii}(k) \right) u_{i,rb}^l(k)}{\sum_{l=1}^{M_{ii}} \mu_{ii,rb}^l \left(\boldsymbol{x}_{ii}(k) \right)} \right] \end{aligned} \tag{4.32}$$

The crisp control variable $u_i(k)$ is derived by defuzzifying $\tilde{u}_i(k)$ in Eq. (4.32) as

$$u_i(k) = \frac{u_{i,lb}(k) + u_{i,rb}(k)}{2} \tag{4.33}$$

Remark 4.1: According to the introduced controller design procedures, in theory, the computational cost to obtain a control variable based on an interval Type–2 ETSM doubles that based on a Type–1 ETSM because of the increased fuzziness in the

coefficients of the Type–2 ETSM.

4.4 Simulation

A three–input–three–output (3×3) nonlinear process is given as follows.

$$\begin{cases} \dot{x}_1 = x_2 + 5x_1^2 x_2 + 6x_2^2 \\ \dot{x}_2 = -4x_1 - 5x_2 + 8x_1 x_2 + u_1 \\ \dot{x}_3 = x_4 \\ \dot{x}_4 = -6x_3 - 5x_4 + 3x_3^3 + 10x_3 x_4 x_5 + u_2 \\ \dot{x}_5 = x_6 + 4x_7^2 \\ \dot{x}_6 = x_7 + 5x_5 x_6^2 x_7 \\ \dot{x}_7 = -14x_5 - 23x_6 - 10x_7 + 7x_5 x_6 x_7 + u_3 \\ y_1 = 5x_1 + 5x_2 + 6x_3 + 2x_4 + 14x_5 + 9x_6 + x_7 \\ y_2 = 8x_1 + 2x_2 + 3x_3 + 4x_5 + 6x_6 + 2x_7 \\ y_3 = x_1 + x_2 + 4x_3 + 2x_4 + 1.4x_5 + 0.2x_6 \end{cases} \tag{4.34}$$

where y_i's ($i=1,2,3$) and u_j's ($j=1,2,3$) are outputs and inputs respectively, x_r's ($r=1,\cdots,7$) are state variables. The time delays in this process are $\tau'_{i1}=\tau'_{i2}=2$ (sec) and $\tau'_{i3}=1$(sec) for $i=1,2,3$. Suppose there are disturbances added to the process when collecting data samples of individual loops as shown in Fig. 3.2, and the disturbances are random but bounded in $[-0.2,\ \ 0.2]$. Choose the sampling interval as $T=0.1$sec. The Type–1 and the Type–2 T–S fuzzy models as the forms of Eq. (4.17) and Eq. (4.18) are constructed based on the sampled input–output data pairs, and the identified results are presented in Appendix B. Given the operating points as

$$\boldsymbol{x}_{0,ij} = \left[u_{0,j}(k_0 - \tau_{ij}) \quad y_{0,i}(k_0 - 1) \quad y_{0,i}(k_0 - 2) \right] = \left[0 \quad 0 \quad 0 \right]$$

for $i, j = 1,2,3$, from the Type–1 T–S fuzzy model matrix, the following results can be obtained as

$$\boldsymbol{K}_{TS} = \begin{bmatrix} 1.2565 & 0.9784 & 1.0782 \\ 2.1238 & 0.5486 & 0.2905 \\ 0.2493 & 0.6743 & 0.1313 \end{bmatrix}, \quad \boldsymbol{E}_{TS} = \begin{bmatrix} 2.1954 & 2.5234 & 2.1538 \\ 2.8221 & 3.5756 & 1.1021 \\ 2.1872 & 2.3181 & 6.9247 \end{bmatrix}$$

$$\boldsymbol{\Lambda}_{TS}=\begin{bmatrix}-0.1498 & -0.1944 & 1.3442\\ 1.2235 & -0.0548 & -0.1687\\ -0.0737 & 1.2492 & -0.1755\end{bmatrix},\quad \boldsymbol{\Phi}_{TS}=\begin{bmatrix}-0.6522 & 0.0945 & 1.5577\\ 1.6075 & -0.1095 & -0.4980\\ -0.0447 & 1.0150 & -0.0598\end{bmatrix}$$

According to the RNGA based loop pairing criterion, the optimal control configuration can be determined: $y_1-u_3\,/\,y_2-u_1\,/\,y_3-u_2$, where $\boldsymbol{N}_{TS}=0.9598>0$. Based on $\boldsymbol{\Lambda}_{TS}$ and $\boldsymbol{\Phi}_{TS}$, the relative normalized integrated error array can be derived as

$$\boldsymbol{\Gamma}_{TS}=\begin{bmatrix}4.3545 & -0.4861 & 1.1589\\ 1.3138 & 1.9981 & 2.9520\\ -0.6065 & 0.8125 & 0.3405\end{bmatrix}$$

For the paired loops, $\lambda_{TS,13}=1.3442>1$, $\lambda_{TS,21}=1.2235>1$, $\lambda_{TS,32}=1.2492>1$, and $\gamma_{TS,13}=1.1589>1$, $\gamma_{TS,21}=1.3138>1$, $\gamma_{TS,32}=0.8125<1$, thus the Type–1 ETSMs of loop y_1-u_3 and loop y_2-u_1 are determined by **Case 3**, and the Type–1 ETSM of loop y_3-u_2 is determined by **Case 4** as described in Section 4.2.

From the Type–2 T–S fuzzy model matrix, the following results can be obtained.

$$\boldsymbol{K}_{TS}=\begin{bmatrix}1.2502 & 0.9762 & 1.0750\\ 2.1205 & 0.5480 & 0.2902\\ 0.2481 & 0.6724 & 0.1316\end{bmatrix},\quad \boldsymbol{E}_{TS}=\begin{bmatrix}2.1939 & 2.5221 & 2.1479\\ 2.8188 & 3.5633 & 1.1018\\ 2.1847 & 2.3172 & 6.8859\end{bmatrix}$$

$$\boldsymbol{\Lambda}_{TS}=\begin{bmatrix}-0.1492 & -0.1961 & 1.3453\\ 1.2228 & -0.0543 & -0.1685\\ -0.0736 & 1.2504 & -0.1768\end{bmatrix},\quad \boldsymbol{\Phi}_{TS}=\begin{bmatrix}-0.6478 & 0.0930 & 1.5548\\ 1.6039 & -0.1093 & -0.4946\\ 0.0439 & 1.0163 & -0.0602\end{bmatrix}$$

According to the RNGA based loop pairing criterion, the optimal control configuration can be determined: $y_1-u_3\,/\,y_2-u_1\,/\,y_3-u_2$, which is same as that obtained from Type–1 T–S fuzzy model matrix, and $\boldsymbol{N}_{TS}=0.9596>0$. Based on $\boldsymbol{\Lambda}_{TS}$ and $\boldsymbol{\Phi}_{TS}$, the relative normalized integrated error array can be derived as

$$\boldsymbol{\Gamma}_{TS}=\begin{bmatrix}4.3415 & -0.4742 & 1.1557\\ 1.3117 & 2.0119 & 2.9356\\ -0.5960 & 0.8127 & 0.3403\end{bmatrix}$$

For the paired loops, $\lambda_{TS,13}=1.3453>1$, $\lambda_{TS,21}=1.2228>1$, $\lambda_{TS,32}=1.2504>1$, and $\gamma_{TS,13}=1.1557>1$, $\gamma_{TS,21}=1.3117>1$, $\gamma_{TS,32}=0.8127<1$, thus the Type–2 ETSMs of loop y_1-u_3 and loop y_2-u_1 are determined by **Case 3**, and the Type–2 ETSM of loop y_3-u_2 is determined by **Case 4**.

Based on the ETSMs of paired loops, by using the control algorithm introduced in Section 4.3, the decentralized fuzzy–model–based controllers can be derived. For comparison, the same control algorithm is employed to design decentralized PID controllers for this MIMO process based on the ETFs in terms of RNGA criterion [38, 64], and the transfer functions are obtained by linearizing the MIMO processes of Eq. (4.34) at the given points without disturbances (the details are in Appendix B). The gain and the phase margin are chosen as $A_{m,i}=3$ and $\Psi_{m,i}=\pi/3$, and reference values are $rv_1=1.5$, $rv_2=1$ and $rv_3=0$. Apply ETF and ETSM based controllers to manipulate this MIMO process, their performances are shown in Fig. 4.7.

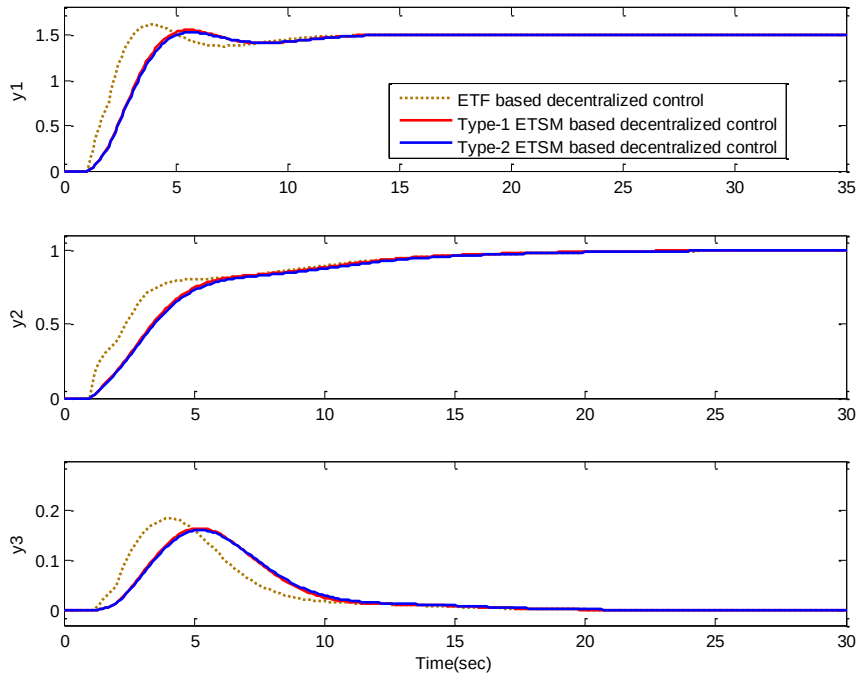

Figure 4.7 Decentralized controls for the MIMO process in Eq. (4.34)

As can be seen in Fig. 4.7, even though the fuzzy models are built based on the data with inexact information, the controllers based on ETSMs can achieve better results

with smaller overshoots compared to that based on the ETFs linearized from exact mathematical models. And in this case, the performances of Type–1 and Type–2 ETSM based decentralized controls are comparable. In a bid to clearly demonstrate their difference, the Integral of the Absolute value of the Error (IAE), a performance criterion given by [70], is employed to reflect the error accumulation of a control result which is defined as

$$\mathrm{IAE}(y_i) = \sum_{k=0}^{\infty} \left| rv_i - y_i(k) \right| \cdot T$$

where T is the sampling interval. The IAEs of three outputs under the Type–1 and the Type–2 ETSM based decentralized controls in this case is given in Table 4.2.

Table 4.2 The IAEs of Type–1 and Type–2 ETSM based decentralized controls for the process in Eq. (4.34)

Type of fuzzy model	IAE(y_1)	IAE(y_2)	IAE(y_3)
Type–1	4.8325	4.9911	0.9011
Type–2	4.7737	4.8073	0.8890

As shown in Table 4.2, the IAEs of Type–1 and Type–2 ETSM based controls, which denote the values of their error accumulations, are very close.

In order to test the robustness of these controllers, we suppose that in the equation group for the process of Eq. (4.34), the third equation $\dot{x}_3 = x_4$ is changed as that in Eq. (4.35) due to the uncertainties

$$\dot{x}_3 = x_4 + 1.5u_1 \tag{4.35}$$

Apply previously designed controllers to the process with changed equation as in Eq. (4.35), the control performances are given in Fig. 4.8, and the comparison of IAEs between Type–1 and Type–2 control is presented in Table 4.3. As illustrated in Fig. 4.8, both Type–1 and Type–2 ETSM based controllers can outperform ETF based controller. And it can be seen that outputs under Type–2 ETSM based control are of a little smaller overshoots than that under Type–1 ETSM based control, which is proved by the values of IAEs presented in Table 4.3 that IAEs of Type–2 control are smaller.

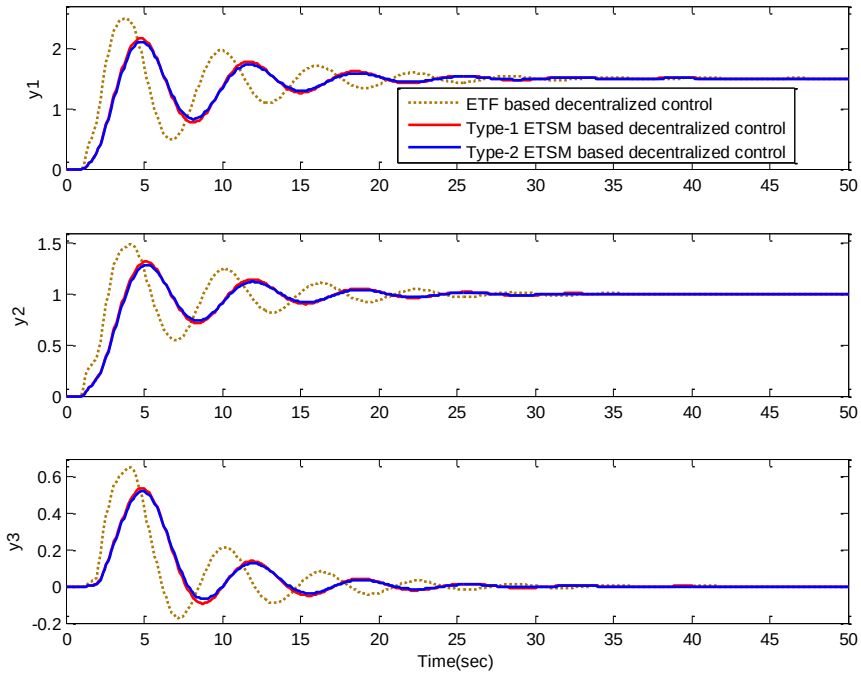

Figure 4.8 Decentralized controls for the process changed as Eq. (4.35)

Table 4.3 The IAEs of Type–1 and Type–2 ETSM based decentralized controls for the process changed as Eq. (4.35)

Type of fuzzy model	IAE(y_1)	IAE(y_2)	IAE(y_3)
Type–1	8.7149	4.8392	2.5867
Type–2	8.1517	4.5987	2.4248

When the changed parameter in the process is further enlarged as

$$\dot{x}_3 = x_4 + 2.31u_1 \tag{4.36}$$

the performances of the previous designed decentralized controllers applied to the process with changed equation as in Eq. (4.36) are shown in Fig. 4.9, and the IAE comparison between Type–1 and Type–2 control is given in Table 4.4. As illustrated in Fig. 4.9, in this case, the outputs under ETF based controller are oscillating and cannot merge with reference values, while the outputs under ETSM based controllers can successfully handle the parametric uncertainties and make the outputs reach their references stably, and the IAEs of Type–2 control are still smaller than that of Type–1 control. Compared with the performances in Fig. 4.8 and Table 4.3, the difference

between Type–1 and Type–2 ETSM based control is more apparent in Fig. 4.9 and Table 4.4 that Type–2 ETSM based controller achieves better results with smaller amplitude of oscillation and error accumulations.

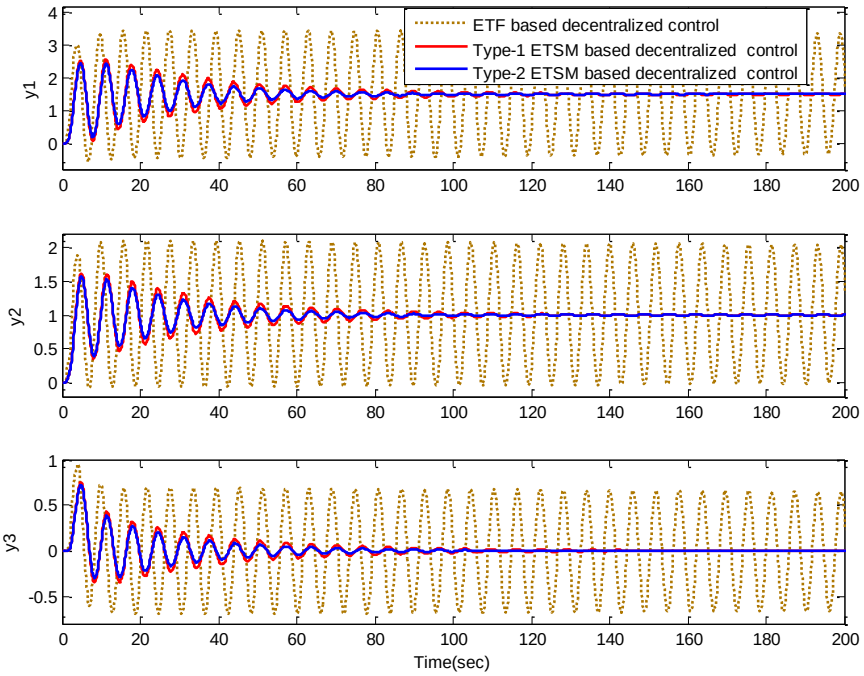

Figure 4.9 Decentralized controls for the process changed as Eq. (4.36)

Table 4.4 The IAEs of Type–1 and Type–2 ETSM based decentralized controls for the process changed as Eq. (4.36)

Type of fuzzy model	IAE(y_1)	IAE(y_2)	IAE(y_3)
Type–1	33.1772	17.8432	11.2063
Type–2	24.7395	13.4902	8.3285

In order to clearly demonstrate the robustness of Type–1 and Type–2 ETSM based controllers, we continue to enlarge the changed parameter as

$$\dot{x}_3 = x_4 + 2.5u_1 \tag{4.37}$$

In this case, the process under ETF based decentralized controller becomes unstable and divergent as in Fig. 4.10, while the process under both Type–1 and Type–2 ETSM based controllers is still stable as shown in Fig. 4.11. And the IAEs are presented in Table 4.5. From Fig. 4.11 and Table 4.5, it is very clear and easy to figure out that

Type–2 ETSM based decentralized controller can provide much improved performance in terms of oscillating amplitude and settling time when compared with Type–1 ETSM based controller.

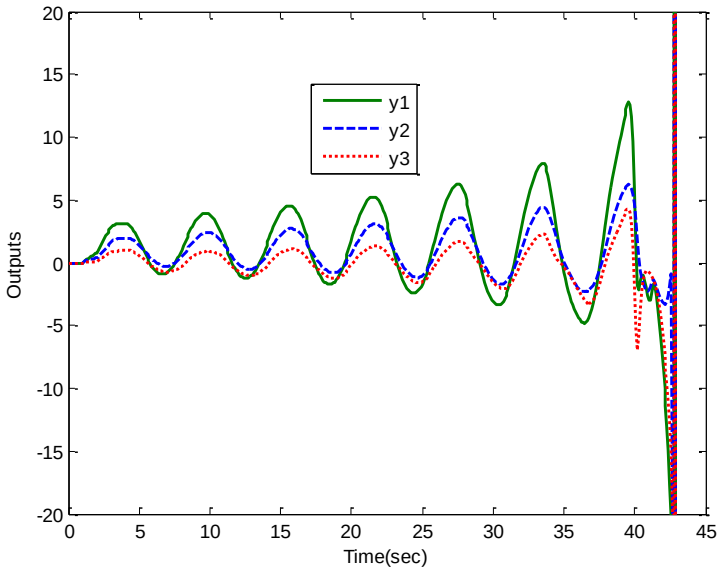

Figure 4.10 ETF based decentralized control for the process changed as Eq. (4.37)

Figs 4.7–4.11 prove that both Type–1 and Type–2 ETSM based decentralized controllers can achieve much better performances than their ETF counterpart. And the IAEs in Tables 4.2–4.5 demonstrate that when large uncertainty appears, Type–2 ETSM based controller can give more robust results than Type–1 ETSM based one.

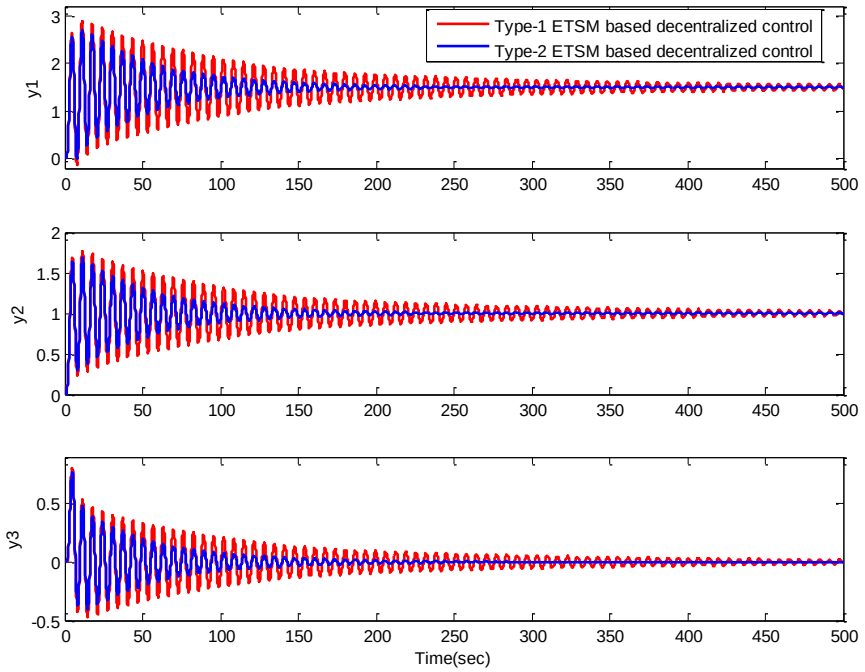

Figure 4.11 ETSM based decentralized controls for process changed as Eq. (4.37)

Table 4.5 The IAEs of Type–1 and Type–2 ETSM based decentralized controls for the process changed as Eq. (4.37)

Type of fuzzy model	IAE(y_1)	IAE(y_2)	IAE(y_3)
Type–1	116.5160	62.4408	40.4200
Type–2	53.1375	28.8519	18.3917

Remark 4.2: The simulation results demonstrate that under the uncertainty with the degree that Type–1 fuzzy model can handle, the decentralized controllers based on Type–1 and Type–2 ETSMs perform comparably. When the degree of uncertainty increases, Type–2 fuzzy model is able to give better performance than Type–1 fuzzy model in terms of robustness. Since the computational cost and complexity based on Type–2 fuzzy model with respect to modeling, loop pairing and controller design are more than that based on Type–1 fuzzy model, in order to achieve satisfactory performance while minimize the cost, which type of fuzzy model should be utilized depends on the degree of uncertainty, the expectation of modeling accuracy and the requirement of controller robustness.

4.5 Summary

In this chapter, both Type–1 and Type–2 ETSMs are proposed to describe the interactions among the loops to facilitate decentralized control for MIMO processes. For a certain loop in an MIMO process, an ETSM is obtained by scaling the parameters of its individual open–loop model according to the quantified interacting effects provided by RNGA based pairing criterion, and the scaled parameters are further revised to adapt different cases such that the integrity of control system can be ensured. The proposed ETSM method can express the interacting results on both steady and dynamic properties of a loop caused by other loops. Based on the ETSMs of paired loops, each local controller of a decentralized control system can be independently designed by using linear SISO control schemes. Compared with the existing decentralized fuzzy control methods adding extra terms in the individual models to characterize the coupling effects, ETSM provides an easier and more

practical way to express the interactions that can reduce complexities in both modeling and controller design. Compared with the existing ETF methods, ETSM method gives an alternative when mathematical functions are unavailable, and offers a basis to develop robust controllers for the process since fuzzy system is strong in handling uncertainties. Simulation results demonstrate that ETSM based controllers outperform their ETF based counterpart, and they can achieve the goals even if the original process parameters change significantly. It is also proved that as the degree of uncertainty increases, Type–2 fuzzy system can give more satisfactory performance than Type–1 fuzzy system. Since the ETSM can embody the interactions from other loops, more interesting control techniques can be developed based on it. In the following chapter, a sparse control method based on ETSM for an MIMO process will be presented.

Chapter 5. Sparse control based on T–S fuzzy models for MIMO processes

5.1 Introduction

For an MIMO process where the interacting effects among the loops are weak or modest, previously proposed decentralized control can generally work with satisfactory performance. However, for an MER system with closely–coupled effects, it may give degraded performance due to the limited control structure. On the other hand, full–dimensional control such as centralized control or full decoupling control generally provide improved performance in manipulating closely–coupled MIMO processes when compared with decentralized control. However, full–dimensional control may result in drastically increased computational cost and complexity, especially for large–scale processes, making the control algorithms difficult to implement.

To develop an efficient controller that can handle strong coupling yet remain viable in applications, sparse control, including “block diagonal control” and “triangular control”, which can make a compromise between decentralized control and full–dimensional control in structure, have been developed. By adding several off–diagonal controllers to the diagonal decentralized control structure, sparse control, if it is well designed, is able to achieve better performance for closely–coupled MIMO processes compared to decentralized control while can be much simpler in calculation and application than full–dimensional control. In [71], an approach using Observability and Controllability Gramian to form a Participation Matrix (PM) for interaction measurement and control structure selection was developed, and in [72] it was further discussed. This work was only used to support linear systems until recently. It was extended to bilinear and nonlinear systems in [73, 74]. These studies have not presented clear criteria to uniquely determine a sparse control structure for an MIMO process, while a clear criterion in terms of RNGA based loop pairing criterion was proposed in [38]. Moreover, [38] presented an independent design method using

ETFs so that the sparse controller design for an MIMO process becomes multiple independent SISO controller designs. Several examples demonstrated its simplicity and effectiveness when compared to decentralized control and full–dimensional control. However, these methods are proposed based on knowing mathematical functions of an MIMO process, which implies that their implementations may be limited when accurate mathematical functions cannot be derived.

Sparse control based on a fuzzy model can be a solution. To the best of the author's knowledge, no studies concerning sparse control structure selection and sparse controller design based on fuzzy model have been developed. In a bid to fill the gap, in this chapter, the study of [38] is extended to fuzzy area to present a guideline for sparse control system design based on both Type–1 and Type–2 T–S fuzzy models with simple and manageable calculations. For an MIMO process, the interactions between process inputs and outputs are analyzed in terms of RNGA loop pairing criterion to determine whether the coupling effects are strong enough that the MIMO process should choose sparse control over decentralized control, and a clear criterion is presented to uniquely determine a sparse control structure. By employing ETSMs, an independent design method is introduced so that the sparse controller design for an MIMO process can be converted to multiple independent single–loop controller designs. The proposed guideline gives an alternative to manipulate closely–coupled multivariable processes where mathematical models are unavailable, and it lays a basis to devise robust fuzzy controllers. Moreover, the comparative studies of Type–1 and Type–2 T–S fuzzy models can be carried out under this guideline. In the simulation section, the performances of ETF, Type–1 and Type–2 ETSM based sparse controls are provided and compared with each other as well as their decentralized control counterparts to demonstrate the effectiveness of the proposed method. Similar to the simulation in Chapter 4, parametric uncertainties are introduced to the process to show the robustness of these controllers.

5.2 Sparse control structure selection

According to RNGA based loop pairing criterion introduced in Chapter 3, the

decentralized control configuration for an MIMO process can be determined. By placing the paired loops in the diagonal position through column swapping, a decentralized controller for the MIMO process in a closed–loop control system as in Fig. 4.6 can be expressed as

$$\boldsymbol{G}_c = \begin{bmatrix} G_{c,1} & 0 & \cdots & 0 \\ 0 & G_{c,2} & \cdots & 0 \\ \vdots & \vdots & \ddots & \vdots \\ 0 & 0 & \cdots & G_{c,n} \end{bmatrix}_{n\times n} \tag{5.1}$$

Decentralized control utilizes the simplest control structure to manipulate an MIMO process, and it can work with satisfactory results when the interactions among the loops are not strong, when for closely–coupled processes, its limited structure may struggle with the interactions. On the other hand, a centralized controller using full–dimensional structure to eliminate interacting effects can be expressed as

$$\boldsymbol{G}_c = \begin{bmatrix} G_{c,11} & G_{c,12} & \cdots & G_{c,1n} \\ G_{c,21} & G_{c,22} & \cdots & G_{c,2n} \\ \vdots & \vdots & \ddots & \vdots \\ G_{c,n1} & G_{c,n2} & \cdots & G_{c,nn} \end{bmatrix}_{n\times n} \tag{5.2}$$

The disadvantage of the full–dimensional controller is that the computational cost will be greatly increased when compared with decentralized control, especially for large–scale processes where the calculations of high–dimensional matrices will be involved that may cause difficulties in the implementation.

To make a compromise between decentralized control structure as in Eq. (5.1) and centralized control structure as in Eq. (5.2), sparse control with the following structure can be employed.

$$\boldsymbol{G}_c = \begin{bmatrix} G_{c,11} & \kappa_{12}G_{c,12} & \cdots & \kappa_{1n}G_{c,1n} \\ \kappa_{21}G_{c,21} & G_{c,22} & \cdots & \kappa_{2n}G_{c,2n} \\ \vdots & \vdots & \ddots & \vdots \\ \kappa_{n1}G_{c,n1} & \kappa_{n2}G_{c,n2} & \cdots & G_{c,nn} \end{bmatrix} \tag{5.3}$$

where κ_{ij} is a selection index with value of 1 or 0. When $\kappa_{ij} = 1$, it means the off–diagonal controller $G_{c,ij}$ is added to the control structure, and when $\kappa_{ij} = 0$, it

means no controller in the position. If $\kappa_{ij}=0$ for $i,j=1,\cdots,n\,(i\neq j)$, Eq. (5.3) becomes a decentralized control as in Eq. (5.1), and if $\kappa_{ij}=1$ for $i,j=1,\cdots,n\,(i\neq j)$, Eq. (5.3) becomes a centralized controller as in Eq. (5.2). For sparse control, the values of κ_{ij}'s ($i,j=1,\cdots,n$, $i\neq j$) are not the same. Compared with decentralized control, sparse control can achieve improved performance in handling the influence of interactions, while its complexity is less than that of centralized control.

One of the key steps for sparse control development is to determine the values of κ_{ij}'s ($i,j=1,\cdots,n$, $i\neq j$) in Eq. (5.3) to select a proper control structure, which can be achieved by virtue of RNGA based loop pairing criterion. By swapping the column of fuzzy model matrix $\boldsymbol{F}_{TS}$, RGA $\boldsymbol{\Lambda}_{TS}$, RNGA $\boldsymbol{\Phi}_{TS}$ and relative normalized integrated error array $\boldsymbol{\Gamma}_{TS}$ to place the paired elements on the diagonal positions, an "interaction index", denoted by $\boldsymbol{B}_{TS}=\left[\beta_{TS,ij}\right]_{n\times n}$ can be defined as

$$\begin{aligned}\beta_{TS,ij}&=\left|\frac{\phi_{TS,ij}}{\phi_{TS,ii}}\right|=\left|\frac{k_{NTS,ij}/\hat{k}_{NTS,ij}}{k_{NTS,ii}/\hat{k}_{NTS,ii}}\right|=\left|\frac{k_{TS,ij}/\hat{k}_{TS,ij}}{k_{TS,ii}/\hat{k}_{TS,ii}}\cdot\frac{\hat{e}_{TS,ij}/e_{TS,ij}}{\hat{e}_{TS,ii}/e_{TS,ii}}\right|\\&=\left|\frac{\lambda_{TS,ij}}{\lambda_{TS,ii}}\cdot\frac{\gamma_{TS,ij}}{\gamma_{TS,ii}}\right|\end{aligned}\tag{5.4}$$

$\beta_{TS,ij}\,(j\neq i)$ can be utilized to analyze the steady and the dynamic interactions between paired and unpaired elements to determine the value of κ_{ij}. Two extreme cases of the values of $\beta_{TS,ij}$ are analyzed as follows [38].

1. $\beta_{TS,ij}$ is very small.

A very small value of $\beta_{TS,ij}$ means either $\left|\lambda_{TS,ij}/\lambda_{TS,ii}\right|$ is very small or $\left|\gamma_{TS,ij}/\gamma_{TS,ii}\right|$ is very small. A very small value of $\left|\lambda_{TS,ij}/\lambda_{TS,ii}\right|$ implies $\left|k_{TS,ij}\right|$ is much smaller than $\left|k_{TS,ii}\right|$, thus the steady–state effect on y_i from u_j is very little when compared with that from u_i. While a very small value of $\left|\gamma_{TS,ij}/\gamma_{TS,ii}\right|$

indicates $\left|e_{TS,ij}\right|$ is much smaller than $\left|e_{TS,ii}\right|$, thus the response speed of loop $y_i - u_j$ is very rapid when compared with that of loop $y_i - u_i$, which can be considered as a high–frequency interference and can be effectively filtered out by the paired loop with relative slow response speed.

2. $\beta_{TS,ij}$ is very large.

A very large value of $\beta_{TS,ij}$ means either $\left|\lambda_{TS,ij} / \lambda_{TS,ii}\right|$ is very large or $\left|\gamma_{TS,ij} / \gamma_{TS,ii}\right|$ is very large. A very large value of $\left|\lambda_{TS,ij} / \lambda_{TS,ii}\right|$ implies $\left|k_{TS,ij}\right|$ is much larger than $\left|k_{TS,ii}\right|$. If loop $y_i - u_j$ is included in the controller, the control system will be quite sensitive to modeling errors, which means a small modeling error or a small change in the control variable u_j will be magnified through this loop and result in a very large error in the output y_i, and then the control would be very hard to achieve for such a loop. On the other hand, a very large value of $\left|\gamma_{TS,ij} / \gamma_{TS,ii}\right|$ indicates $\left|e_{TS,ij}\right|$ is much larger than $\left|e_{TS,ii}\right|$, thus loop $y_i - u_j$ presents quite slow reactions and can be regarded as a constant disturbance that can be easily handled by the paired loop controller.

According to the above analysis, the off–diagonal loops with the value of $\beta_{TS,ij}$ neither too small nor too large should be considered into controller design. As in Fig. 4.6 where a closed–loop control system for an MIMO process is shown, it is easy to learn that in the controller matrix $\boldsymbol{G}_c$, $G_{c,ji}$ is the controller using d_i to determine control variable u_j, which implies $G_{c,ji}$ is based on y_i to calculate u_j. Therefore, in $\boldsymbol{G}_c$, the controller $G_{c,ji}$ related to loop $y_i - u_j$ is at the transposed position of $f_{TS,ij}$ in $\boldsymbol{F}_{TS}$. When the value of $\beta_{TS,ij}$ is modest, $\kappa_{ji} = 1$ to add controller $G_{c,ji}$ to $\boldsymbol{G}_c$ such that loop $y_i - u_j$ can be included into controller design. An example of determining sparse control structure for $\boldsymbol{G}_c$, based on selected elements in $\boldsymbol{F}_{TS}$, is

given as follows (with * in the positions of selected elements).

$$\boldsymbol{F}_{TS}=\begin{bmatrix} * & * & * & \\ & * & & \\ & & * & \\ * & & & * \end{bmatrix} \Rightarrow \boldsymbol{G}_c=\begin{bmatrix} * & & & * \\ * & * & & \\ * & & * & \\ & & & * \end{bmatrix}.$$

To develop an effective control structure that facilitate the controller design while saving the computational cost as much as possible, the following criterion to determine the value of κ_{ij} to select a proper sparse control structure can be used [38].

$$\kappa_{ij}=\begin{cases} 1, & 0.15 \le \beta_{TS,ji} \le 8 \\ 0, & \text{otherwise} \end{cases} \quad \text{for } i \ne j \tag{5.5}$$

Remark 5.1: Since the RGA $\boldsymbol{\Lambda}_{TS}$ and RNGA $\boldsymbol{\Phi}_{TS}$ for a 2×2 process is symmetric, the control type for 2×2 process is either centralized structure or decentralized structure. Whereas for an $n\times n$ process with $n>2$, sparse control can be applied. In the practical applications, it is rare to find a process suitable for centralized control or full decoupling control, therefore, decentralized control of sparse control methods are generally more appropriate for MIMO control system designs [38].

5.3 Independent design based on ETSMs

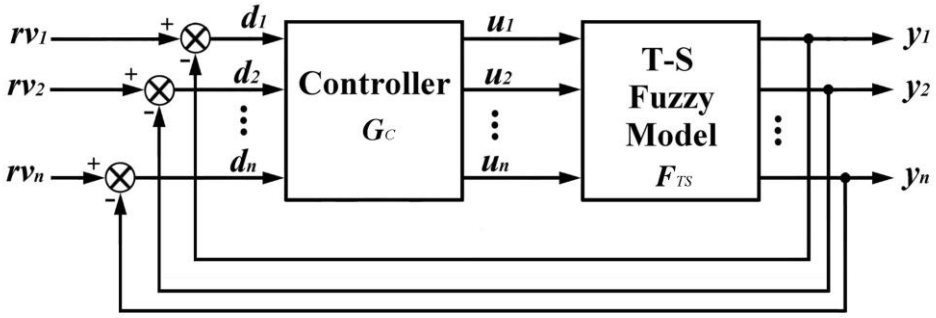

Figure 5.1 A closed–loop MIMO control system

The fuzzy model matrix for an MIMO process is a discrete system that can be denoted by $\boldsymbol{F}_{TS}(z^{-1})=\left[\, f_{TS,ij}(z^{-1})\right]_{n\times n}$. As the closed–loop control system shown in Fig. 5.1, a general controller design pattern is to satisfy

$$\boldsymbol{F}_{TS}(z^{-1})\boldsymbol{G}_c(z^{-1}) \approx \frac{T}{1-z^{-1}}\cdot \boldsymbol{I} \tag{5.6}$$

where $\boldsymbol{I}$ is an identity matrix. The controller matrix can then be obtained by

$$\boldsymbol{G}_c(z^{-1}) \approx \boldsymbol{F}_{TS}^{-1}(z^{-1}) \cdot \frac{T}{1-z^{-1}} \tag{5.7}$$

Given the nonlinear nature and special structure with "IF–THEN" rules of a T–S fuzzy model, it is quite difficult or even impossible to directly calculate the inverse matrix $\boldsymbol{F}_{TS}^{-1}(z^{-1})$, which causes an obstacle in devising the control system $\boldsymbol{G}_c(z^{-1})$. In this section, an independent controller design method based on ETSMs for sparse control is introduced to provide a simple and feasible manner to solve this problem.

The calculating method to obtain ETSM introduced in Chapter 4 can be used for paired loops while may not be applicable to other loops since their $\lambda_{TS,ij}$'s and $\gamma_{TS,ij}$'s may be negative, and $\gamma_{TS,ij}$'s may not be close to 1. Hence the ETSM calculating method given in Chapter 4 is revised for deriving the ETSMs of unpaired elements as shown in Table 5.1.

Table 5.1 Coefficient calculations of ETSMs for unpaired loops in different cases

Interacting Cases	Values of coefficients $\hat{a}_{ij,r}^{l}$	$\hat{a}_{ij,lb,r}^{l}$ and $\hat{a}_{ij,rb,r}^{l}$	$\hat{\tau}_{ij}$
1. $\lvert\lambda_{TS,ij}\rvert \le 1, \lvert\gamma_{TS,ij}\rvert > 1$	By Eq. (4.7)	By Eq. (4.16)	By Eq. (4.10)
2. $\lvert\lambda_{TS,ij}\rvert \le 1, \lvert\gamma_{TS,ij}\rvert \le 1$	By Eq. (4.7)	By Eq. (4.16)	$\hat{\tau}_{ij} = \tau_{ij}$
3. $\lvert\lambda_{TS,ij}\rvert > 1, \lvert\gamma_{TS,ij}\rvert > 1$	$\text{sign}(\lambda_{TS,ij}) \cdot a_{ij,r}^{l}$	$\begin{cases} \hat{a}_{ij,lb,r}^{l} = \text{sign}(\lambda_{TS,ij}) \cdot a_{ij,lb,r}^{l} \\ \hat{a}_{ij,rb,r}^{l} = \text{sign}(\lambda_{TS,ij}) \cdot a_{ij,rb,r}^{l} \end{cases}$	By Eq. (4.10)
4. $\lvert\lambda_{TS,ij}\rvert > 1, \lvert\gamma_{TS,ij}\rvert \le 1$	$\text{sign}(\lambda_{TS,ij}) \cdot a_{ij,r}^{l}$	$\begin{cases} \hat{a}_{ij,lb,r}^{l} = \text{sign}(\lambda_{TS,ij}) \cdot a_{ij,lb,r}^{l} \\ \hat{a}_{ij,rb,r}^{l} = \text{sign}(\lambda_{TS,ij}) \cdot a_{ij,rb,r}^{l} \end{cases}$	$\hat{\tau}_{ij} = \tau_{ij}$

Subsequently, based on the fuzzy model matrix $\boldsymbol{F}_{TS}$, for an $n \times n$ MIMO process, we can obtain an ETSM matrix $\hat{\boldsymbol{F}}_{TS}$ expressed as

$$\hat{\boldsymbol{F}}_{TS} = \left[\hat{f}_{TS,ij} \right]_{n\times n} = \begin{bmatrix} \hat{f}_{TS,11} & \hat{f}_{TS,12} & \cdots & \hat{f}_{TS,1n} \\ \hat{f}_{TS,21} & \hat{f}_{TS,22} & \cdots & \hat{f}_{TS,2n} \\ \vdots & \vdots & \ddots & \vdots \\ \hat{f}_{TS,n1} & \hat{f}_{TS,n2} & \cdots & \hat{f}_{TS,nn} \end{bmatrix} \tag{5.8}$$

where $\hat{\boldsymbol{F}}_{TS}$ is a discrete system denoted by $\hat{\boldsymbol{F}}_{TS}(z^{-1}) = \left[\hat{f}_{TS,ij}(z^{-1}) \right]_{n\times n}$. For loop $y_i - u_j$, the interactions from other closed–loops can be measured using dynamic relative gain defined as [55, 59, 75]

$$\lambda_{TS,ij}(z^{-1}) = \frac{f_{TS,ij}(z^{-1})}{\hat{f}_{TS,ij}(z^{-1})} = f_{TS,ij}(z^{-1}) \cdot \hat{f}^{-1}_{TS,ij}(z^{-1}) \tag{5.9}$$

Let $\hat{\boldsymbol{F}}^{*}_{TS}(z^{-1}) = \left[\hat{f}^{-1}_{TS,ij}(z^{-1}) \right]_{n\times n}$, according to Eq. (5.9), for the overall process, the dynamic RGA can be derived as

$$\boldsymbol{\Lambda}_{TS}(z^{-1}) = \left[\lambda_{TS,ij}(z^{-1}) \right]_{n\times n} = \boldsymbol{F}_{TS}(z^{-1}) \otimes \hat{\boldsymbol{F}}^{*}_{TS}(z^{-1}) \tag{5.10}$$

According to the calculation of $\boldsymbol{\Lambda}_{TS}$ as in Eq. (3.6), the dynamic RGA can be calculated as

$$\boldsymbol{\Lambda}_{TS}(z^{-1}) = \boldsymbol{F}_{TS}(z^{-1}) \otimes \boldsymbol{F}^{-T}_{TS}(z^{-1}) \tag{5.11}$$

Comparing Eq. (5.10) with Eq. (5.11), an important relationship can be revealed as

$$\boldsymbol{F}^{-1}_{TS}(z^{-1}) = \left(\hat{\boldsymbol{F}}^{*}_{TS}(z^{-1}) \right)^{T} = \begin{bmatrix} \hat{f}^{-1}_{TS,11} & \hat{f}^{-1}_{TS,21} & \cdots & \hat{f}^{-1}_{TS,n1} \\ \hat{f}^{-1}_{TS,12} & \hat{f}^{-1}_{TS,22} & \cdots & \hat{f}^{-1}_{TS,n2} \\ \vdots & \vdots & \ddots & \vdots \\ \hat{f}^{-1}_{TS,1n} & \hat{f}^{-1}_{TS,2n} & \cdots & \hat{f}^{-1}_{TS,nn} \end{bmatrix} \tag{5.12}$$

By considering Eq. (5.12), Eq. (5.7) can be rewritten as

$$\boldsymbol{G}_c(z^{-1}) \approx \hat{\boldsymbol{F}}^{-1}_{TS}(z^{-1}) \cdot \frac{T}{1-z^{-1}} = \left(\hat{\boldsymbol{F}}^{*}_{TS}(z^{-1}) \right)^{T} \cdot \frac{T}{1-z^{-1}} \tag{5.13}$$

Let the error function for Eq. (5.13) be defined as

$$\boldsymbol{J}(z^{-1}) = \left[J_{ij}(z^{-1}) \right]_{n\times n} = \boldsymbol{G}_c(z^{-1}) - \left(\hat{\boldsymbol{F}}^{*}_{TS}(z^{-1}) \right)^{T} \cdot \frac{T}{1-z^{-1}} \tag{5.14}$$

and an index function $\boldsymbol{J}_{\min}$ for minimizing the error function $\boldsymbol{J}(z^{-1})$ in Eq. (5.14)

can be defined as the minimum value of the sum of the absolute error between each element in $\boldsymbol{G}_c(z^{-1})$ and $\left(\hat{\boldsymbol{F}}_{TS}^{*}(z^{-1})\right)^{T}\cdot T/(1-z^{-1})$ as

$$\boldsymbol{J}_{\min}=\min\sum_{i=1}^{n}\sum_{j=1}^{n}\left|J_{ij}(z^{-1})\right|=\min\sum_{i=1}^{n}\sum_{j=1}^{n}\left|G_{c,ij}(z^{-1})-\hat{f}_{TS,ji}^{-1}\cdot T/(1-z^{-1})\right| \qquad (5.15)$$

Form Eq. (5.15), the minimization of $\boldsymbol{J}(z^{-1})$ requires the controller $G_{c,ij}(z^{-1})$ where $\kappa_{ij}\neq 0$ is determined by

$$G_{c,ij}(z^{-1})-\hat{f}_{TS,ji}^{-1}\cdot T/(1-z^{-1})=0 \;\Rightarrow\; G_{c,ij}(z^{-1})\cdot\hat{f}_{TS,ji}=T/(1-z^{-1}) \qquad (5.16)$$

In Eq. (5.16), $G_{c,ij}(z^{-1})\cdot\hat{f}_{TS,ji}$ can be regarded as the forward function of a closed–loop SISO control system as shown in Fig. 5.2.

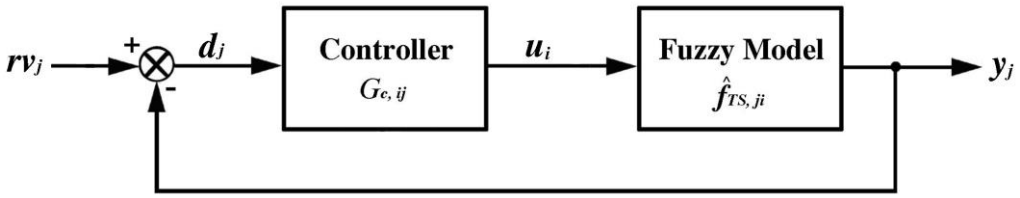

Figure 5.2 A closed–loop SISO control system

And the controller $G_{c,ij}(z^{-1})$ that satisfies Eq. (5.16) is the objective of a general controller design pattern for SISO processes similar to that in Eq. (5.6) for MIMO processes. Therefore, based on ETSMs, each element of $\boldsymbol{G}_c$ can be independently designed using SISO control algorithms to realize a multivariable control system and avoid directly calculating inverse matrix $\boldsymbol{F}_{TS}^{-1}(z^{-1})$.

The steps of using the proposed method to devise sparse control for an MIMO process are briefly given as follows.

i). At an operating condition, determine paired loops using RNGA based criterion, and then select several unpaired elements according to Eq. (5.5).

ii). According to the information provided by the RNGA based criterion, scale the individual T–S fuzzy model coefficients of each selected loop to obtain ETSMs.

Afterwards independently devise a SISO controller for each ETSM through linear control algorithms to form a sparse control system for the whole process.

iii). When the operating condition changes, repeat step i) and step ii) to update control structure and the ETSMs for sparse control variable calculations.

The significances of the proposed guideline including control structure selection and ETSM based independent design for sparse control include the following.

- The guideline is implemented based on T–S fuzzy models that can be built from data samples, which provides an alternative where the accurate mathematical models of the processes are unavailable. It offers a basis to develop robust fuzzy controllers. Moreover, only the information of the identifiable individual open–loop models is utilized. Therefore, this method is effective and feasible in real MER control applications.
- The guideline provides a clear, reasonable and low–computational–cost manner to select the off–diagonal loops for sparse controller design. And when the working condition changes, the control structure and the corresponding ETSMs can be rapidly updated, which makes it suitable to be applied in real–time control systems.
- The sparse controller for an MIMO process can be achieved by independently designing a SISO controller for each selected loop based on the ETSM, which can greatly reduce the computational complexity. Furthermore, since linear control algorithms can be applied to develop control systems based on ETSMs, this method provides a way to employ the simple and mature linear SISO control algorithms to manipulate complex and closely–coupled nonlinear MER systems.
- This method can be applied on both Type–1 and Type–2 T–S fuzzy models to devise sparse control under a uniform frame for an MIMO process, which provides a platform to carry out the comparative studies of these two types of T–S fuzzy model to demonstrate and analyze their properties and differences.

5.4 Simulation

Consider the 3×3 nonlinear MIMO process in Eq. (4.34), given the operating points as $\boldsymbol{x}_{0,ij}=\left[u_{0,j}(k_0-\tau_{ij}) \quad y_{0,i}(k_0-1) \quad y_{0,i}(k_0-2)\right]=\left[0 \quad 0 \quad 0\right]$ for $i,j=1,2,3$, based on the Type–1 T–S fuzzy model matrix, $\boldsymbol{K}_{TS}$, $\boldsymbol{E}_{TS}$, $\boldsymbol{\Lambda}_{TS}$, $\boldsymbol{\Phi}_{TS}$ and $\boldsymbol{\Gamma}_{TS}$ can be calculated. Place the paired loops in the diagonal positions through column swap, we can have the following arrays.

$$\boldsymbol{K}_{TS}=\begin{bmatrix}1.0782 & 1.2565 & 0.9784\\ 0.2905 & 2.1238 & 0.5486\\ 0.1313 & 0.2493 & 0.6743\end{bmatrix},\quad \boldsymbol{E}_{TS}=\begin{bmatrix}2.1538 & 2.1954 & 2.5234\\ 1.1021 & 2.8221 & 3.5756\\ 6.9247 & 2.1872 & 2.3181\end{bmatrix}$$

$$\boldsymbol{\Lambda}_{TS}=\begin{bmatrix}1.3442 & -0.1498 & -0.1944\\ -0.1687 & 1.2235 & -0.0548\\ -0.1755 & -0.0737 & 1.2492\end{bmatrix},\quad \boldsymbol{\Phi}_{TS}=\begin{bmatrix}1.5577 & -0.6522 & 0.0945\\ -0.4980 & 1.6075 & -0.1095\\ -0.0598 & -0.0447 & 1.0150\end{bmatrix}$$

$$\boldsymbol{\Gamma}_{TS}=\begin{bmatrix}1.1589 & 4.3545 & -0.4861\\ 2.9520 & 1.3138 & 1.9981\\ 0.3405 & -0.6065 & 0.8125\end{bmatrix}$$

Based on $\boldsymbol{\Phi}_{TS}$, the interaction index $\boldsymbol{B}_{TS}$ for Type–1 T–S fuzzy model matrix can be derived as

$$\boldsymbol{B}_{TS}=\begin{bmatrix}1.0000 & \mathbf{0.4187} & 0.0607\\ \mathbf{0.3098} & 1.0000 & 0.0681\\ 0.0589 & 0.0441 & 1.0000\end{bmatrix} \tag{5.17}$$

According to Eq. (5.5), two off–diagonal loops (their $\beta_{TS,ij}$'s in $\boldsymbol{B}_{TS}$ of Eq. (5.17) are in bold) should be selected and added to the controller design.

Based on Type–2 T–S fuzzy model matrix, $\boldsymbol{K}_{TS}$, $\boldsymbol{E}_{TS}$, $\boldsymbol{\Lambda}_{TS}$, $\boldsymbol{\Phi}_{TS}$ and $\boldsymbol{\Gamma}_{TS}$ can be computed. Placing the paired elements of these matrices in the diagonal positions through column swap yields

$$\boldsymbol{K}_{TS}=\begin{bmatrix}1.0750 & 1.2502 & 0.9762\\ 0.2902 & 2.1205 & 0.5480\\ 0.1316 & 0.2481 & 0.6724\end{bmatrix},\quad \boldsymbol{E}_{TS}=\begin{bmatrix}2.1479 & 2.1939 & 2.5221\\ 1.1018 & 2.8188 & 3.5633\\ 6.8859 & 2.1847 & 2.3172\end{bmatrix}$$

$$\boldsymbol{\Lambda}_{TS}=\begin{bmatrix}1.3453 & -0.1492 & -0.1961\\ -0.1685 & 1.2228 & -0.0543\\ -0.1768 & -0.0736 & 1.2504\end{bmatrix},\quad \boldsymbol{\Phi}_{TS}=\begin{bmatrix}1.5548 & -0.6478 & 0.0930\\ -0.4946 & 1.6039 & -0.1093\\ -0.0602 & 0.0439 & 1.0163\end{bmatrix}$$

$$\boldsymbol{\Gamma}_{TS}=\begin{bmatrix}1.1557 & 4.3415 & -0.4742\\ 2.9356 & 1.3117 & 2.0119\\ 0.3403 & -0.5960 & 0.8127\end{bmatrix}$$

Based on $\boldsymbol{\Phi}_{TS}$, the interaction index $\boldsymbol{B}_{TS}$ for Type–2 T–S fuzzy model matrix can be obtained as

$$\boldsymbol{B}_{TS}=\begin{bmatrix}1.0000 & \mathbf{0.4167} & 0.0598\\ \mathbf{0.3084} & 1.0000 & 0.0681\\ 0.0592 & 0.0432 & 1.0000\end{bmatrix} \tag{5.18}$$

The two off–diagonal loops selected based on Type–2 T–S fuzzy models are the same as that selected based on Type–1 T–S fuzzy models (their $\beta_{TS,ij}$'s in $\boldsymbol{B}_{TS}$ of Eq. (5.18) are in bold). And these two elements are loop y_2-u_3 and loop y_1-u_1 in the original process. Therefore, the selected loops for controller design in $\boldsymbol{F}_{TS}$ of the original MIMO process in Eq. (4.34) can be expressed as (set 0 to the unselected elements)

$$\boldsymbol{F}_{TS}=\begin{bmatrix}f_{TS,11} & 0 & f_{TS,13}\\ f_{TS,21} & 0 & f_{TS,23}\\ 0 & f_{TS,32} & 0\end{bmatrix} \tag{5.19}$$

And then the controller matrix is

$$\boldsymbol{G}_c=\begin{bmatrix}G_{c,11} & G_{c,12} & 0\\ 0 & 0 & G_{c,23}\\ G_{c,31} & G_{c,32} & 0\end{bmatrix} \tag{5.20}$$

Based on the ETSMs of the selected loops, each nonzero element in $\boldsymbol{G}_c$ of Eq. (5.20) can be designed independently using linear SISO control algorithms. Same as the decentralized control simulation in Section 4.4, in this section, the gain and phase margins based control algorithm introduced in Section 4.3 using $A_{m,i}=3$ and $\Psi_{m,i}=\pi/3$ is employed to devise both Type–1 and Type–2 ETSM based sparse

control systems. And the sparse controller based on ETFs in terms of RNGA pairing criterion [38] is also calculated for comparison (the details are presented in Appendix B). Set reference values same as that in the simulation of Chapter 4 which are $rv_1 = 1.5$, $rv_2 = 1$ and $rv_3 = 0$, the performances of these sparse control systems when manipulating the MIMO process in Eq. (4.34) without uncertainty are shown in Fig. 5.3. The IAEs of three outputs under Type–1 and Type–2 ETSM based sparse controls in this case are presented in Table 5.2. And the comparisons between these sparse controllers and their decentralized counterparts in this case are given in Fig. 5.4.

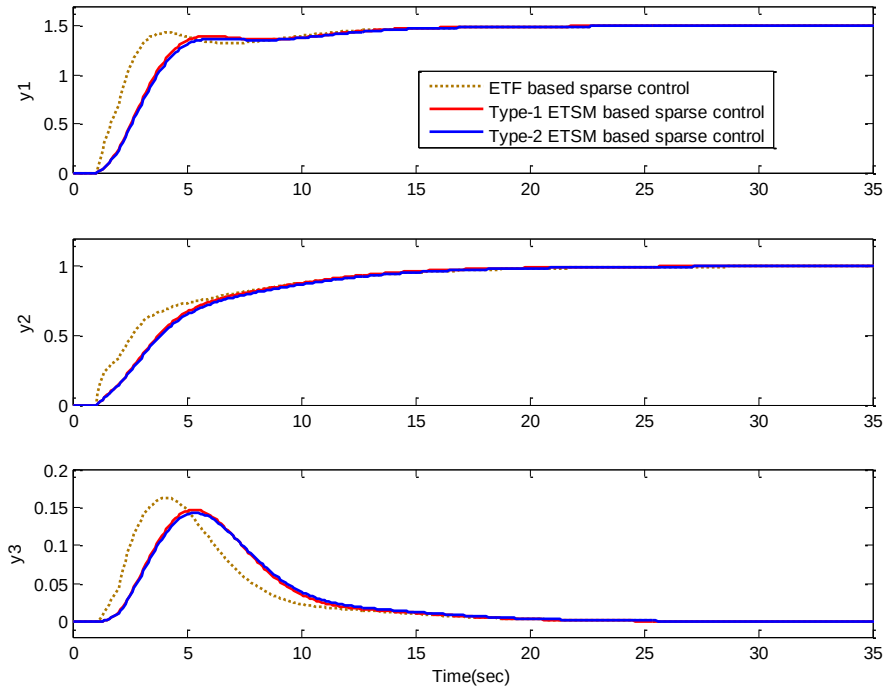

Figure 5.3 Sparse controls for the MIMO process in Eq. (4.34)

Table 5.2 The IAEs of Type–1 and Type–2 ETSM based sparse controls for the process in Eq. (4.34)

Type of fuzzy model	IAE(y_1)	IAE(y_2)	IAE(y_3)
Type–1	6.0915	5.4253	0.9012
Type–2	5.8638	5.2152	0.8892

As can be seen in Fig. 5.3 and Table 5.2, Type–1 and Type–2 ETSM based sparse controllers achieve comparable performances with close IAE values. And both of them can obtain better results than ETF based sparse controller. And as the comparisons

illustrated in Fig. 5.4, sparse controllers can achieve smaller overshoots in the outputs than their decentralized controller counterparts.

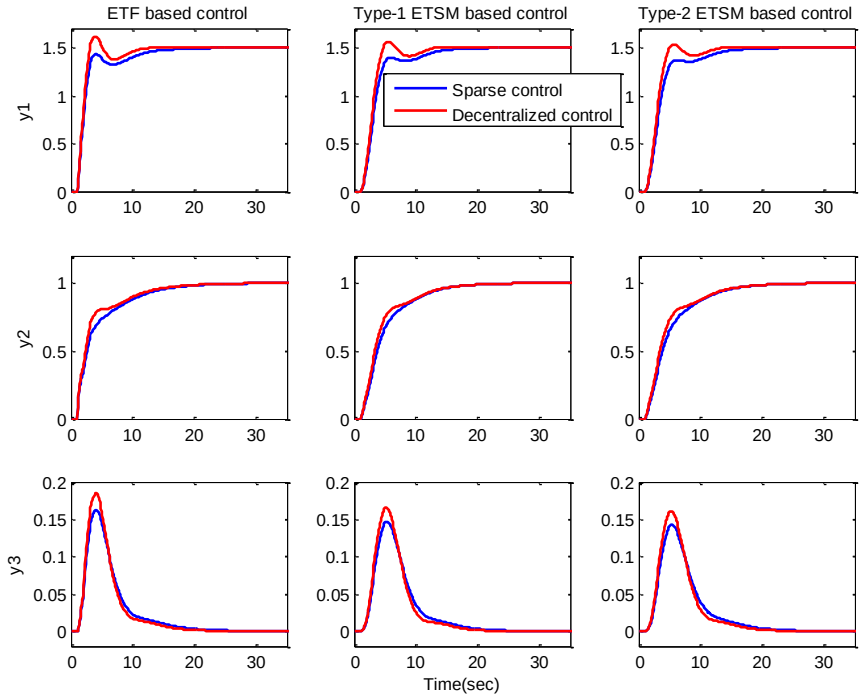

Figure 5.4 The comparisons of sparse and decentralized controls for the MIMO process in Eq. (4.34)

To test the robustness of these sparse controllers, similar as that in Section 4.4, parametric uncertainty is introduced to the process and then these sparse control systems designed based on original process are applied to manipulate the changed process. Consider the process with changed equation as in Eq. (4.36) where $\dot{x}_3 = x_4 + 2.31u_1$, the performances of ETF and ETSM based sparse controllers in this case are shown in Fig. 5.5. The IAEs of Type–1 and Type–2 ETSM based sparse controls are given in Table 5.3. And the comparisons between sparse control and decentralized control in this case are given in Fig. 5.6.

Table 5.3 The IAEs of Type–1 and Type–2 ETSM based sparse controls for the process changed as Eq. (4.36)

Type of fuzzy model	IAE(y_1)	IAE(y_2)	IAE(y_3)
Type–1	13.7481	7.7032	4.6465
Type–2	12.0882	6.8659	4.0580

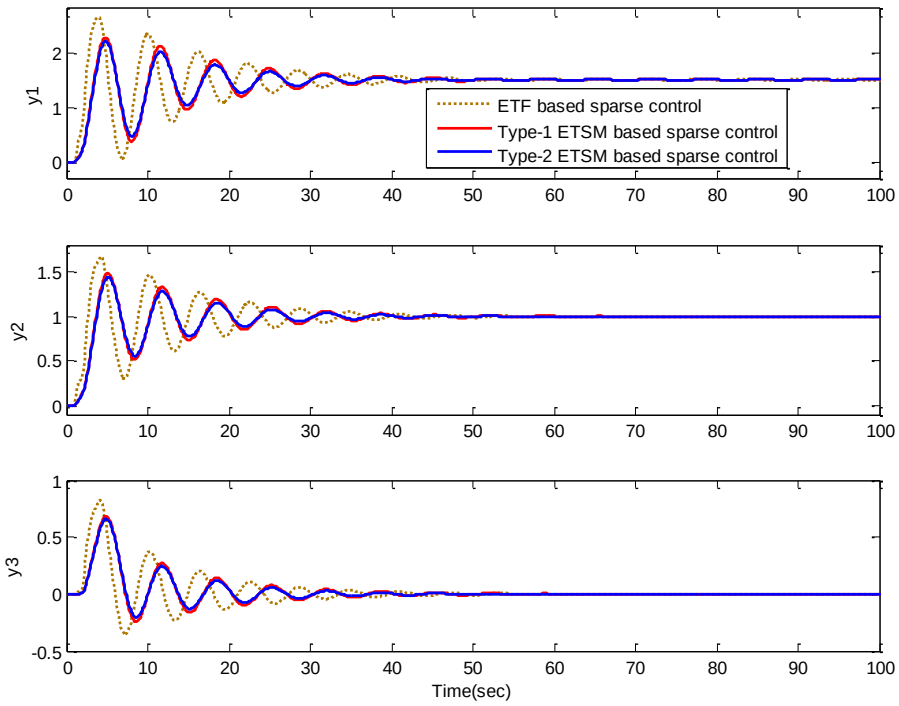

Figure 5.5 Sparse controls for the process changed as Eq. (4.36)

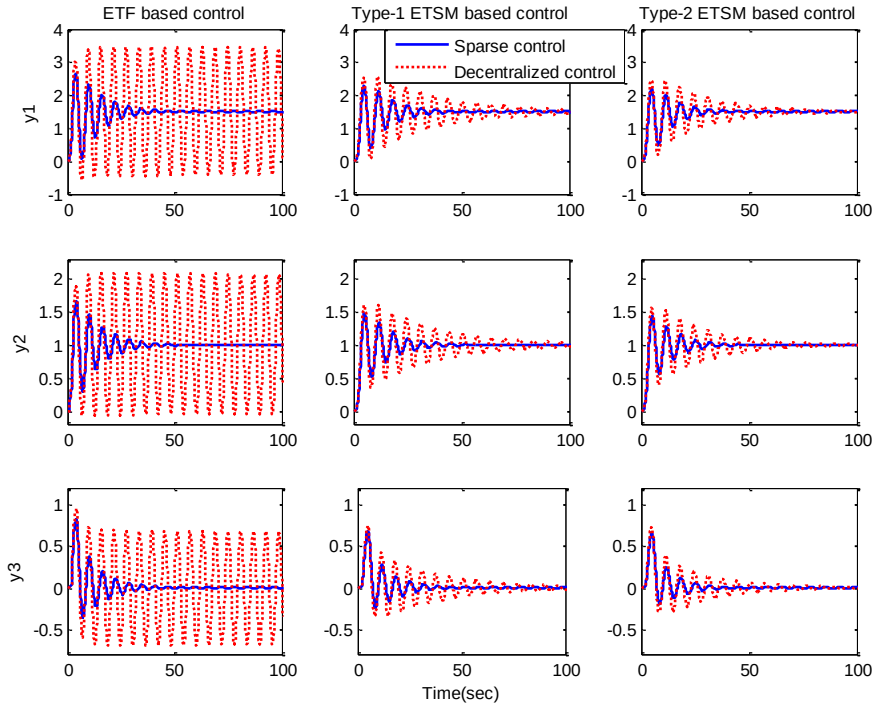

Figure 5.6 The comparisons of sparse and decentralized controls for the process changed as Eq. (4.36)

From Fig. 5.5, it can be seen that ETSM based controls can give better results when compared with ETF based control. And Type–2 ETSM based sparse control can achieve a little smaller amplitude of oscillation than Type–1 ETSM based sparse

control, which can be proved by the values of IAEs that the error accumulations of the outputs under the Type–2 ETSM based control are smaller than that under the Type–1 ETSM based control. The comparisons in Fig. 5.6 demonstrate that ETF based sparse control can make the outputs reach the references stably in this case while its decentralized control cannot, and both Type–1 and Type–2 ETSM based sparse controls outperform their decentralized control counterparts with respect to the amplitude of oscillation and settling time.

When the parametric uncertainty is further enlarged as in Eq. (4.37) where $\dot{x}_3 = x_4 + 2.5u_1$, the performances of ETF and ETSM based sparse controllers and the comparisons of sparse and decentralized control are illustrated in Fig. 5.7 and Fig. 5.8,

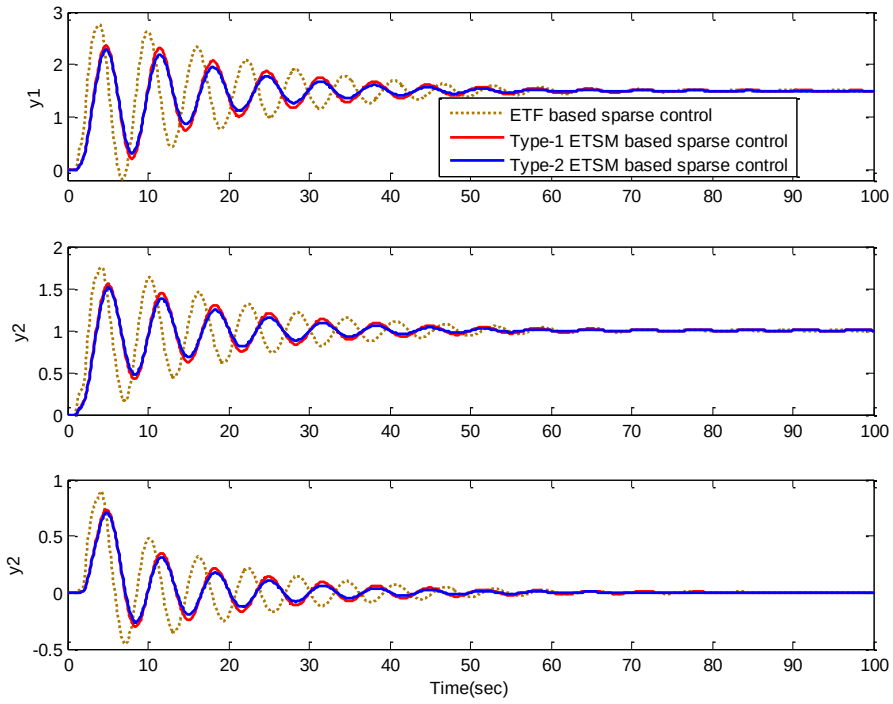

Figure 5.7 Sparse controls for the process changed as Eq. (4.37)

Table 5.4 The IAEs of Type–1 and Type–2 ETSM based sparse controls for the process changed as Eq. (4.37)

Type of fuzzy model	IAE(y_1)	IAE(y_2)	IAE(y_3)
Type–1	18.5367	10.3292	6.4409
Type–2	15.5261	8.7686	5.3595

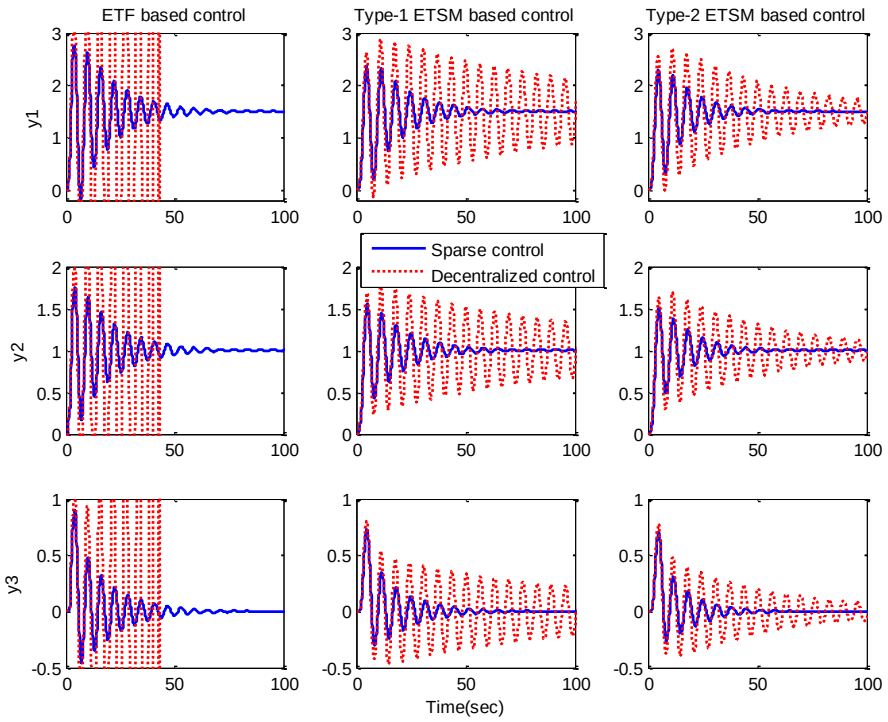

Figure 5.8 The comparisons of sparse and decentralized controls for the process changed as Eq. (4.37)

respectively. And the IAEs of Type–1 and Type–2 ETSM based sparse controls are presented in Table 5.4. In this case, ETSM based sparse controls can still provide smaller oscillations than ETF based sparse control. The superiority of Type–2 ETSM based sparse control over Type–1 ETSM based sparse control with respect to oscillation amplitudes and error accumulations as shown in Fig. 5.7 and Table 5.4 is more apparent than that in Fig. 5.5 and Table 5.3. According to the comparison in Fig. 5.8, three sparse control systems can achieve much better performance than their decentralized control counterparts.

To clearly demonstrate the robustness of these sparse controllers, the parametric uncertainty can be further enlarged as follows

$$\dot{x}_3 = x_4 + 2.95u_1 \tag{5.21}$$

In this case, the process under ETF based sparse control becomes unstable and divergent as in Fig. 5.9, while the process under both Type–1 and Type–2 ETSM based sparse controllers is still stable as shown in Fig. 5.10. And their IAEs are presented in Table 5.5. From Fig. 5.10 it can be seen that as the degree of parametric uncertainty

increases, the advantage of Type–2 fuzzy system over Type–1 fuzzy system in terms of robustness become more evident that the process outputs under Type–2 ETSM based sparse control have smaller oscillations and much smaller settling time than that under Type–1 ETSM based sparse control. And the IAEs in Table 5.5 demonstrate that the error accumulations of the outputs under Type–2 ETSM based sparse control are much smaller than that under Type–1 ETSM based sparse control in this case.

Table 5.5 The IAEs of Type–1 and Type–2 ETSM based sparse controls for the process changed as Eq. (5.21)

Type of fuzzy model	IAE(y_1)	IAE(y_2)	IAE(y_3)
Type–1	134.6823	74.5896	49.7393
Type–2	56.0107	31.3793	20.5908

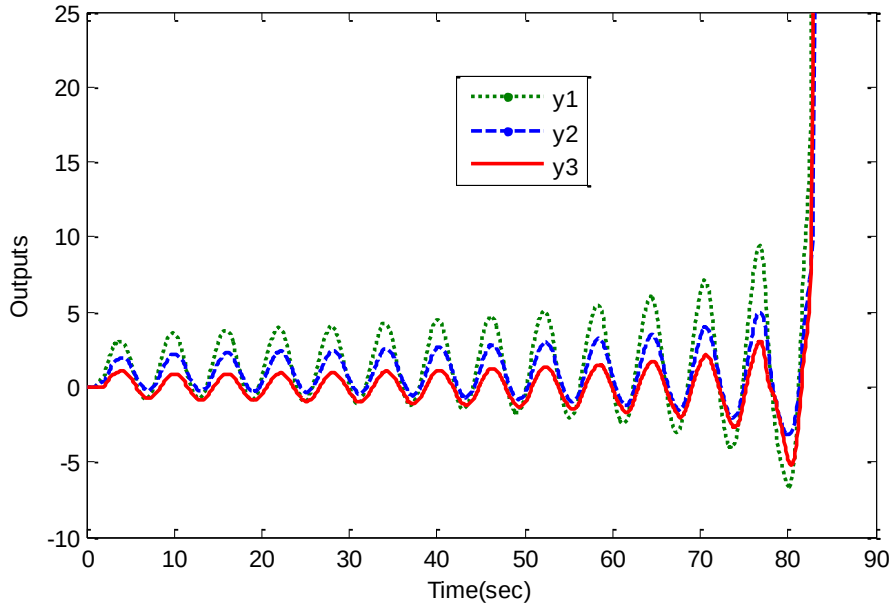

Figure 5.9 ETF based sparse control for the process changed as Eq. (5.21)

Remark 5.2: The simulation results prove that by adding several off–diagonal controllers to the control structure, sparse control has the capability to achieve much better results than decentralized control that it can be applied to manipulate the process with strong interacting effects and uncertainties where decentralized control is not able to provide satisfactory results. The sparse controllers based on Type–1 and Type–2 fuzzy models perform comparably when the process is under the uncertainty with the degree that Type–1 fuzzy model can handle. When larger uncertainties appear, it is

proved that Type–2 fuzzy model can give more robust performance than Type–1 fuzzy model. Since the computational cost and complexity based on Type–2 fuzzy system in respect of modeling, loop pairing, sparse control structure selection and controller design are more than that based on Type–1 fuzzy model, in order to use minimum cost to achieve satisfactory control results in the applications, the degree of uncertainty, the expectation of modeling accuracy and the requirement of controller robustness should be well considered when making decision of the selection between Type–1 and Type–2 fuzzy systems.

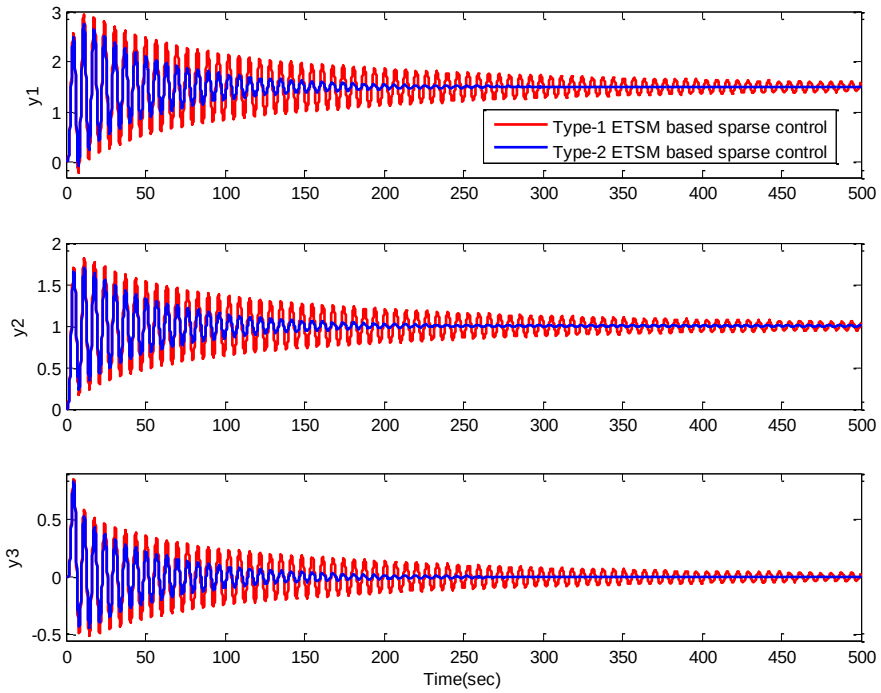

Figure 5.10 ETSM based sparse controls for the process changed as Eq. (5.21)

5.5 Summary

In a bid to improve the control performance for strong coupling MIMO processes of MER systems, a guideline to devise T–S fuzzy model based sparse control was presented in this chapter. Through analyzing the interactions using RNGA for an MIMO process, a selecting criterion that adding several off–diagonal controllers to the diagonal control structure to form a sparse control structure is given. Afterwards, an independent design method was introduced that the sparse control system design for an MIMO process can be transformed to a group of independent SISO controllers in

terms of ETSMs. This guideline paves the way to utilize linear SISO control algorithms to manipulate nonlinear and strongly coupled MIMO processes, and robust controller can be derived since fuzzy system is powerful to handle the uncertainties. Moreover, the comparative research of Type–1 and Type–2 fuzzy systems can be launched to analyze and study their properties. The simulation results demonstrate that sparse control outperforms its decentralized control counterpart. And compared with the ETF based sparse control, both Type–1 and Type–2 ETSM based sparse controls can obtain better performances. As the degree of uncertainty increases, control system based on Type–2 ETSMs is able to achieve more robust and satisfactory results than that based on Type–1 ETSMs. In the next chapter, the proposed methods in this thesis are applied to an experimental MER system to demonstration their practicability and effectiveness in MER systems.

Chapter 6. Applications in MER systems

6.1 Introduction

In this chapter, the proposed Type–1 and Type–2 T–S fuzzy model based methods are applied to evaluate the interactions, select control structures and design decentralized and sparse controllers for an experimental MER system. The photo of this system is shown in Fig. 6.1. Its schematic diagram and the corresponding pressure (P)–enthalpy (h) chart are given in Fig. 6.2 and Fig. 6.3. This MER system utilizes a single compressor (COMP) and a single condenser (COND) but three evaporators (EVAP1, EVAP2 and EVAP3) each working at a specified evaporating temperatures to simultaneously cater for three different cooling requirements: air–conditioning, food storage and freezing. In this experimental MER system, the pressure regulation (PR) is composed of throttles, and R134a is used as the refrigerant. For EVAP1, water is used as heat transfer fluid to convey the cooling to meet the air–conditioning requirements. And for EVAP 2 (food storage) and EVAP3 (freezing) whose evaporating temperatures are low that water may be frozen, ethylene glycol solution is used instead.

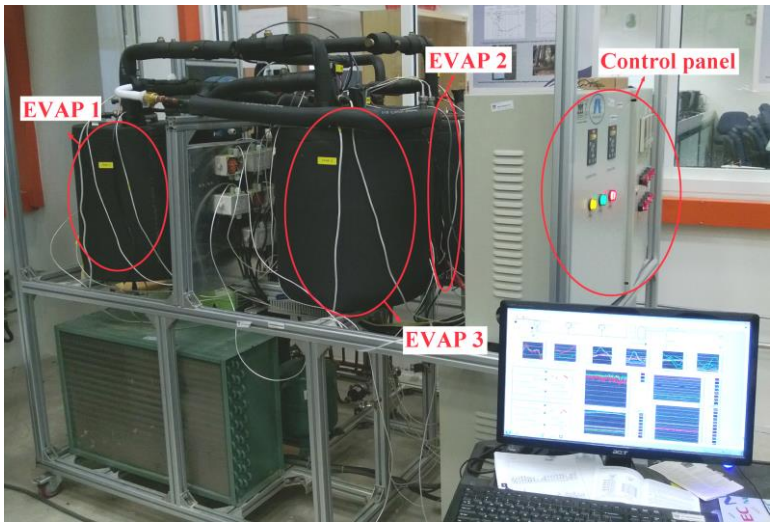

Figure 6.1 An experimental MER system

As shown in Fig. 6.2 and Fig. 6.3, the working process of this MER system can be introduced by the following steps.

1). The refrigerant as a saturated vapor with a low pressure at state **1** enters the

compressor and is compressed isentropically to a superheated vapor with a high pressure at state **2**.

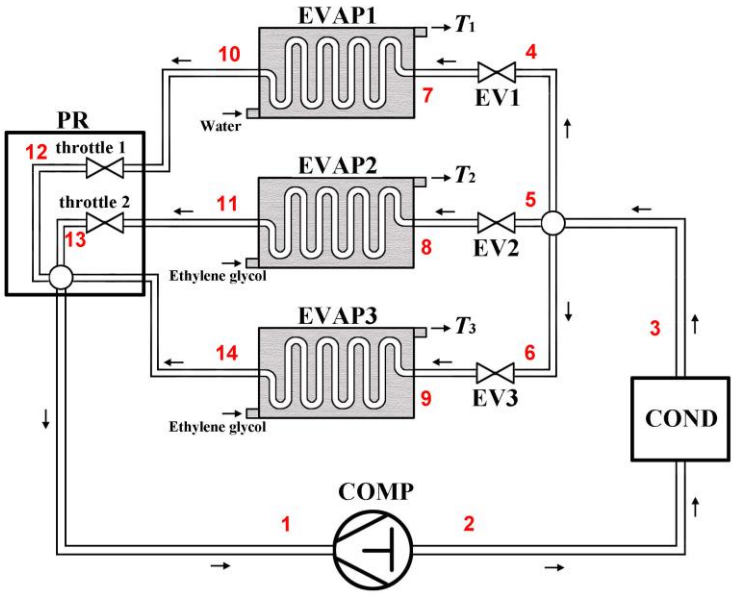

Figure 6.2 Schematic diagram of the MER system

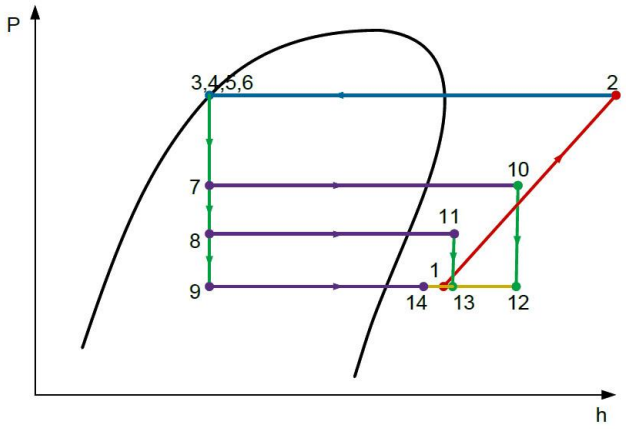

Figure 6.3 Pressure (P)–enthalpy (h) chart of the MER system

2). The superheated refrigerant enters into the condenser where it is cooled and condensed into liquid phase at state **3** by rejecting heat to the external environment.

3). The sub–cooled liquid refrigerant at a high pressure is divided into three flows (states **4**, **5** and **6)**, which go into EVAP1 (state **7**), EVAP2 (state **8**) and EVAP3 (state **9**) after reducing the pressures through EV1, EV2, and EV3 respectively.

4). By absorbing heats from the ambient environments of the evaporators, the three refrigerant flows evaporate at specified temperatures to become saturated vapor at

states **10**, **11** and **14**.

5). In the PR, the flows at state **10** and state **11** are throttled to state **12** and state **13** respectively such that their pressures are equal to that of the flow at state **14** from EVAP3 which has the lowest evaporating pressure and temperature.

6). The three flows of states **12**, **13** and **14** mix up into one flow at state **1** and return to compressor to complete the entire refrigeration cycle of this MER system.

6.2 Experimental results of MER system control

In the experiment, the compressor power and the speeds of fans in this MER system are fixed. The flow rate of refrigerant in three evaporators can be adjusted to satisfy different cooling loads through regulating the opening degrees of three EVs. And the opening change in any one of the EVs will have impacts on three refrigerant flow rates of three evaporators subsequently affect the temperatures of heat transfer fluids T_1, T_2 and T_3 as shown in Fig. 6.2. Therefore, an interconnected three–input–three–output (3×3) process can be formed where the three EV opening degrees are used to manipulate the heat transfer fluid temperatures of three evaporators.

The designed working condition for this MER system is that the heat transfer fluid temperatures of three evaporators related to air–conditioning, food storage and freeze are $T_{1,d}=17$ ℃, $T_{2,d}=3$ ℃ and $T_{3,d}=-8$ ℃, and the corresponding EV opening degrees are 85%, 43% and 16% respectively. The operating ranges of EV1, EV2 and EV3 in this experiment are given as [70%, 100%], [31%, 55%] and [12%, 20%]. For fuzzy modeling, they are uniformly scaled as [–3, 3] to be the ranges of inputs u_j ($j=1,2,3$), and let the outputs be temperature differences $y_i=T_i-T_{i,d}$ ($i=1,2,3$). Choose the sampling interval as $0.1(\min)$, the step responses of y_i ($i=1,2,3$) to u_j ($j=1,2,3$) at designed working condition are shown in Fig. 6.4. As can be seen in Fig. 6.4, when the *i*th input is a unit step signal and other inputs are 0, the value of the *i*th output decreases and the values of other outputs increase. The time delay of this

3×3 process can be measured as: $\tau'_{11}=0.6\,(\text{min})$, $\tau'_{12}=1.2(\text{min})$, $\tau'_{13}=1.1(\text{min})$, $\tau'_{21}=1(\text{min})$, $\tau'_{22}=0.8(\text{min})$, $\tau'_{23}=1(\text{min})$, $\tau'_{31}=1(\text{min})$, $\tau'_{32}=1.1(\text{min})$ and $\tau'_{33}=0.8(\text{min})$. Based on the sampled input–output data pairs, the Type–1 and the Type–2 T–S fuzzy models can be constructed for this MER system using the methods given in Chapter 2 and are presented in Appendix C.

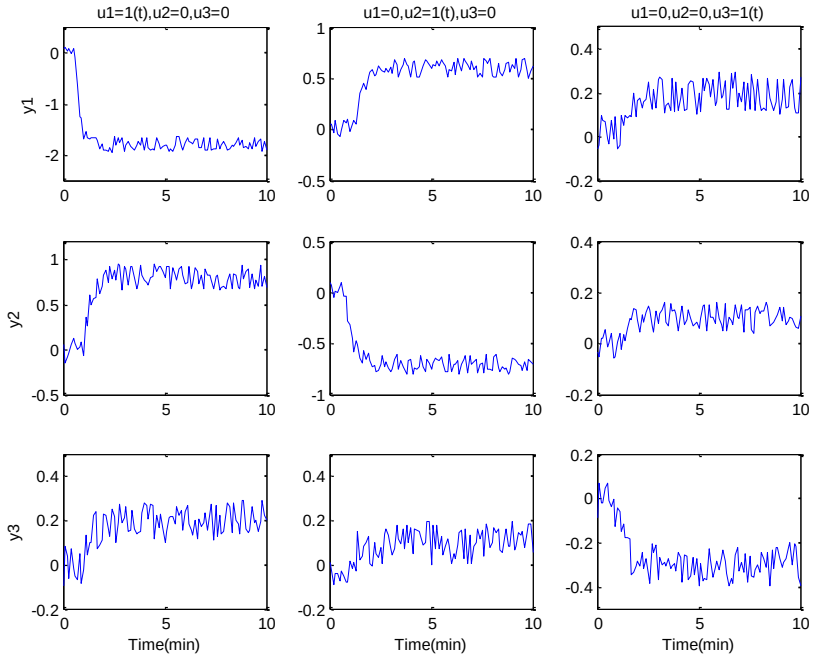

Figure 6.4 Step responses of the three outputs of the MER system

6.2.1 Control structures for the MER system

According to the RNGA based loop pairing rules for choosing decentralized control configuration described in Section 3.2 and the off–diagonal element selection criterion for sparse control structure introduced in Section 5.2, the control structures for this MER system can be determined based on the T–S fuzzy models. The experiment for the MER system control is carried out in the area of designed working condition around the points as $\boldsymbol{x}_{0,ij}=\left[u_{0,j}(k_0-\tau_{ij})\quad y_{0,i}(k_0-1)\quad y_{0,i}(k_0-2)\right]=\left[0\quad 0\quad 0\right]$ for $i,j=1,2,3$, from Type–1 T–S fuzzy models, the following results can be obtained as

$$\boldsymbol{K}_{TS}=\begin{bmatrix}-1.7952 & 0.5882 & 0.2275\\ 0.7752 & -0.7009 & 0.1006\\ 0.1973 & 0.1002 & -0.2794\end{bmatrix},\quad \boldsymbol{E}_{TS}=\begin{bmatrix}0.7524 & 1.5937 & 1.5742\\ 1.2484 & 1.0486 & 1.3959\\ 1.3315 & 1.4550 & 1.2464\end{bmatrix}$$

$$\boldsymbol{\Lambda}_{TS}=\begin{bmatrix} 2.2957 & -0.9574 & -0.3382 \\ -0.9987 & 2.2037 & -0.2050 \\ -0.2970 & -0.2462 & 1.5432 \end{bmatrix},\quad \boldsymbol{\Phi}_{TS}=\begin{bmatrix} 1.2809 & -0.2050 & -0.0759 \\ -0.2133 & 1.2718 & -0.0585 \\ -0.0676 & -0.0668 & 1.1344 \end{bmatrix}$$

According to the RNGA based criterion, the paired loops for decentralized control are in the diagonal positions: $y_1-u_1 / y_2-u_2 / y_3-u_3$. Based on RNGA $\boldsymbol{\Phi}_{TS}$, the interaction index $\boldsymbol{B}_{TS}$ can be obtained as

$$\boldsymbol{B}_{TS}=\begin{bmatrix} 1.0000 & \mathbf{0.1600} & 0.0593 \\ \mathbf{0.1677} & 1.0000 & 0.0460 \\ 0.0596 & 0.0589 & 1.0000 \end{bmatrix}$$

where $\boldsymbol{B}_{TS}$ shows that the interactions among part of paired and unpaired elements are strong that requires sparse control to manipulate this MER system. According to the selection criterion in Eq. (5.5), two off–diagonal loops y_1-u_2 and y_2-u_1 should be considered and added to diagonal control structure to form a sparse control.

From Type–2 T–S fuzzy models, the following results can be obtained.

$$\boldsymbol{K}_{TS}=\begin{bmatrix} -1.7973 & 0.5894 & 0.2292 \\ 0.7806 & -0.6999 & 0.1005 \\ 0.1995 & 0.1000 & -0.2805 \end{bmatrix},\quad \boldsymbol{E}_{TS}=\begin{bmatrix} 0.7524 & 1.5968 & 1.5751 \\ 1.2497 & 1.0467 & 1.3970 \\ 1.3357 & 1.4563 & 1.2419 \end{bmatrix}$$

$$\boldsymbol{\Lambda}_{TS}=\begin{bmatrix} 2.3246 & -0.9781 & -0.3464 \\ -1.0203 & 2.2278 & -0.2075 \\ -0.3043 & -0.2496 & 1.5539 \end{bmatrix},\quad \boldsymbol{\Phi}_{TS}=\begin{bmatrix} 1.2822 & -0.2059 & -0.0763 \\ -0.2143 & 1.2722 & -0.0579 \\ -0.0680 & -0.0663 & 1.1343 \end{bmatrix}$$

The paired loops can be determined as $y_1-u_1 / y_2-u_2 / y_3-u_3$, which is same as that determined based on Type–1 T–S fuzzy models. And then the interaction index $\boldsymbol{B}_{TS}$ can be calculated from RNGA $\boldsymbol{\Phi}_{TS}$ as

$$\boldsymbol{B}_{TS}=\begin{bmatrix} 1.0000 & \mathbf{0.1606} & 0.0595 \\ \mathbf{0.1684} & 1.0000 & 0.0455 \\ 0.0599 & 0.0584 & 1.0000 \end{bmatrix}$$

Same as that obtained from Type–1 T–S fuzzy models, $\boldsymbol{B}_{TS}$ demonstrates that sparse

control should be adopted and the selected off–diagonal elements for sparse control structure are $y_1 - u_2$ and $y_2 - u_1$.

Based on the above Type–1 and Type–2 T–S fuzzy model based interaction analyses and control structure selections, it can be concluded that the decentralized control configuration of this experimental MER system is that the openings of EV1, EV2 and EV3 are used to regulate the heat transfer fluid temperatures of EVAP1, EVAP 2 and EVAP 3 respectively. While for sparse control, the adjustment of EV1 opening degree should consider the heat transfer fluid temperature of EVAP 2, and the adjustment of EV2 opening degree should consider the heat transfer fluid temperature of EVAP1.

6.2.2 ETSMs for the MER system

Based on the RGA $\boldsymbol{\Lambda}_{TS}$ and RNGA $\boldsymbol{\Phi}_{TS}$ of Type–1 T–S fuzzy models, the relative normalized integrated error array $\boldsymbol{\Gamma}_{TS}$ can be derived according to Eq.(4.4).

$$\boldsymbol{\Gamma}_{TS} = \begin{bmatrix} 0.5580 & 0.2141 & 0.2245 \\ 0.2136 & 0.5771 & 0.2854 \\ 0.2278 & 0.2712 & 0.7351 \end{bmatrix}$$

Based on $\boldsymbol{\Lambda}_{TS}$ and $\boldsymbol{\Gamma}_{TS}$ calculated from Type–1 T–S fuzzy models, the Type–1 ETSMs of the selected loops can be obtained according to the approaches given in Chapter 4 and 5. For the paired loops, $\lambda_{TS,11} = 2.2957 > 1$, $\lambda_{TS,22} = 2.2037 > 1$, $\lambda_{TS,33} = 1.5432 > 1$, and $\gamma_{TS,11} = 0.5580 < 1$, $\gamma_{TS,22} = 0.5771 < 1$, $\gamma_{TS,33} = 0.7351 < 1$, thus their Type–1 ETSMs are determined according to **Case 4** as described in Section 4.2. While for off–diagonal loops, $\left|\lambda_{TS,12}\right| = \left|-0.9574\right| < 1$, $\left|\lambda_{TS,21}\right| = \left|-0.9987\right| < 1$ and $\gamma_{TS,12} = 0.2141 < 1$, $\gamma_{TS,21} = 0.2136 < 1$, thus their Type–1 ETSMs are determined by **Case 2** as described in Table 5.1.

Based on RGA $\boldsymbol{\Lambda}_{TS}$ and RNGA $\boldsymbol{\Phi}_{TS}$ calculated from Type–2 T–S fuzzy models, the relative normalized integrated error array $\boldsymbol{\Gamma}_{TS}$ can be obtained by Eq.(4.4).

$$\boldsymbol{\Gamma}_{TS} = \begin{bmatrix} 0.5516 & 0.2105 & 0.2203 \\ 0.2100 & 0.5711 & 0.2792 \\ 0.2234 & 0.2655 & 0.7299 \end{bmatrix}$$

Based on $\boldsymbol{\Lambda}_{TS}$ and $\boldsymbol{\Gamma}_{TS}$ calculated from Type–2 T–S fuzzy models and the approaches described in Chapters 4 and 5, the Type–2 ETSMs of the selected loops can be derived. For the paired loops, $\lambda_{TS,11} = 2.3246 > 1$, $\lambda_{TS,22} = 2.2278 > 1$, $\lambda_{TS,33} = 1.5539 > 1$, and $\gamma_{TS,11} = 0.5516 < 1$, $\gamma_{TS,22} = 0.5711 < 1$, $\gamma_{TS,33} = 0.7299 < 1$, thus their Type–2 ETSMs are determined by **Case 4** as introduced in Section 4.2. While for off–diagonal loops, $|\lambda_{TS,12}| = |-0.9781| < 1$, $|\lambda_{TS,21}| = |-1.0203| > 1$ and $\gamma_{TS,12} = 0.2105 < 1$, $\gamma_{TS,21} = 0.2100 < 1$, thus their Type–2 ETSMs are determined by **Case 2** and **Case 4** respectively as described in Table 5.1.

6.2.3 Decentralized and sparse controls for the MER system

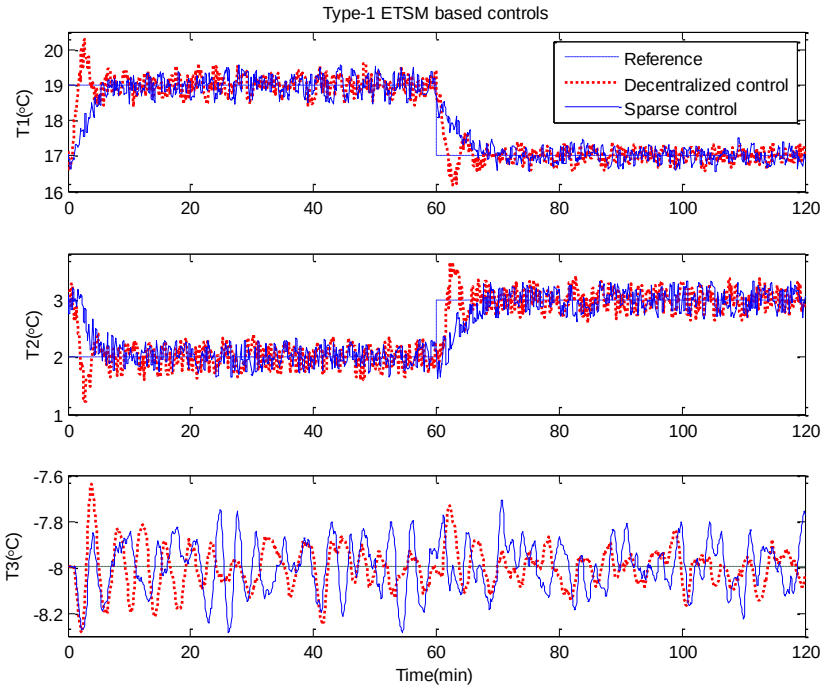

Figure 6.5 Type–1 ETSM based controls for the MER system

Using the control algorithm introduced in Section 4.3 and choosing $A_{m,i} = 3$ and $\Psi_{m,i} = \pi/3$, the decentralized and sparse controllers based on Type–1 and Type–2 ETSMs can be obtained and applied to manipulate the MER system. In the

experiments, the references for three outputs are given as 19℃ for T_1, 2℃ for T_2 and –8℃ for T_3, and the reference values for T_1 and T_2 are changed to 17℃ and 3℃ at $t = 60(\text{min})$ while the reference value for T_3 are unchanged during the whole experiment. The performances of decentralized and sparse controllers designed based on Type–1 and Type–2 ETSMs for this MER system are presented in Fig. 6.5 and Fig. 6.6 respectively.

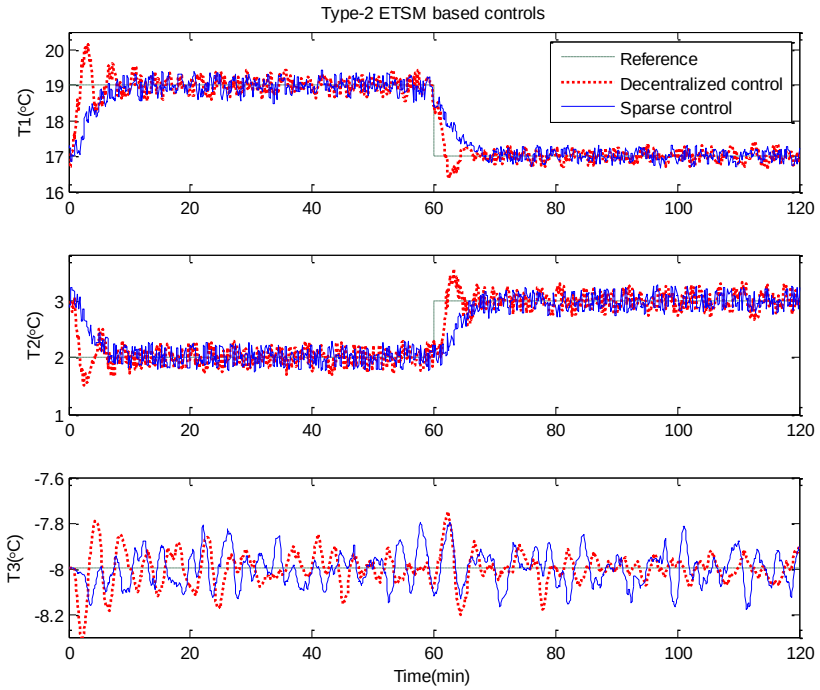

Figure 6.6 Type–2 ETSM based controls for the MER system

As shown in Fig. 6.5 and Fig. 6.6, despite the interactions and noise, the outputs can track their references under both decentralized and sparse controls. The outputs under decentralized controls have overshoots at the beginning and at $t = 60(\text{min})$. While the sparse controls, by adding two off–diagonal controllers to the diagonal control structure, are able to achieve smoother curves of the outputs, which proves sparse control can effectively handle the interactions by using a little more complicated control structure compared to decentralized control.

On the other hand, as in Fig. 6.7 where the manipulation variables are illustrated, the changes of EV opening degree under sparse controls are more moderate when

compared to that under decentralized controls. In practice, the gentle changes of inputs and outputs can avoid unnecessary waste of energy, reduce wear and friction on the machine components and prolong service life of the device.

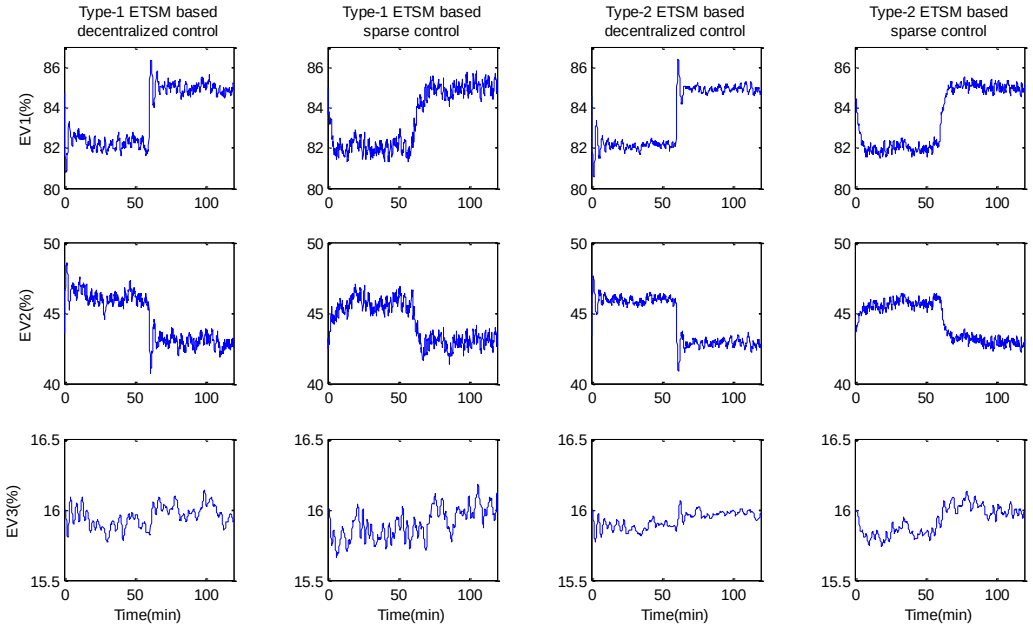

Figure 6.7 The manipulation variables of the MER system

6.2.4 Comparisons of Type–1 and Type–2 ETSM based controls

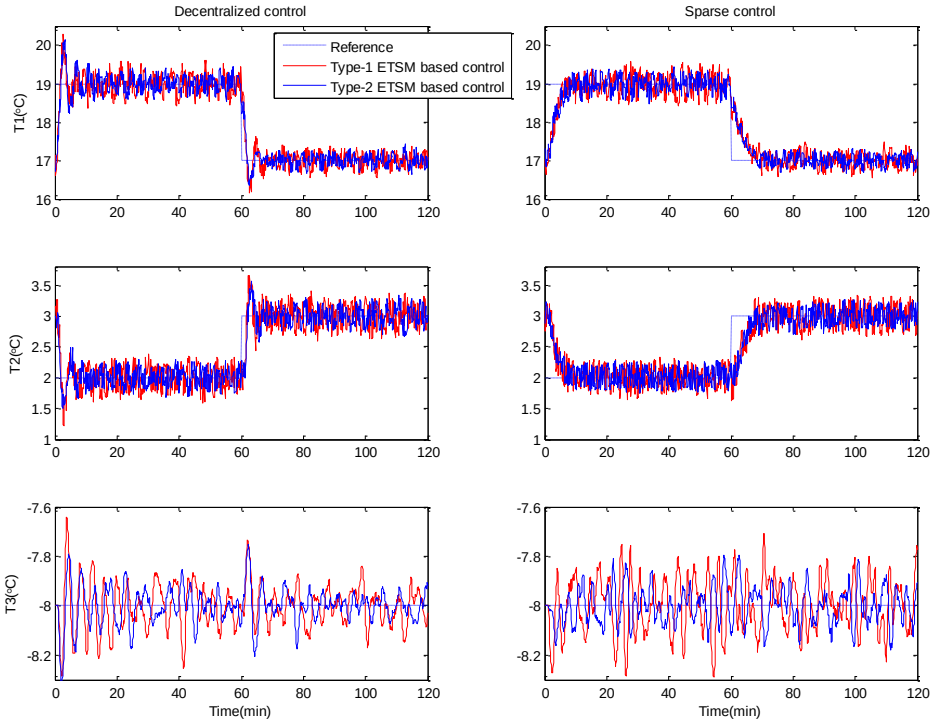

Figure 6.8 Comparisons between Type–1 and Type–2 ETSM based controls

The comparisons of Type–1 and Type–2 ETSMs based control performances are presented in Fig. 6.8. And the integrals of the absolute value of the errors (IAE) from $t = 0$ to $t = 120(\text{min})$ of each output under four controls are shown in Table 6.1. From Fig. 6.8 and Table 6.1, it can be figure out that the outputs manipulated by Type–2 ETSM based controls can achieve smaller values in overshoot, oscillation and IAE when compared to that manipulated by their Type–1 ETSM based counterparts, which demonstrates that Type–2 fuzzy control systems can provide more robust results than Type–1 fuzzy control systems in real applications. The comparison of the calculating time to derive a control variable based on a Type–1 and a Type–2 ETSM with 6 fuzzy rules in this application is given in Table 6.2, which shows that the calculating time based on an ETSM to obtain a control variable using the gain and phase margins based tuning algorithm given in Section 4.3 is very short, and the calculating time based on a Type–2 ETSM is about twice as long as that based on a Type–1 ETSM.

Table 6.1 The IAEs of Type–1 and Type–2 ETSM based controls for the MER system

Controls	IAE(y_1)	IAE(y_2)	IAE(y_3)
Type–1 decentralized control	31.3006	24.2762	10.0530
Type–2 decentralized control	28.2043	22.7316	8.5021
Type–1 sparse control	27.6832	21.8937	7.2410
Type–2 sparse control	25.9449	20.4427	6.2014

Table 6.2 Comparison of the control variable calculating time based on a Type–1 and a Type–2 ETSM

ETSM	Calculating time
Type–1	0.004913(sec)
Type–2	0.010508(sec)

According to the control performances in Fig. 6.5–6.8 and Table 6.1–6.2, several analyses can be given as below:

1). In this application, compared to Type–1 ETSM based decentralized control system which is designed based on three diagonal loops, Type–1 ETSM based sparse control considers two more off–diagonal input–output relations so its online computational

cost is about 67% more than that of Type–1 decentralized control. The online computational cost of Type–2 control systems doubles that of their Type–1 counterparts, which means, Type–2 ETSM based decentralized control requires 100% more computational cost than Type–1 decentralized control, and the computational cost of Type–2 sparse control is more than three times as much as that of Type–1 decentralized control.

2). Type–2 control systems can achieve better and more robust performance than their Type–1 counterparts especially when the degree of uncertainty is large. And from Fig. 6.8 and Table 6.1, it can be learned that the performance differences between Type–1 and Type–2 control systems utilizing same control structures are not significant, which implies the uncertainties of this MER system in the given operating range are of the degree that Type–1 fuzzy system can handle. On the other hand, sparse control with a little more complex control structure than diagonal structure can provide great improvement on decentralized control for this MER system.

3). Based on the analyses in 1) and 2), it can be concluded that Type–1 sparse control can provide significant improvement on the decentralized controls for this MER system, and its computational cost is even less than that of Type–2 decentralized control. Moreover, compared with Type–2 sparse control, it can give almost comparable control performance while only requires half of the computational cost. Hence, Type–1 ETSM based sparse control should be the most cost–effective manner to manipulate the MER system in this application. However, the calculating time to derive a control variable as shown in Table 6.2 is very short which means even the computational cost of the Type–2 ETSM based sparse control is quite manageable. Moreover, as can be seen in Fig. 6.7 that the manipulation variable changes of Type–2 ETSM based sparse control are smoother and gentler than that of Type–1 sparse control, which can save unnecessary cost of energy and reduce wear and tear on the device. Therefore, Type–2 ETSM based sparse control can be a good choice for the MER system control in this application.

6.3 Summary

In this chapter, the proposed Type–1 and Type–2 fuzzy model based methods for multivariable process control are applied to manipulate an experimental MER system which is comprised of a single compressor and a single condenser but three evaporators that can economically satisfy different cooling demands for air–conditioning, perishable food storage and freezing. According to the interaction analysis, the paired loops for decentralized control are in diagonal positions, and two off–diagonal controllers can be added to the diagonal control structure for sparse control system design. The results of Type–1 and Type–2 ETSM based decentralized and sparse controls for the MER system indicate that sparse control can achieve improved performances over decentralized control, and Type–2 ETSM based control systems are more robust than their Type–1 counterparts. The experiments validate the practicality and effectiveness of the proposed control structure selection criteria and ETSM based controller designs for MER systems in this thesis.

Chapter 7. Conclusions and future work

7.1 Conclusions

To develop practical and efficient control strategies for MER systems, in this thesis, a series of novel methods based on both Type–1 and Type–2 T–S fuzzy models were proposed and tested on an experimental MER system to validate their practicability and effectiveness. The main contributions of this thesis are summarized as follows:

1. Fuzzy–model–based RNGA loop pairing criterion

Decentralized control is the most popular method to manipulate MIMO processes, and the main difficulty for it is to deal with the interactions among the loops. By defining steady–state gain and normalized integrated error based on T–S fuzzy model, this thesis presented fuzzy–model–based RNGA loop pairing criterion to analyze the interactions and determine the optimal decentralized control configuration where the resulting control–loops have minimum coupling effects from other loops, such that the burden of controller for an MER system to deal with interactions can be minimized. Simple calculation procedures of RNGA paring criterion based on both Type–1 and Type–2 T–S fuzzy models were given. The proposed method is an alternative for the existing transfer function based loop pairing approaches when the accurate mathematical functions of the processes are unavailable. Compared with the existing fuzzy–model–based pairing methods that only steady–state gain is considered, this method takes both steady and dynamic information into account such that a more appropriate control configuration can be provided. Simulation proved that both Type–1 and Type–2 T–S fuzzy models constructed based on the data sampled from the process with inexactness can give accurate control configuration, and the calculated results from Type–2 T–S fuzzy models can achieve smaller errors than that from Type–1 T–S fuzzy models.

2. ETSM method for decentralized control

To facilitate decentralized fuzzy controller design for an MER system in handling the interactions, both Type–1 and Type–2 ETSM methods were proposed. In an MIMO

process formed from an MER system, the ETSM for a certain loop has same structure but revised coefficients as that of its individual T–S fuzzy model. And the revised coefficients, calculated in terms of RNGA based loop pairing criterion, are able to express the interacting results on this loop caused by other closed loops. Based on the ETSMs of the paired loops, an MIMO process can be approximately regarded as a group of non–interacting single–loops and the decentralized control system can be independently designed by using linear SISO control algorithms. Compared with the existing decentralized fuzzy control using extra terms to characterize interactions, ETSM offers a viable, easier and more practical manner to express the interactions that can reduce the complexities in both process modeling and controller design. While compared with existing ETF methods, ETSM is an alternative where accurate mathematical models are unavailable, and saves the time and cost for new transfer function identification when operating condition changes in a real–time application since fuzzy model can describe a global nonlinear process. Moreover, it gives a base to develop robust controllers since fuzzy system has strong power to handle uncertainty, and to carry out comparative studies of Type–1 and Type–2 T–S fuzzy models. Simple calculating approaches were presented to determine the coefficients of both Type–1 and Type–2 ETSMs by using the quantified interacting effects provided form RNGA criterion. And the simulation results of decentralized control demonstrated they were superior over their ETF counterpart. As the degree of uncertainty increased, Type–2 ETSM was able to achieve more satisfactory performance than Type–1 ETSM.

3. A guideline for sparse fuzzy control

For closely–coupled processes of MER systems, sparse control with compromised control structure between diagonal and full–dimensional can achieve improved performance than decentralized control, while requiring less computational cost compared with centralized control. A guideline to devise sparse control based on T–S fuzzy models was presented. By virtue of RNGA based loop pairing criterion, an approach to selecting sparse control structure was given. With the help of ETSMs, an independent design method was introduced to convert an MIMO control system design

to multiple non–interacting single–loop controller designs. The proposed guideline gives a platform to utilize the mature linear SISO control techniques to devise robust fuzzy controllers for manipulating nonlinear and strong–coupled MER systems. Furthermore, comparative studies of Type–1 and Type–2 fuzzy systems can be launched. In the simulation, sparse control performances based on ETF, Type–1 and Type–2 ETSMs were given and compared with each other as well as their decentralized counterparts. The results demonstrated that sparse control outperformed decentralized control, and ETSM based control worked better than ETF based control. When larger uncertainty appeared, the superiority of Type–2 fuzzy system in terms of robustness over Type–1 fuzzy system was more apparent.

4. Applications

The proposed Type–1 and Type–2 T–S fuzzy model based methods of this thesis were applied to manipulate an experimental MER system with three evaporators that can simultaneously cater cooling requirements for air–conditioning, perishable food storage and freezing. A 3×3 process can be formed from this MER system. Based on the sampled data, a Type–1 and a Type–2 T–S fuzzy model matrix were constructed. According to the interaction analysis using RNGA based pairing criterion, decentralized control configuration for this process was determined as the diagonal loops. And the analysis indicated that the interacting effects among part of the paired and unpaired elements are strong that two off–diagonal loops can be included to design sparse control systems for this process. The experimental results of Type–1 and Type–2 ETSM based controllers demonstrated that Type–2 fuzzy control systems were more robust than their Type–1 counterparts, and sparse control achieved much better performance than decentralized control, which validated the effectiveness of the proposed control structure selections and ETSM methods for multivariable process control of MER systems.

7.2 Future work

More efforts are needed in this study and the future work including the following.

1. Fuzzy modeling

As the foundation of the studies in this thesis, a Type–1 or a Type–2 T–S fuzzy model with its parameters well determined is able to guarantee accurate results and satisfactory performances in control structure selection and controller design while minimizing the computational cost. A well identified Type–2 fuzzy system can achieve significant improved performance than its Type–1 counterpart when a large number of uncertainties appear. The modeling methods to construct Type–1 and Type–2 T–S fuzzy models could potentially be improved in future study. An effective method can be developed to determine the fuzzy rule number which was roughly evaluated according to human experience in this thesis, and a more efficient clustering algorithm can be studied to divide data samples into several fuzzy sets, and a more accurate approach with lower computational complexity could be investigated to identify the left and the right bounds of the fuzzy memberships and local model coefficients in Type–2 fuzzy system.

2. Loop pairing criteria

In this thesis, the control structure was selected according to RNGA based loop pairing criterion in terms of steady–state gains and response speeds of individual loops such that the steady–state and dynamic interactions on the paired loops can be minimized and control system can achieve optimal performance. However, in real applications, the energy costs or the environmental impacts should be considered when selecting the controlled loops. Sometimes a control system would choose the pairing structure with suboptimal control performance to reduce the energy consumption and protect the environment. Therefore, the loop pairing criteria which take into account the energy cost or other consumptions should be developed. And how to define the energy cost and implement the new loop pairing criteria based on the fuzzy model could be studied.

3. Control algorithm

The gain and phase margin based control algorithm was employed to design controllers based on fuzzy models and applied to manipulate refrigeration system in

this thesis. The outputs of MER system can stably reach their references under both decentralized and sparse control even though there are disturbances and interactions. However, it still leaves room for improvement: the overshoots under decentralized controllers can be reduced or even eliminated, and smaller settling time can be provided. Since the proposed method of this thesis provides a base that linear SISO control methods can be utilized to manipulate nonlinear MIMO processes, more advanced and sophisticated control algorithms can be applied to improve the control performance for MER systems in future study.

References

[1] R. J. Dossat and T. J. Horan, *Principles of refrigeration*, 5th ed. Upper Saddle River, N.J.,U.S.A: Prentice Hall, 2002.

[2] *Green Building Design Guide*. Singapore: Building & Construction Authority, 2007.

[3] X.-D. He and H. H. Asada, "A new feedback linearization approach to advanced control of multi-unit HVAC systems," in *American Control Conference 2003*, Denver, Colorado, USA, June 4-6, 2003, pp. 2311-2316.

[4] J.-L. Lin and T. J. Yeh, "Identification and control of multi-evaporator air-conditioning systems," *International Journal of Refrigeration*, vol. 30, pp. 1374-1385, 2007.

[5] J.-L. Lin and T. J. Yeh, "Control of multi-evaporator air-conditioning systems for flow distribution," *Energy Conversion and Management*, vol. 50, pp. 1529-1541, 2009.

[6] M. S. Elliott and B. P. Rasmussen, "Model-based predictive control of a multi-evaporator vapor compression cooling cycle," in *American Control Conference 2008*, Seattle, Washington, USA, June 11-13, 2008, pp. 1463-1468.

[7] M. S. Elliott and B. P. Rasmussen, "A model-based predictive supervisory controller for multi-evaporator HVAC systems," in *American Control Conference 2009*, St. Louis, Missouri, USA, June 10-12, 2009, pp. 3669-3674.

[8] M. S. Elliott and B. P. Rasmussen, "Decentralized model predictive control of a multi-evaporator air conditioning system," *Control Engineering Practice*, vol. 21, pp. 1665-1677, 2013.

[9] X. Xiangguo, P. Yan, D. Shiming, X. Liang, and C. Mingyin, "Experimental study of a novel capacity control algorithm for a multi-evaporator air conditioning system," *Applied Thermal Engineering*, vol. 50, pp. 975-984, 2013.

[10] Y. You, A. Wu, and S. Yang, "An Optimal Control Strategy for Multi-evaporator Vapor Compression Systems," in *Electrical and Control Engineering (ICECE), 2010 International Conference on*, Wuhan, China, June 25-27, 2010, pp. 410-413.

[11] C. Wu, Z. Xingxi, and D. Shiming, "Development of control method and dynamic model for multi-evaporator air conditioners (MEAC)," *Energy Conversion and Management*, vol. 46, pp. 451-465, 2005.

[12] J. Xu and Z. Feng, "A Novel Self-adaptive Fuzzy-PID Controller for Temperature Control in Variable Refrigerant Volume (VRV) Air Conditioning Systems," *International Conference on Intelligent Systems and Knowledge Engineering (ISKE 2007)*, Chengdu, China, October 15-16, 2007.

[13] R.-E. Precup and H. Hellendoorn, "A survey on industrial applications of fuzzy control," *Computers in Industry*, vol. 62, pp. 213-226, 2011.

[14] L. X. Wang and J. M. Mendel, "Fuzzy basis functions, universal approximation, and orthogonal least-squares learning," *IEEE Trans Neural Netw*, vol. 3, pp. 807-14, 1992.

[15] K. Tanaka and H. O. Wang, *Fuzzy Control Systems Design and Analysis: A Linear Matrix Inequality Approach*: John Wiley & Sons, 2001.

[16] Y. Hao, "General SISO Takagi-Sugeno fuzzy systems with linear rule consequent are universal approximators," *Fuzzy Systems, IEEE Transactions on*, vol. 6, pp. 582-587, 1998.

[17] C. Fantuzzi and R. Rovatti, "On the approximation capabilities of the homogeneous Takagi-Sugeno model," in *Fuzzy Systems, 1996., Proceedings of the Fifth IEEE International*

Conference on, New Orleans, LA, USA, September 8-11, 1996, pp. 1067-1072.

[18] G. Feng, "A Survey on Analysis and Design of Model-Based Fuzzy Control Systems," *Fuzzy Systems, IEEE Transactions on,* vol. 14, pp. 676-697, 2006.

[19] E. H. Mamdani, "Application of fuzzy algorithms for control of simple dynamic plant," *Electrical Engineers, Proceedings of the Institution of,* vol. 121, pp. 1585-1588, 1974.

[20] T. Takagi and M. Sugeno, "Fuzzy identification of systems and its applications to modeling and control," *Systems, Man and Cybernetics, IEEE Transactions on,* vol. SMC-15, pp. 116-132, 1985.

[21] C.-C. Cheng and S.-H. Chien, "Adaptive sliding mode controller design based on T–S fuzzy system models," *Automatica,* vol. 42, pp. 1005-1010, 2006.

[22] M. He, W.-J. Cai, and S.-Y. Li, "Multiple fuzzy model-based temperature predictive control for HVAC systems," *Information Sciences,* vol. 169, pp. 155-174, 2005.

[23] N. Li, S.-Y. Li, and Y.-G. Xi, "Multi-model predictive control based on the Takagi–Sugeno fuzzy models: a case study," *Information Sciences,* vol. 165, pp. 247-263, 2004.

[24] Q. Liao, N. Li, and S. Li, "Type-II T-S fuzzy model-based predictive control," in *Decision and Control, 2009 held jointly with the 2009 28th Chinese Control Conference. CDC/CCC 2009. Proceedings of the 48th IEEE Conference on*, Shanghai, China, December 15-18, 2009, pp. 4193-4198.

[25] R. Qi and M. A. Brdys, "T-S Model Based Indirect Adaptive Fuzzy Control for a Class of MIMO Uncertain Nonlinear Systems," in *Intelligent Control and Automation, 2006. WCICA 2006. The Sixth World Congress on*, Dalian, China, June 21-23, 2006, pp. 3943-3947.

[26] Q. Xin and R. Zhang, "Adaptive robust control based on T-S fuzzy-neural systems for a hypersonic vehicle," in *Electrical and Control Engineering (ICECE), 2011 International Conference on*, Yichang, China, September 16-18, 2011, pp. 535-538.

[27] R. Z. Homod, K. S. M. Sahari, H. A. F. Almurib, and F. H. Nagi, "Gradient auto-tuned Takagi-Sugeno Fuzzy Forward control of a HVAC system using predicted mean vote index," *Energy and Buildings,* vol. 49, pp. 254-267, 2012.

[28] H. Lv, L. Jia, S. Kong, and Z. Zhang, "Predictive functional control based on fuzzy T-S model for HVAC systems temperature control," *Journal of Control Theory and Applications,* vol. 5, pp. 94-8, 2007.

[29] Z. Guo and Z. Yanhua, "Decentralized robust control for nonlinear interconnected systems based on T-S fuzzy bilinear model," *Sensors and Transducers,* vol. 20, pp. 53-63, 2013.

[30] C. Hua and S. X. Ding, "Decentralized networked control system design using T-S fuzzy approach," *IEEE Transactions on Fuzzy Systems,* vol. 20, pp. 9-21, 2012.

[31] S.-W. Lin, C.-H. Sun, and C.-H. Chiu, "Decentralized guaranteed cost control for large-scale T-S fuzzy systems," *International Journal of Fuzzy Systems,* vol. 12, pp. 300-310, 2010.

[32] T. Wang and L.-J. Qu, "Robust decentralized control for T-S uncertain fuzzy interconnected systems with time-delay," in *6th International Conference on Machine Learning and Cybernetics, ICMLC 2007*, Hong Kong, China, August 19-22, 2007, pp. 631-636.

[33] M.-S. Chiu and Y. Arkun, "Decentralized control structure selection based on integrity considerations," *Industrial and Engineering Chemistry Research,* vol. 29, pp. 374-382, 1990.

[34] P. Grosdidier and M. Morari, "A computer aided methodology for the design of decentralized controllers," *Computers & Chemical Engineering,* vol. 11, pp. 423-433, 1987.

[35] M.-J. He, W.-J. Cai, W. Ni, and L.-H. Xie, "RNGA based control system configuration for

multivariable processes," *Journal of Process Control,* vol. 19, pp. 1036-1042, 2009.

[36] C. Xu and Y. C. Shin, "Interaction analysis for MIMO nonlinear systems based on a fuzzy basis function network model," *Fuzzy Sets and Systems,* vol. 158, pp. 2013-2025, 2007.

[37] H.-P. Huang, J.-C. Jeng, C.-H. Chiang, and W. Pan, "A direct method for multi-loop PI/PID controller design," *Journal of Process Control,* vol. 13, pp. 769-786, 2003.

[38] Y. Shen, W.-J. Cai, and S. Li, "Multivariable process control: Decentralized, decoupling, or sparse?," *Industrial and Engineering Chemistry Research,* vol. 49, pp. 761-771, 2010.

[39] H. Mei, S. Li, W.-J. Cai, and Q. Xiong, "Decentralized closed-loop parameter identification for multivariable processes from step responses," *Mathematics and Computers in Simulation,* vol. 68, pp. 171-192, 2005.

[40] L. A. Zadeh, "The concept of a linguistic variable and its application to approximate reasoning—I," *Information Sciences,* vol. 8, pp. 199-249, 1975.

[41] L. A. Zadeh, "Fuzzy sets," *Information and Control,* vol. 8, pp. 338-353, 1965.

[42] N. N. Karnik, J. M. Mendel, and L. Qilian, "Type-2 fuzzy logic systems," *Fuzzy Systems, IEEE Transactions on,* vol. 7, pp. 643-658, 1999.

[43] R. John and S. Coupland, "Type-2 Fuzzy Logic: A Historical View," *Computational Intelligence Magazine, IEEE,* vol. 2, pp. 57-62, 2007.

[44] J. M. Mendel and R. I. B. John, "Type-2 fuzzy sets made simple," *Fuzzy Systems, IEEE Transactions on,* vol. 10, pp. 117-127, 2002.

[45] Q. Liang and J. M. Mendel, "Interval type-2 fuzzy logic systems: theory and design," *Fuzzy Systems, IEEE Transactions on,* vol. 8, pp. 535-550, 2000.

[46] N. N. Karnik and J. M. Mendel, "Type-2 fuzzy logic systems: type-reduction," in *Systems, Man, and Cybernetics, 1998. 1998 IEEE International Conference on*, San Diego, CA, USA, October 11-14, 1998, vol.2, pp. 2046-2051.

[47] Q. Liang and J. M. Mendel, "An introduction to type-2 TSK fuzzy logic systems," in *Fuzzy Systems Conference Proceedings, 1999. FUZZ-IEEE '99. 1999 IEEE International*, Seoul, South Korea, August 22-25 1999, vol.3, pp. 1534-1539.

[48] D. E. Gustafson and W. C. Kessel, "Fuzzy clustering with a fuzzy covariance matrix," in *Decision and Control including the 17th Symposium on Adaptive Processes, 1978 IEEE Conference on*, San Diego, CA, USA, January 10-12, 1978, pp. 761-766.

[49] W. Mengling, L. Ning, and L. Shaoyuan, "Type-2 T-S fuzzy modeling for the dynamic systems with measurement noise," in *2008 IEEE 16th International Conference on Fuzzy Systems (FUZZ-IEEE)*, Piscataway, NJ, USA, June 1-6, 2008, pp. 443-448.

[50] R. Qun, L. Baron, and M. Balazinski, "Type-2 takagi-sugeno-kang fuzzy logic modeling using subtractive clustering," in *NAFIPS 2006 - 2006 Annual Meeting of the North American Fuzzy Information Processing Society*, Montreal, QC, Canada, June 3- 6, 2006, pp. 120-125.

[51] Q. Xiong, W.-J. Cai, and M.-J. He, "A practical loop pairing criterion for multivariable processes," *Journal of Process Control,* vol. 15, pp. 741-747, 2005.

[52] E. Bristol, "On a new measure of interaction for multivariable process control," *Automatic Control, IEEE Transactions on,* vol. 11, pp. 133-134, 1966.

[53] A. Niederlinski, "A heuristic approach to the design of linear multivariable interacting subsystems," *Automatica,* vol. 7, pp. 691-701, 1971.

[54] P. Grosdidier, M. Morari, and B. R. Holt, "Closed-loop properties from steady-state gain information," *Industrial & Engineering Chemistry, Fundamentals,* vol. 24, pp. 221-235,

1985.

[55] M. F. Witcher and T. J. McAvoy, "Interacting control systems: steady state and dynamic measurement of interaction," *ISA Transactions*, vol. 16, pp. 35-41, 1977.

[56] E. H. Bristol, "Recent results on interactions in multivariable process control," in *in Proceedings of the 71st Annual AIChE Meeting*, Houston, TX, USA, 1979.

[57] L. S. Tung and T. F. Edgar, "Analysis of control output interactions in dynamic systems," *AIChE Journal*, vol. 27, pp. 690-693, 1981.

[58] H.-P. Huang, M. Ohshima, and I. Hashimoto, "Dynamic interaction and multiloop control system design," *Journal of Process Control*, vol. 4, pp. 15-27, 1994.

[59] T. Mc Avoy, Y. Arkun, R. Chen, D. Robinson, and P. D. Schnelle, "A new approach to defining a dynamic relative gain," *Control Engineering Practice*, vol. 11, pp. 907-914, 2003.

[60] Q.-F. Liao, W.-J. Cai, S.-Y. Li, and Y.-Y. Wang, "Interaction analysis and loop pairing for MIMO processes described by T–S fuzzy models," *Fuzzy Sets and Systems*, vol. 207, pp. 64-76, 2012.

[61] Q.-F. Liao, W.-J. Cai, and Y.-Y. Wang, "Interaction analysis and loop pairing for MIMO processes described by type-2 T-S fuzzy models," in *Industrial Electronics and Applications (ICIEA), 2013 8th IEEE Conference on*, Melbourne, VIC, Australia, June 19-21, 2013, pp. 622-627.

[62] E. I. Jury, *Theory and Application of the Z-Transform Method*: John Wiley and Sons, 1964.

[63] Q. Xiong and W.-J. Cai, "Effective transfer function method for decentralized control system design of multi-input multi-output processes," *Journal of Process Control*, vol. 16, pp. 773-784, 2006.

[64] W. Hu, W.-J. Cai, and G. Xiao, "Decentralized control system design for MIMO processes with integrators/differentiators," *Industrial and Engineering Chemistry Research*, vol. 49, pp. 12521-12528, 2010.

[65] I. L. Chien, H.-P. Huang, and J.-C. Yang, "A simple multiloop tuning method for PID controllers with no proportional kick," *Industrial and Engineering Chemistry Research*, vol. 38, pp. 1456-1468, 1999.

[66] T. J. McAvoy, *Interaction Analysis: Principles and Applications*: Instrument Society of America, 1985.

[67] W. L. Luyben, "Simple method for tuning SISO controllers in multivariable systems," *Industrial & Engineering Chemistry, Process Design and Development*, vol. 25, pp. 654-660, 1986.

[68] S.-H. Shen and C.-C. Yu, "Use of relay-feedback test for automatic tuning of multivariable systems," *AIChE Journal*, vol. 40, pp. 627-646, 1994.

[69] Y.-G. Wang and W.-J. Cai, "Advanced proportional-integral-derivative tuning for integrating and unstable processes with gain and phase margin specifications," *Industrial and Engineering Chemistry Research*, vol. 41, pp. 2910-2914, 2002.

[70] P. B. Deshpande and R. H. Ash, *Computer process control with advanced control applications*: Instrument Society of America, 1988.

[71] A. Conley and M. E. Salgado, "Gramian based interaction measure," in *Decision and Control, 2000. Proceedings of the 39th IEEE Conference on*, Sydney, NSW, Australia, Decmber 2000, vol.5, pp. 5020-5022.

[72] A. Conley and M. E. Salgado, "MIMO interaction measure and controller structure selection,"

International Journal of Control, vol. 77, pp. 367-383, 2004.

[73] H. R. Shaker and M. Komareji, "Control configuration selection for multivariable nonlinear systems," *Industrial and Engineering Chemistry Research*, vol. 51, pp. 8583-8587, 2012.

[74] H. R. Shaker and J. Stoustrup, "An interaction measure for control configuration selection for multivariable bilinear systems," *Nonlinear Dynamics*, vol. 72, pp. 165-174, 2013.

[75] W.-J. Cai, W. Ni, M.-J. He, and C.-Y. Ni, "Normalized decoupling - a new approach for MIMO process control system design," *Industrial and Engineering Chemistry Research*, vol. 47, pp. 7347-7356, 2008.

Author’s publications

1. Liao Qianfang, Cai Wenjian, Li Shaoyuan, and Wang Youyi, Interaction analysis and loop pairing for MIMO processes described by T–S fuzzy models, Fuzzy Sets and Systems, vol. 207, pp. 64–76, 2012.

2. Liao Qianfang, Cai Wenjian, and Wang Youyi, Interaction analysis and loop pairing for MIMO processes described by Type–2 T–S fuzzy models, 8th IEEE Conference on Industrial Electronics and Applications (ICIEA), Melbourne, VIC, Australia, June 19-21, 2013, pp. 622-627.

3. Liao Qianfang, Cai Wenjian, and Wang Youyi, Effective T-S Fuzzy Model for Decentralized Control, International Conference on Information and Automation for Sustainability (ICIAfS), Colombo, Sri Lanka, December 22-24, 2014.

4. Liao Qianfang, Cai Wenjian, and Wang Youyi, A method to describe interactions based on Type-1 and Type-2 T-S fuzzy models for decentralized control, submitted to *IEEE Transactions on Fuzzy Systems*.

5. Liao Qianfang, Cai Wenjian, and Wang Youyi, Control Structure Selection based on Type-1 and Type-2 T-S Fuzzy Models for MIMO Processes, submitted to *IEEE Conference on Industrial Electronics and Applications (ICIEA)*, 2015.

Appendix A

The parameters of Type–1 and Type–2 T–S fuzzy models for the process in Eq. (3.27) are given in Table A.1 and Table A.2, where $M_{ij}=5\,(i,j=1,2,3)$, $p=0$, $q=1$, and the centers of the fuzzy clusters are denoted by $\boldsymbol{z}_{c,ij}^{l}=[\boldsymbol{x}_{c,ij}^{l}(k)\quad y_{c,i}^{l}(k)]$, $l=1,\cdots M_{ij}$ where $\boldsymbol{x}_{c,ij}^{l}=\left[u_{c,j}^{l}(k-\tau_{ij})\quad y_{c,i}^{l}(k-1)\right]$.

Table A.1 The centers of fuzzy clusters for the process in Eq. (3.27)

Centers of C_{ij}^{l}'s in loop y_i–u_j	No. of fuzzy clusters				
	$R^1(l=1)$	$R^2(l=2)$	$R^3(l=3)$	$R^4(l=4)$	$R^5(l=5)$
$f_{TS,11}(\triangle\mu_{11}^{l}=0.05)$					
$u_{c,1}^{l}(k-\tau_{11})$	1.6881	0.2826	0.8640	1.2239	0.9509
$y_{c,1}^{l}(k-1)$	0.9440	0.9661	1.1162	1.0476	0.8503
$y_{c,1}^{l}(k)$	1.0857	0.9391	1.0985	0.8589	0.9803
$f_{TS,12}(\triangle\mu_{12}^{l}=0.05)$					
$u_{c,2}^{l}(k-\tau_{12})$	0.3206	1.6531	1.4627	0.6281	1.0298
$y_{c,1}^{l}(k-1)$	–9.0536	–10.1313	–8.8250	–9.4707	–8.8443
$y_{c,1}^{l}(k)$	–7.5243	–9.9624	–11.0131	–9.9958	–7.7846
$f_{TS,13}(\triangle\mu_{13}^{l}=0.05)$					
$u_{c,3}^{l}(k-\tau_{13})$	0.3496	1.5875	0.9516	1.4122	0.6395
$y_{c,1}^{l}(k-1)$	12.3573	12.3563	10.7962	13.6367	14.2000
$y_{c,1}^{l}(k)$	11.0114	14.4953	12.5767	11.5162	13.9655
$f_{TS,21}(\triangle\mu_{21}^{l}=0.05)$					
$u_{c,1}^{l}(k-\tau_{21})$	0.4666	1.4521	1.6092	0.6933	0.7626
$y_{c,2}^{l}(k-1)$	–5.5415	–4.7532	–5.3411	–4.3274	–5.4302
$y_{c,2}^{l}(k)$	–5.3912	–5.7632	–4.9253	–5.0379	–4.2886
$f_{TS,22}(\triangle\mu_{22}^{l}=0.05)$					
$u_{c,2}^{l}(k-\tau_{22})$	0.3195	1.6728	1.4050	0.8598	0.9380
$y_{c,2}^{l}(k-1)$	8.6326	7.6052	9.3473	7.5834	7.3755
$y_{c,2}^{l}(k)$	8.0689	8.5623	8.0160	7.1403	9.0516
$f_{TS,23}(\triangle\mu_{23}^{l}=0.05)$					
$u_{c,3}^{l}(k-\tau_{23})$	1.5026	0.8895	0.2893	1.6557	0.7306
$y_{c,2}^{l}(k-1)$	6.3499	7.1417	7.3157	7.5541	6.7085
$y_{c,2}^{l}(k)$	8.0459	6.0599	5.9112	7.4529	7.5278
$f_{TS,31}(\triangle\mu_{31}^{l}=0.05)$					
$u_{c,1}^{l}(k-\tau_{31})$	1.6859	0.2749	0.8664	1.1277	0.9371
$y_{c,3}^{l}(k-1)$	–15.9007	–15.6053	–13.8958	–15.4377	–18.3150
$y_{c,3}^{l}(k)$	–18.0692	–13.5629	–16.7078	–13.2566	–17.5821
$f_{TS,32}(\triangle\mu_{32}^{l}=0.05)$					
$u_{c,2}^{l}(k-\tau_{32})$	0.3045	1.6653	1.4744	0.8694	0.9377
$y_{c,3}^{l}(k-1)$	3.1739	2.7924	3.5533	2.9549	2.7779

$y^l_{c,3}(k)$	2.9749	3.2452	3.1260	2.6437	3.3411
$f_{TS,33}(\triangle\mu^l_{33}=0.05)$					
$u^l_{c,3}(k-\tau_{33})$	1.5269	0.4890	1.5415	0.6104	0.6702
$y^l_{c,3}(k-1)$	0.8886	1.1303	1.1108	0.8981	0.9526
$y^l_{c,3}(k)$	1.0192	0.9615	0.9978	0.8766	1.1238

Table A.2 The consequent parameters of Type–1 and Type–2 T–S fuzzy models for the process in Eq. (3.27)

No. of	Type–1 fuzzy model		Type–2 fuzzy model			
Fuzzy rules	a^l_0	b^l_1	$a^l_{lb,0}$	$a^l_{rb,0}$	$b^l_{lb,1}$	$b^l_{rb,1}$
$f_{TS,11}$						
$R^1(l=1)$	0.1940	0.7994	0.2553	0.1541	0.8218	0.7398
$R^2(l=2)$	0.0690	0.9274	0.1268	0.0147	1.0432	0.8179
$R^3(l=3)$	0.0047	0.9757	–0.0177	0.0146	1.1040	0.8565
$R^4(l=4)$	0.0828	0.6914	0.0875	0.0725	0.8019	0.5798
$R^5(l=5)$	–0.0141	1.1962	0.0511	–0.0006	1.2717	1.0356
$f_{TS,12}$						
$R^1(l=1)$	–1.7878	0.7354	–1.5435	–2.6297	0.6285	0.8339
$R^2(l=2)$	–1.5533	0.7173	–1.1113	–1.8700	0.6785	0.7793
$R^3(l=3)$	–2.9283	0.7749	–2.3906	–3.3330	0.7488	0.8312
$R^4(l=4)$	–1.8857	0.9432	–1.6750	–2.0111	0.8416	1.0403
$R^5(l=5)$	–2.5211	0.5619	–2.2091	–3.0199	0.4685	0.6402
$f_{TS,13}$						
$R^1(l=1)$	0.1026	0.8508	0.2554	0.3201	0.9698	0.7247
$R^2(l=2)$	3.6331	0.6978	4.0737	3.2117	0.7726	0.6291
$R^3(l=3)$	–1.6635	1.3286	–1.6495	–1.9860	1.4758	1.2051
$R^4(l=4)$	1.1240	0.6976	1.3434	0.6406	0.7925	0.6298
$R^5(l=5)$	–0.1765	0.9831	–0.2713	–0.2573	1.1008	0.8792
$f_{TS,21}$						
$R^1(l=1)$	–0.3665	0.9434	–0.3141	–0.3819	0.8324	1.0510
$R^2(l=2)$	–1.1682	0.8685	–0.9845	–1.2695	0.7960	0.9669
$R^3(l=3)$	–0.7616	0.6738	–0.4995	–1.0041	0.6399	0.7133
$R^4(l=4)$	0.0629	1.1831	0.1643	0.1785	1.0567	1.3459
$R^5(l=5)$	–0.4387	0.7044	–0.5099	–0.4416	0.5815	0.8164
$f_{TS,22}$						
$R^1(l=1)$	–1.2034	0.9552	–1.3359	–1.1730	1.0813	0.8415
$R^2(l=2)$	0.9832	0.9086	1.2625	0.7451	0.9532	0.8266
$R^3(l=3)$	–0.5864	0.9405	–0.4684	–0.7199	1.0233	0.8579
$R^4(l=4)$	0.9384	0.8219	1.2423	0.7619	0.9295	0.7114
$R^5(l=5)$	0.1908	1.2335	0.4378	–0.0922	1.3480	1.1167
$f_{TS,23}$						
$R^1(l=1)$	1.7449	0.8761	2.1569	1.4309	0.9118	0.8096
$R^2(l=2)$	1.2623	0.6714	1.8984	0.7977	0.7062	0.6180
$R^3(l=3)$	1.7304	0.7214	2.6071	1.8280	0.8064	0.6039

$R^4(l=4)$	1.1926	0.7168	1.5367	0.7444	0.7504	0.7019
$R^5(l=5)$	1.7836	0.9468	2.0758	1.5141	1.0457	0.8428
$f_{TS,31}$						
$R^1(l=1)$	–4.3140	0.6779	–3.3001	–5.0657	0.6601	0.7219
$R^2(l=2)$	–1.1953	0.8223	–0.7083	–1.5506	0.7115	0.9383
$R^3(l=3)$	–3.0603	1.0538	–2.7721	–3.6269	0.9338	1.1585
$R^4(l=4)$	–2.4143	0.6460	–1.9430	–2.9091	0.5515	0.7509
$R^5(l=5)$	–3.6005	0.7720	–3.2143	–4.3153	0.6890	0.8440
$f_{TS,32}$						
$R^1(l=1)$	0.2404	0.8945	0.1470	0.1534	1.0153	0.7887
$R^2(l=2)$	0.2770	1.0068	0.4082	0.1769	1.0599	0.9301
$R^3(l=3)$	–0.1070	0.9236	–0.0058	–0.1500	0.9820	0.8382
$R^4(l=4)$	0.5912	0.6879	0.7214	0.4146	0.7763	0.6205
$R^5(l=5)$	0.2727	1.1425	0.3374	0.1684	1.2551	1.0273
$f_{TS,33}$						
$R^1(l=1)$	0.1583	0.8887	0.1613	0.1102	1.0343	0.8175
$R^2(l=2)$	0.0171	0.8276	0.0237	–0.0021	0.9311	0.7316
$R^3(l=3)$	0.1072	0.7431	0.1463	0.0880	0.7962	0.6587
$R^4(l=4)$	–0.0386	0.9898	–0.0229	–0.0533	1.1243	0.8648
$R^5(l=5)$	0.1102	1.1210	0.1250	0.1041	1.2401	0.9911

Appendix B

The parameters of Type–1 and Type–2 T–S fuzzy models for the process in Eq. (4.34) are given in Table B.1 and Table B.2, where $M_{ij}=6\,(i,j=1,2,3)$, $p=0$ and $q=2$, and the centers of the fuzzy clusters are denoted by $\mathbf{z}_{c,ij}^{l}=[\mathbf{x}_{c,ij}^{l}(k)\quad y_{c,i}^{l}(k)]$, $l=1,\cdots.M_{ij}$ where $\mathbf{x}_{c,ij}^{l}=\left[u_{c,j}^{l}(k-\tau_{ij})\quad y_{c,i}^{l}(k-1)\quad y_{c,i}^{l}(k-2)\right]$.

Table B.1 The centers of fuzzy clusters for the process in Eq. (4.34)

Centers of C_{ij}^{l}'s in loop y_i–u_j	No. of fuzzy clusters					
	$R^1(l=1)$	$R^2(l=2)$	$R^3(l=3)$	$R^4(l=4)$	$R^5(l=5)$	$R^6(l=6)$
$f_{TS,11}(\triangle\mu_{11}^{l}=0.05)$						
$u_{c,1}^{l}(k-\tau_{11})$	0.5622	1.3647	0.8080	1.2917	1.3446	0.6003
$y_{c,1}^{l}(k-1)$	1.3286	0.9915	1.2043	1.1904	1.5125	0.9530
$y_{c,1}^{l}(k-2)$	1.1450	1.1523	1.3147	1.0916	1.3482	1.1075
$y_{c,1}^{l}(k)$	1.1055	1.2062	1.0991	1.3174	1.6284	0.8485
$f_{TS,12}(\triangle\mu_{12}^{l}=0.05)$						
$u_{c,2}^{l}(k-\tau_{12})$	1.2909	0.8570	1.3501	0.5789	0.6350	1.2364
$y_{c,1}^{l}(k-1)$	1.0727	0.9838	0.9385	1.0686	0.9503	1.0267
$y_{c,1}^{l}(k-2)$	1.0145	1.0085	0.9997	1.0040	1.0149	0.9979
$y_{c,1}^{l}(k)$	1.1222	0.9727	1.0153	0.9847	0.8888	1.0575
$f_{TS,13}(\triangle\mu_{13}^{l}=0.05)$						
$u_{c,3}^{l}(k-\tau_{13})$	0.6910	0.6976	1.2953	1.2328	1.3997	0.6252
$y_{c,1}^{l}(k-1)$	1.1078	1.0586	1.0414	1.0761	1.0703	1.0272
$y_{c,1}^{l}(k-2)$	1.0911	1.0471	1.0593	1.0804	1.0460	1.0584
$y_{c,1}^{l}(k)$	1.0822	1.0196	1.0782	1.0774	1.1201	1.0064
$f_{TS,21}(\triangle\mu_{21}^{l}=0.05)$						
$u_{c,1}^{l}(k-\tau_{21})$	1.1255	0.9491	0.5658	1.4285	0.5358	1.3894
$y_{c,2}^{l}(k-1)$	2.0363	2.1622	2.1112	2.0109	1.9872	2.1456
$y_{c,2}^{l}(k-2)$	1.9934	2.2249	2.0555	2.0733	2.0470	2.0585
$y_{c,2}^{l}(k)$	2.0275	2.1363	2.0055	2.1058	1.9364	2.2626
$f_{TS,22}(\triangle\mu_{22}^{l}=0.05)$						
$u_{c,2}^{l}(k-\tau_{22})$	1.1127	0.8016	0.5747	1.4044	1.2765	0.7716
$y_{c,2}^{l}(k-1)$	0.5326	0.4769	0.5144	0.5023	0.4934	0.5007
$y_{c,2}^{l}(k-2)$	0.5303	0.4824	0.5160	0.4970	0.5015	0.4931
$y_{c,2}^{l}(k)$	0.5327	0.4761	0.5152	0.5022	0.5039	0.4902
$f_{TS,23}(\triangle\mu_{23}^{l}=0.05)$						
$u_{c,3}^{l}(k-\tau_{23})$	1.2047	0.7098	1.3109	0.6307	0.8037	1.2922
$y_{c,2}^{l}(k-1)$	0.3152	0.2388	0.2396	0.3261	0.2656	0.3328
$y_{c,2}^{l}(k-2)$	0.2842	0.2888	0.2839	0.2673	0.2936	0.2966
$y_{c,2}^{l}(k)$	0.3275	0.2264	0.3076	0.2541	0.2461	0.3571
$f_{TS,31}(\triangle\mu_{31}^{l}=0.05)$						

$u^l_{c,1}(k-\tau_{31})$	1.3618	0.6121	0.7111	1.2980	1.3706	0.6179
$y^l_{c,3}(k-1)$	0.2010	0.2782	0.2186	0.2335	0.2980	0.2037
$y^l_{c,3}(k-2)$	0.2405	0.2419	0.2171	0.2216	0.2627	0.2448
$y^l_{c,3}(k)$	0.2425	0.2354	0.1998	0.2574	0.3258	0.1773
$f_{TS,32}$ ($\triangle\mu^l_{32}$=0.05)						
$u^l_{c,2}(k-\tau_{32})$	1.3431	0.6205	1.2799	0.6305	1.2034	0.8962
$y^l_{c,3}(k-1)$	0.6055	0.7323	0.7242	0.6044	0.7122	0.6536
$y^l_{c,3}(k-2)$	0.6633	0.6627	0.6880	0.6667	0.6706	0.6782
$y^l_{c,3}(k)$	0.6858	0.6514	0.7517	0.5572	0.7462	0.6429
$f_{TS,33}$($\triangle\mu^l_{33}$=0.03)						
$u^l_{c,3}(k-\tau_{33})$	0.8772	1.2857	0.6684	1.2590	0.5560	1.3119
$y^l_{c,3}(k-1)$	0.1077	0.1117	0.1109	0.1092	0.1096	0.1102
$y^l_{c,3}(k-2)$	0.1080	0.1111	0.1090	0.1113	0.1105	0.1093
$y^l_{c,3}(k)$	0.1082	0.1130	0.1086	0.1100	0.1109	0.1086

Table B.2 The consequent parameters of Type–1 and Type–2 T–S fuzzy models for the process in Eq. (4.34)

No. of fuzzy rules	Type–1 fuzzy model			Type–2 fuzzy model					
	a^l_0	b^l_1	b^l_2	$a^l_{lb,0}$	$b^l_{lb,1}$	$b^l_{lb,2}$	$a^l_{rb,0}$	$b^l_{rb,1}$	$b^l_{rb,2}$
$f_{TS,11}$									
$R^1(l=1)$	0.4168	0.6234	0.0503	0.4362	0.6849	0.0205	0.3974	0.5620	0.0801
$R^2(l=2)$	0.3746	0.8545	-0.1103	0.4063	0.8622	-0.1055	0.3429	0.8468	-0.1150
$R^3(l=3)$	0.3863	0.8449	-0.1765	0.4012	0.8446	-0.1448	0.3714	0.8452	-0.2082
$R^4(l=4)$	0.3621	0.7834	-0.1002	0.3859	0.8059	-0.0979	0.3383	0.7608	-0.1025
$R^5(l=5)$	0.4159	0.7726	-0.0442	0.4317	0.8055	-0.0558	0.4001	0.7396	-0.0327
$R^6(l=6)$	0.3931	0.7623	-0.0971	0.4217	0.7919	-0.0774	0.3646	0.7327	-0.1169
$f_{TS,12}$									
$R^1(l=1)$	0.1853	0.7450	0.0959	0.1948	0.7958	0.0751	0.1758	0.6943	0.1168
$R^2(l=2)$	0.1745	0.6941	0.1611	0.1825	0.7393	0.1618	0.1665	0.6489	0.1604
$R^3(l=3)$	0.1845	0.7492	0.0625	0.1997	0.7782	0.0625	0.1693	0.7202	0.0626
$R^4(l=4)$	0.1831	0.7475	0.0791	0.1858	0.8249	0.0418	0.1805	0.6702	0.1164
$R^5(l=5)$	0.1519	0.6249	0.1768	0.1594	0.6537	0.1946	0.1443	0.5960	0.1590
$R^6(l=6)$	0.1822	0.6979	0.0894	0.1916	0.7502	0.0701	0.1727	0.6456	0.1086
$f_{TS,13}$									
$R^1(l=1)$	0.0980	0.7854	0.1420	0.0991	0.8415	0.1272	0.0969	0.7293	0.1569
$R^2(l=2)$	0.0931	0.8095	0.0692	0.0971	0.8475	0.0773	0.0891	0.7716	0.0610
$R^3(l=3)$	0.0946	0.8083	0.1186	0.1047	0.8468	0.1152	0.0845	0.7699	0.1219
$R^4(l=4)$	0.0919	0.7504	0.1254	0.0987	0.7647	0.1474	0.0851	0.7361	0.1034
$R^5(l=5)$	0.1062	0.6681	0.2587	0.1147	0.7141	0.2457	0.0978	0.6222	0.2717
$R^6(l=6)$	0.0956	0.8711	0.0580	0.1010	0.9326	0.0447	0.0902	0.8096	0.0712
$f_{TS,21}$									
$R^1(l=1)$	0.1881	1.0126	-0.1523	0.2011	1.0316	-0.1280	0.1751	0.9935	-0.1766
$R^2(l=2)$	0.2028	0.8467	0.0421	0.2154	0.8228	0.0992	0.1903	0.8705	-0.0151

$R^3(l=3)$	0.2350	1.0616	-0.1896	0.2459	1.0841	-0.1675	0.2242	1.0391	-0.2116
$R^4(l=4)$	0.2127	0.8061	0.0828	0.2404	0.8094	0.1061	0.1851	0.8028	0.0595
$R^5(l=5)$	0.2605	1.0580	-0.1312	0.2805	1.0763	-0.1038	0.2406	1.0397	-0.1586
$R^6(l=6)$	0.1848	0.9333	0.0234	0.2087	0.9642	0.0203	0.1608	0.9024	0.0265
$f_{TS,22}$									
$R^1(l=1)$	0.0254	1.1676	-0.2225	0.0262	1.2035	-0.2183	0.0245	1.1316	-0.2267
$R^2(l=2)$	0.0159	1.2794	-0.2973	0.0166	1.3471	-0.3081	0.0151	1.2116	-0.2864
$R^3(l=3)$	0.0326	1.1339	-0.1470	0.0336	1.1633	-0.1308	0.0316	1.1045	-0.1632
$R^4(l=4)$	0.0242	1.3626	-0.4637	0.0299	1.4041	-0.4739	0.0185	1.3212	-0.4534
$R^5(l=5)$	0.0173	1.4796	-0.4639	0.0218	1.5131	-0.4600	0.0128	1.4460	-0.4678
$R^6(l=6)$	0.0140	1.4328	-0.5218	0.0169	1.4874	-0.5301	0.0112	1.3782	-0.5134
$f_{TS,23}$									
$R^1(l=1)$	0.1431	0.4784	0.0008	0.1470	0.5093	-0.0062	0.1393	0.4475	0.0078
$R^2(l=2)$	0.1472	0.5180	0.0102	0.1520	0.5509	0.0226	0.1424	0.4850	-0.0023
$R^3(l=3)$	0.1460	0.4818	-0.0028	0.1525	0.4978	-0.0001	0.1395	0.4657	-0.0055
$R^4(l=4)$	0.1448	0.4781	0.0295	0.1475	0.5224	0.0189	0.1422	0.4337	0.0400
$R^5(l=5)$	0.1413	0.4808	-0.0026	0.1466	0.5059	0.0115	0.1360	0.4557	-0.0167
$R^6(l=6)$	0.1495	0.5094	-0.0118	0.1539	0.5300	-0.0112	0.1451	0.4889	-0.0124
$f_{TS,31}$									
$R^1(l=1)$	0.0788	0.8838	-0.1595	0.0849	0.8820	-0.1458	0.0727	0.8857	-0.1731
$R^2(l=2)$	0.0852	0.6130	0.0631	0.0864	0.6812	0.0276	0.0839	0.5447	0.0985
$R^3(l=3)$	0.0823	0.6856	-0.0409	0.0855	0.7638	-0.0673	0.0792	0.6073	-0.0145
$R^4(l=4)$	0.0747	0.7549	-0.0992	0.0796	0.7771	-0.0971	0.0698	0.7328	-0.1014
$R^5(l=5)$	0.0802	0.7467	-0.0008	0.0841	0.7766	-0.0119	0.0763	0.7168	0.0103
$R^6(l=6)$	0.0818	0.8178	-0.1564	0.0864	0.7850	-0.0949	0.0773	0.8506	-0.2180
$f_{TS,32}$									
$R^1(l=1)$	0.1778	0.6767	0.0550	0.1896	0.7009	0.0570	0.1661	0.6526	0.0530
$R^2(l=2)$	0.1789	0.6433	0.1093	0.1830	0.7056	0.0848	0.1748	0.5811	0.1338
$R^3(l=3)$	0.1711	0.6716	0.0518	0.1784	0.7101	0.0411	0.1639	0.6331	0.0624
$R^4(l=4)$	0.1670	0.6305	0.0966	0.1762	0.6755	0.1000	0.1579	0.5854	0.0932
$R^5(l=5)$	0.1775	0.7149	0.0543	0.1857	0.7500	0.0474	0.1693	0.6797	0.0613
$R^6(l=6)$	0.1799	0.6413	0.0997	0.1944	0.6931	0.0796	0.1654	0.5895	0.1198
$f_{TS,33}$									
$R^1(l=1)$	0.0024	1.0770	-0.0830	0.0029	1.1021	-0.0621	0.0019	1.0520	-0.1040
$R^2(l=2)$	0.0038	0.6604	0.3255	0.0045	0.6959	0.3242	0.0030	0.6248	0.3268
$R^3(l=3)$	0.0005	1.0561	-0.1007	0.0007	1.0956	-0.0965	0.0003	1.0166	-0.1050
$R^4(l=4)$	0.0035	0.6166	0.3367	0.0041	0.5863	0.4023	0.0029	0.6469	0.2711
$R^5(l=5)$	0.0027	0.9986	0.0155	0.0029	1.0034	0.0547	0.0025	0.9938	-0.0236
$R^6(l=6)$	0.0029	0.8095	0.1177	0.0035	0.8531	0.1108	0.0023	0.7660	0.1246

Linearized the nonlinear MIMO process in Eq. (4.34) at the given operating points, a transfer function matrix can be obtained as:

$$\boldsymbol{G}(s)=\left[g_{ij}(s)\right]_{n\times n}=\begin{bmatrix}\dfrac{1.25}{0.25s+1}e^{-2s} & \dfrac{1}{0.5s+1}e^{-2s} & \dfrac{1}{s+1}e^{-s}\\ \dfrac{2}{s+1}e^{-2s} & \dfrac{0.5}{0.1667s^2+0.8333s+1}e^{-2s} & \dfrac{0.2857}{0.1429s+1}e^{-s}\\ \dfrac{0.25}{0.25s+1}e^{-2s} & \dfrac{0.6667}{0.3333s+1}e^{-2s} & \dfrac{0.1}{0.5s^2+1.5s+1}e^{-s}\end{bmatrix}$$

Based on $\boldsymbol{G}(s)$, the steady–state gain matrix $\boldsymbol{K}$, the normalized integrated error matrix $\boldsymbol{E}$, the RGA $\boldsymbol{\Lambda}$, and the RNGA $\boldsymbol{\Phi}_{TS}$, can be calculated as:

$$\boldsymbol{K}=\begin{bmatrix}1.25 & 1 & 1\\ 2 & 0.5 & 0.2857\\ 0.25 & 0.6667 & 0.1\end{bmatrix},\quad \boldsymbol{E}=\begin{bmatrix}2.25 & 2.5 & 2\\ 3 & 2.8333 & 1.1429\\ 2.25 & 2.3333 & 2.5\end{bmatrix}$$

$$\boldsymbol{\Lambda}=\begin{bmatrix}-0.1942 & -0.1422 & 1.3364\\ 1.2535 & -0.0691 & -0.1843\\ -0.0592 & 1.2113 & -0.1521\end{bmatrix},\quad \boldsymbol{\Phi}=\begin{bmatrix}-0.7135 & 0.0089 & 1.7047\\ 1.6875 & -0.1174 & -0.5701\\ 0.0261 & 1.1085 & -0.1346\end{bmatrix}$$

According to the RNGA based loop pairing criterion, the optimal control configuration can be determined: $y_1-u_3\,/\,y_2-u_1\,/\,y_3-u_2$, where NI is $\boldsymbol{N}=0.9608>0$. Based on $\boldsymbol{\Lambda}$ and $\boldsymbol{\Phi}$, the relative normalized integrated error array $\boldsymbol{\Gamma}$ for $\boldsymbol{G}(s)$ can be derived:

$$\boldsymbol{\Gamma}=\begin{bmatrix}3.6741 & -0.0624 & 1.2756\\ 1.3462 & 1.6980 & 3.0927\\ -0.4402 & 0.9151 & 0.8850\end{bmatrix}$$

And then the ETFs $\hat{g}_{ij}(s)$ of paired loops and the ETF based decentralized controllers according to the methods in [38] can be derived:

Loop y_1-u_3: $\hat{g}_{13}(s)=\dfrac{1}{1.2756s+1}e^{-1.2756s}$, and $G_{c,1}(s)=\dfrac{0.5236s+0.4105}{s}$.

Loop y_2-u_1: $\hat{g}_{21}(s)=\dfrac{2}{1.3462s+1}e^{-2\times1.3462s}$, and $G_{c,2}(s)=\dfrac{0.1309s+0.0972}{s}$.

Loop y_3-u_2: $\hat{g}_{32}(s)=\dfrac{0.6667}{0.3333s+1}e^{-2}$, and $G_{c,3}(s)=\dfrac{0.1309s+0.3927}{s}$.

Place the paired loops in the diagonal positions, the interaction index $\boldsymbol{B}$ for $\boldsymbol{G}(s)$ can be computed:

$$\boldsymbol{B} = \begin{bmatrix} 1.0000 & \mathbf{0.4186} & 0.0052 \\ \mathbf{0.3378} & 1.0000 & 0.0696 \\ 0.1214 & 0.0235 & 1.0000 \end{bmatrix}$$

And the positions of bold numbers in $\boldsymbol{B}$ are the off–diagonal loops selected for sparse controller design, and they are loop $y_2 - u_3$ and loop $y_1 - u_1$ in the original process. For the original process, the selected loops in $\boldsymbol{G}(s)$ (set 0 to the unselected loops) and the corresponding controller matrix are as follows:

$$\boldsymbol{G}(s) = \begin{bmatrix} g_{11}(s) & 0 & g_{13}(s) \\ g_{21}(s) & 0 & g_{23}(s) \\ 0 & g_{32}(s) & 0 \end{bmatrix} \Rightarrow \boldsymbol{G}_c = \begin{bmatrix} G_{c,11} & G_{c,2} & 0 \\ 0 & 0 & G_{c,3} \\ G_{c,1} & G_{c,32} & 0 \end{bmatrix}$$

where

$G_{11}(s) = \dfrac{-0.0102s - 0.0111}{s}$ is designed based on $\hat{g}_{11}(s) = \dfrac{-6.4367}{0.9185s + 1} e^{-7.3482s}$, and

$G_{32}(s) = \dfrac{-0.0482s - 0.1092}{s}$ is designed based on $\hat{g}_{23}(s) = \dfrac{-1.5503}{0.4418s + 1} e^{-3.0927s}$

Appendix C

The parameters of Type–1 and Type–2 T–S fuzzy models for the MER system are given in Table C.1 and Table C.2, where $M_{ij} = 6\,(i, j = 1,2,3)$, $p = 0$ and $q = 2$.

Table C.1 The centers of fuzzy clusters for the MER system

Centers of C_{ij}^{l}'s in loop y_i–u_j	No. of fuzzy clusters $R^1(l=1)$	$R^2(l=2)$	$R^3(l=3)$	$R^4(l=4)$	$R^5(l=5)$	$R^6(l=6)$
$f_{TS,11}(\triangle\mu_{11}^{l}=0.05)$						
$u_{c,1}^{l}(k-\tau_{11})$	-1.1075	0.9168	-0.9836	0.6944	-0.7639	0.5346
$y_{c,1}^{l}(k-1)$	-0.0459	0.6269	0.9628	-0.5856	-0.4118	0.6717
$y_{c,1}^{l}(k-2)$	0.1432	0.0124	0.0059	0.1681	0.4828	0.3950
$y_{c,1}^{l}(k)$	0.7461	-0.2806	1.2813	-0.8496	0.3038	0.0405
$f_{TS,12}(\triangle\mu_{12}^{l}=0.05)$						
$u_{c,2}^{l}(k-\tau_{12})$	-1.5913	1.1459	-0.8951	0.8294	-0.8667	0.6068
$y_{c,1}^{l}(k-1)$	0.1416	-0.1342	-0.1296	0.0827	-0.1732	-0.1205
$y_{c,1}^{l}(k-2)$	-0.0085	-0.0002	-0.0318	-0.0764	-0.0736	-0.1232
$y_{c,1}^{l}(k)$	-0.0761	0.0305	-0.2057	0.1655	-0.2476	-0.0250
$f_{TS,13}(\triangle\mu_{13}^{l}=0.03)$						
$u_{c,3}^{l}(k-\tau_{13})$	0.4006	-0.1076	-1.1684	0.8121	-1.5640	1.0682
$y_{c,1}^{l}(k-1)$	0.0067	-0.0445	-0.0569	0.0003	0.0421	-0.0545
$y_{c,1}^{l}(k-2)$	-0.0185	-0.0016	-0.0222	-0.0394	-0.0004	-0.0198
$y_{c,1}^{l}(k)$	0.0200	-0.0419	-0.0897	0.0330	-0.0259	-0.0029
$f_{TS,21}(\triangle\mu_{21}^{l}=0.05)$						
$u_{c,1}^{l}(k-\tau_{21})$	-1.5427	0.9795	0.9616	-1.4330	0.6577	-0.2576
$y_{c,2}^{l}(k-1)$	0.2760	-0.2305	0.1525	-0.3532	-0.0878	-0.2279
$y_{c,2}^{l}(k-2)$	0.0243	0.0202	-0.0900	-0.1022	-0.2184	-0.0645
$y_{c,2}^{l}(k)$	-0.1501	0.0528	0.3296	-0.5815	0.0809	-0.2131
$f_{TS,22}(\triangle\mu_{22}^{l}=0.05)$						
$u_{c,2}^{l}(k-\tau_{22})$	0.9258	-0.9146	-1.5075	0.5925	1.0956	-0.7863
$y_{c,2}^{l}(k-1)$	-0.1721	0.1859	-0.2414	0.1337	0.2376	0.2467
$y_{c,2}^{l}(k-2)$	0.0977	-0.0767	-0.0252	0.1864	0.0020	0.1610
$y_{c,2}^{l}(k)$	-0.3066	0.3140	0.1240	-0.0261	-0.0452	0.3376
$f_{TS,23}(\triangle\mu_{23}^{l}=0.03)$						
$u_{c,3}^{l}(k-\tau_{23})$	-0.9778	0.8690	-0.7579	0.5809	-1.4618	1.1641
$y_{c,2}^{l}(k-1)$	-0.0230	0.0043	-0.0239	-0.0071	0.0236	-0.0267
$y_{c,2}^{l}(k-2)$	-0.0157	-0.0194	0.0012	-0.0161	-0.0001	-0.0033
$y_{c,2}^{l}(k)$	-0.0377	0.0221	-0.0350	0.0056	-0.0118	0.0029
$f_{TS,31}(\triangle\mu_{31}^{l}=0.03)$						
$u_{c,1}^{l}(k-\tau_{31})$	-0.4131	0.8793	1.0785	-1.2529	-1.5736	0.6802
$y_{c,3}^{l}(k-1)$	-0.0305	0.0339	-0.0408	-0.0809	0.0558	-0.0538
$y_{c,3}^{l}(k-2)$	-0.0300	-0.0240	-0.0258	-0.0279	0.0036	-0.0084
$y_{c,3}^{l}(k)$	-0.0430	0.0687	0.0187	-0.1213	-0.0333	-0.0071

$f_{TS,32}$ ($\triangle\mu^l_{32}$=0.05)						
$u^l_{c,2}(k-\tau_{32})$	-1.3177	0.9899	0.7682	-1.0458	-1.1509	0.9353
$y^l_{c,3}(k-1)$	0.0208	-0.0256	-0.0194	0.0003	-0.0386	0.0116
$y^l_{c,3}(k-2)$	-0.0079	0.0022	-0.0215	-0.0015	-0.0077	-0.0148
$y^l_{c,3}(k)$	-0.0126	0.0023	0.0016	-0.0239	-0.0552	0.0300
$f_{TS,33}$($\triangle\mu^l_{33}$=0.05)						
$u^l_{c,3}(k-\tau_{33})$	1.2731	-1.5564	1.0375	-1.2268	-0.2238	0.0997
$y^l_{c,3}(k-1)$	0.0774	-0.0578	-0.0230	0.0862	0.0764	0.0113
$y^l_{c,3}(k-2)$	0.0156	0.0012	0.0378	0.0210	0.0381	0.0475
$y^l_{c,3}(k)$	-0.0058	0.0374	-0.0767	0.1354	0.0771	0.0047

Table C.2 The consequent parameters of Type–1 and Type–2 T–S fuzzy models for the MER system

No. of fuzzy rules	Type–1 fuzzy model			Type–2 fuzzy model					
	a^l_0	b^l_1	b^l_2	$a^l_{lb,0}$	$b^l_{lb,1}$	$b^l_{lb,2}$	$a^l_{rb,0}$	$b^l_{rb,1}$	$b^l_{rb,2}$
$f_{TS,11}$									
$R^1(l=1)$	-0.6986	0.6177	-0.0099	-0.7192	0.6124	-0.0054	-0.6781	0.6230	-0.0145
$R^2(l=2)$	-0.7156	0.5987	0.0020	-0.7009	0.6152	-0.0077	-0.7304	0.5823	0.0117
$R^3(l=3)$	-0.7121	0.6041	-0.0010	-0.7213	0.6239	-0.0146	-0.7028	0.5842	0.0125
$R^4(l=4)$	-0.6996	0.6166	-0.0108	-0.6898	0.5945	0.0025	-0.7094	0.6388	-0.0241
$R^5(l=5)$	-0.7181	0.6021	0.0027	-0.7299	0.5836	0.0186	-0.7064	0.6206	-0.0131
$R^6(l=6)$	-0.7029	0.6246	-0.0130	-0.6930	0.6474	-0.0230	-0.7129	0.6019	-0.0031
$f_{TS,12}$									
$R^1(l=1)$	0.1184	0.7945	-0.0015	0.1139	0.8251	-0.0244	0.1229	0.7638	0.0214
$R^2(l=2)$	0.1201	0.8014	0.0014	0.1243	0.7686	0.0331	0.1160	0.8342	-0.0302
$R^3(l=3)$	0.1163	0.7816	0.0109	0.1116	0.7501	0.0337	0.1210	0.8130	-0.0119
$R^4(l=4)$	0.1215	0.7857	0.0094	0.1250	0.8300	-0.0253	0.1180	0.7414	0.0442
$R^5(l=5)$	0.1240	0.8134	-0.0082	0.1191	0.7826	0.0101	0.1288	0.8442	-0.0264
$R^6(l=6)$	0.1170	0.7989	-0.0033	0.1226	0.7887	-0.0111	0.1113	0.8092	0.0045
$f_{TS,13}$									
$R^1(l=1)$	0.0375	0.7819	0.0264	0.0387	0.8278	-0.0092	0.0362	0.7359	0.0620
$R^2(l=2)$	0.0391	0.8538	-0.0221	0.0387	0.7909	0.0220	0.0394	0.9167	-0.0663
$R^3(l=3)$	0.0379	0.7891	0.0206	0.0363	0.7633	0.0371	0.0395	0.8148	0.0042
$R^4(l=4)$	0.0393	0.8308	-0.0175	0.0408	0.8684	-0.0566	0.0378	0.7933	0.0216
$R^5(l=5)$	0.0385	0.8094	-0.0026	0.0369	0.8379	-0.0245	0.0401	0.7810	0.0193
$R^6(l=6)$	0.0379	0.7894	0.0120	0.0393	0.7558	0.0353	0.0365	0.8231	-0.0113
$f_{TS,21}$									
$R^1(l=1)$	0.2247	0.7095	0.0023	0.2183	0.7297	-0.0111	0.2311	0.6893	0.0156
$R^2(l=2)$	0.2269	0.7272	-0.0102	0.2315	0.6998	0.0133	0.2222	0.7546	-0.0336
$R^3(l=3)$	0.2290	0.7192	-0.0061	0.2349	0.7463	-0.0258	0.2232	0.6921	0.0136
$R^4(l=4)$	0.2313	0.7122	0.0008	0.2248	0.6959	0.0102	0.2379	0.7286	-0.0087
$R^5(l=5)$	0.2254	0.6903	0.0289	0.2288	0.7108	-0.0040	0.2221	0.6699	0.0617
$R^6(l=6)$	0.2259	0.6812	0.0220	0.2241	0.6391	0.0472	0.2276	0.7233	-0.0033

$f_{TS,22}$									
$R^1(l=1)$	-0.1984	0.7119	0.0067	-0.1944	0.6811	0.0273	-0.2025	0.7426	-0.0140
$R^2(l=2)$	-0.1981	0.7015	0.0020	-0.2015	0.7280	-0.0232	-0.1948	0.6751	0.0272
$R^3(l=3)$	-0.1968	0.7102	0.0060	-0.2024	0.6908	0.0194	-0.1911	0.7296	-0.0075
$R^4(l=4)$	-0.2041	0.7210	-0.0104	-0.1981	0.7172	0.0080	-0.2102	0.7248	-0.0287
$R^5(l=5)$	-0.1956	0.7128	0.0044	-0.1908	0.7366	-0.0144	-0.2003	0.6891	0.0233
$R^6(l=6)$	-0.2034	0.7183	0.0011	-0.2091	0.7276	0.0083	-0.1978	0.7091	-0.0061
$f_{TS,23}$									
$R^1(l=1)$	0.0201	0.7654	0.0201	0.0192	0.7464	0.0246	0.0210	0.7844	0.0156
$R^2(l=2)$	0.0210	0.8084	-0.0151	0.0217	0.8434	-0.0484	0.0203	0.7734	0.0181
$R^3(l=3)$	0.0211	0.8025	-0.0007	0.0207	0.7586	0.0367	0.0215	0.8463	-0.0380
$R^4(l=4)$	0.0202	0.7605	0.0367	0.0211	0.7897	0.0022	0.0192	0.7312	0.0711
$R^5(l=5)$	0.0207	0.7840	0.0091	0.0200	0.8151	-0.0131	0.0215	0.7529	0.0313
$R^6(l=6)$	0.0206	0.7869	0.0068	0.0213	0.7515	0.0344	0.0200	0.8224	-0.0208
$f_{TS,31}$									
$R^1(l=1)$	0.0448	0.7639	0.0100	0.0421	0.7537	-0.0076	0.0475	0.7740	0.0277
$R^2(l=2)$	0.0474	0.7739	-0.0138	0.0484	0.8136	-0.0432	0.0464	0.7343	0.0157
$R^3(l=3)$	0.0462	0.7724	-0.0087	0.0483	0.7597	-0.0008	0.0441	0.7851	-0.0165
$R^4(l=4)$	0.0466	0.7809	-0.0130	0.0452	0.7541	0.0041	0.0479	0.8077	-0.0300
$R^5(l=5)$	0.0477	0.7564	0.0071	0.0461	0.7811	-0.0098	0.0493	0.7317	0.0241
$R^6(l=6)$	0.0480	0.7328	0.0202	0.0489	0.6892	0.0509	0.0471	0.7763	-0.0104
$f_{TS,32}$									
$R^1(l=1)$	0.0221	0.7940	-0.0094	0.0214	0.8232	-0.0350	0.0227	0.7648	0.0162
$R^2(l=2)$	0.0223	0.7722	0.0070	0.0228	0.7359	0.0399	0.0218	0.8084	-0.0259
$R^3(l=3)$	0.0214	0.7673	0.0138	0.0224	0.7691	-0.0045	0.0204	0.7655	0.0321
$R^4(l=4)$	0.0232	0.7782	0.0030	0.0220	0.7799	0.0028	0.0245	0.7764	0.0032
$R^5(l=5)$	0.0219	0.7765	0.0010	0.0214	0.7435	0.0227	0.0225	0.8095	-0.0207
$R^6(l=6)$	0.0222	0.7775	-0.0036	0.0228	0.8147	-0.0337	0.0216	0.7403	0.0265
$f_{TS,33}$									
$R^1(l=1)$	-0.0539	0.8131	0.0085	-0.0516	0.8467	-0.0202	-0.0562	0.7794	0.0372
$R^2(l=2)$	-0.0543	0.8149	-0.0002	-0.0568	0.7871	0.0213	-0.0517	0.8427	-0.0217
$R^3(l=3)$	-0.0556	0.8087	-0.0041	-0.0530	0.7744	0.0244	-0.0581	0.8431	-0.0325
$R^4(l=4)$	-0.0554	0.7792	0.0235	-0.0571	0.8190	-0.0045	-0.0537	0.7394	0.0516
$R^5(l=5)$	-0.0557	0.8653	-0.0304	-0.0565	0.9315	-0.0753	-0.0549	0.7991	0.0144
$R^6(l=6)$	-0.0518	0.7675	0.0398	-0.0505	0.7107	0.0999	-0.0530	0.8243	-0.0203